NOTICE

The quality of this microform is heavily dependent upon the quality of the original thesis submitted for microfilming. Every effort has been made to ensure the highest quality of reproduction possible.

If pages are missing, contact the university which granted the degree.

Some pages may have indistinct print especially if the original pages were typed with a poor typewriter ribbon or if the university sent us an inferior photocopy.

Reproduction in full or in part of this microform is governed by the Canadian Copyright Act, R.S.C. 1970, c. C-30, and subsequent amendments.

AVIS

La qualité de cette microforme dépend grandement de la qualité de la thèse soumise au microfilmage. Nous avons tout fait pour assurer une qualité supérieure de reproduction.

S'il manque des pages, veuillez communiquer avec l'université qui a conféré le grade.

La qualité d'impression de certaines pages peut laisser à désirer, surtout si les pages originales ont été dactylographiées à l'aide d'un ruban usé ou si l'université nous a fait parvenir une photocopie de qualité inférieure.

La reproduction, même partielle, de cette microforme est soumise à la Loi canadienne sur le droit d'auteur, SRC 1970, c. C-30, et ses amendements subséquents.

ISBN 0-315-56442-3

A PROTON NUCLEAR MAGNETIC RESONANCE STUDY

OF

HUMAN TUMOUR BIOPSY SAMPLES

Eva J. Princz

Thesis submitted to the School of Graduate Studies and Research
in partial fulfillment of the requirements for the M.Sc. degree
in Biochemistry

University of Ottawa
Ottawa, Ontario, Canada
July, 1988

UNIVERSITÉ D'OTTAWA
UNIVERSITY OF OTTAWA

Abstract

To the present there has been no method to assess the metastatic potential of human tumours. In a rat mammary adenocarcinoma cell line, the transverse relaxation time (T_2) of the methylene or lipid (CH_2) peak in the ^1H NMR spectrum had been successfully used to differentiate a metastatic from a non-metastatic variant. An extensive clinical study was thus undertaken to test the hypothesis that a long T_2 value was indicative of metastatic potential in the human situation.

While no sample directly violated the initial hypothesis, it was necessary to discern whether biopsy samples with long T_2 values but no clinical evidence of metastasis at the time of surgery would indeed develop metastases in the future. The two year time span of this thesis appears insufficient for conclusive results from follow-up questionnaires.

The colon data base was therefore selected for more intensive study. A statistically significant elevation in T_2 values at the premalignant and early stages of colon cancer progression provided strong implications for the early diagnosis of colorectal cancer. The feasibility of unequivocal diagnosis of malignancy in the colon is addressed using a combination of T_2 and other NMR parameters, notably the presence of a cross peak unique to tumour samples in a 2-dimensional NMR experiment. From the data examined, it would appear that all human colon cancers possess the potential for metastasis, the question being the matter of time involved.

The molecular origin of the NMR parameters unique to tumour samples was investigated. From 2-dimensional NMR studies, it is proposed that the terminal sugar fucose on cell-surface oligosaccharide chains is responsible. Lactate analysis on colon tumour and normal samples eliminated lactate as the source of the long T_2. NMR experiments using the enzyme lactate oxidase to alter the lactate content of human placental homogenates showed that lactate was not the sole source of the cross peak evident in 2-D NMR spectra.

As a result of this study, the feasibility of employing a combination of Magnetic Resonance Imaging (MRI) and Magnetic Resonance Spectroscopy (MRS) for non-invasive diagnosis of colorectal cancer is addressed.

to my family, Gyula, Katalina, Juliska,
Márti and Daniel,
whom I love, for their patience,

to my parents, Ilona and László Adamovich,
who have given me love and support in all my endeavors,

and to the memory of Lydia Love,
who was not given a second chance at life,
and made me wonder what I could do with mine,

this thesis is dedicated.

Acknowledgements

I wish to acknowledge our collaborator in Australia, Dr. Carolyn E. Mountford, a courageous and caring lady, upon whose pioneering work this thesis project was based. I thank her for all her help in understanding our results, and for her heartfelt encouragement in my scientific endeavors.

This project would not have been possible without the cooperation of the Ottawa Civic Hospital. I wish to thank in particular Dr. J. Robin Barr, former Acting Chief, Division of Anatomical Pathology, for histological analysis of the samples for NMR, and for invaluable help in understanding the pathology of cancer, notably colon cancer. Mollie Stokes, Chief Technologist, Anatomical Pathology, deserves much credit for her untiring diligence in coordinating the acquisition of our samples and obtaining the histology reports. The enthusiasm and hard work of both Dr. Barr and Mollie are much appreciated.

Many people have taken part in this extensive project, and I would like to acknowledge several in particular :

- Dr. John K. Saunders - who can work wonders with an NMR machine, for NMR of many samples, and for teaching me how to run an NMR machine
- Myrna Monck - my colleague on the Cancer Project, for sharing the learning and much of the work with me
- Thérèse Kroft - for invaluable, and always cheery, Laboratory assistance:
- Dr. Roxanne Deslauriers and Dr. Ray Somorjai - for helpful discussions on T_2 analysis and CONTIN runs. I wish to thank Roxanne, an exemplary scientist, and also a wife and mother, for her encouragement and understanding.
- Sylvain Lareau - for development of tissue lactate analysis protocol
- Dr. M. Remin - for extensive T_2 analysis of many samples
- Joanne Ridgeway and Lise Bramall - for cheerful assistance with the computing facilities, T_2 runs, and statistical analysis
- Noreen Brady - for many library searches, always with a warm smile.

I thank the National Research Council of Canada, Biological Sciences Division, Ottawa, for the use of their facilities and the opportunity to learn at such a distinguished centre of scientific research.

I wish to thank Dr. Irena Ekiel for assistance with NMR analysis, much appreciated encouragement and help with thesis writing, and inspiration to be "a good scientist", Dr. Keith Butler for introducing me to the magnetic stirrer and other wonders of science, and Dr. Harold Jarrell for informative and interesting discussions on NMR theory.

I thank Dr. Myer Bloom of the Physics Department at U.B.C. for sharing with me his extraordinary insight into the NMR phenomenon during several lengthy discussions on the analysis of our NMR data.

A special thank you goes to Dr. Nicole Bégin-Heick, a terrific lady who has successfully combined science with family life, and encouraged me to undertake Graduate Studies, always with a concerned interest in my progress and well-being.

My fellow students and friends in the lab - among them Laura Stewart (countless explanations of the basics of NMR and "therapeutic teas"), Michèle Auger (my "chemical advisor"), and of course Myrna Monck, whose friendship I hope to treasure for a long time - I thank for their wonderful support.

This thesis might still be in progress, were it not for Mrs. Jean Watson, my amazingly energetic babysitter and good friend.

I have saved until last the person to whom I am most indebted in my present scientific adventure, the initiator of the Cancer Project and my supervisor and friend, Dr. Ian C.P. Smith. I thank him for having faith in an inexperienced 35-year-old-mother-of-three (now four), and his kindness in helping me through a few rough times in my studentship. He has taught me many things, about NMR, about science, about taking a chance on a risky and difficult, but worthwhile project. His enthusiasm for science is inexhaustible and contagious. He is a man of vision in the world of science, with the courage to take risks, characteristics that I am sure will serve him well as Director of Biological Sciences at NRC. It has been an honour and a privilege to have been his graduate student. I will always remember, during long hours in the lab, "Science is not work, it's play!"

Table of Contents

List of Tables

List of Figures and Illustrations

CHAPTER 1

INTRODUCTION

Cancer. The clawlike peripheral extensions of malignant epithelial neoplasms have given the disease its name. The analogy goes further, as they will attest who have gone wading at a rock-strewn seashore and been pinched by a crab whose hiding place had been disturbed. Like its namesake, cancer is silent, and hidden until its bite is felt, many times too late. Early diagnosis is crucial for successful treatment of the disease. A non-invasive means of diagnosis would be the ideal.

Nuclear Magnetic Resonance (NMR) is non-invasive, having as its "probes", certain nuclei occurring naturally in the material to be studied. Phosphorus (^{31}P) and hydrogen (^{1}H) are naturally abundant nuclei in biological tissues which are conducive to examination by NMR. To date, most NMR work in cancer has been performed on these two nuclei. The sample to be examined is placed in a superconducting magnet, and various NMR experiments can be run. Spectra are obtained, and several NMR parameters, such as relaxation times, are calculated for the nucleus under examination in order to characterize the tissue of interest. This procedure will be explained in greater detail in the course of this thesis.

We have limited our study to ^{1}H NMR. Hydrogen is the

most abundant nucleus in biological specimens, most notably in the form of water, but lipids, carbohydrates, and proteins contribute their fair share. Compared to other nuclei, such as carbon (^{13}C), hydrogen spectra are relatively simple, and cover a narrow chemical shift range - approximately 10 ppm as opposed to 200 ppm for ^{13}C for example. Due to the high detection sensitivity of hydrogen, less sample is required and less time is needed for acquisition of data. Thus, hydrogen was the nucleus of choice for the study of something as complicated as cancer. In the long run, of course, all the information provided by other nuclei should be integrated, because each tells its own story. In the same way, other disciplines are contributing to the study of cancer. The solution to the problem will result from the integration of knowledge obtained from several disciplines. This study involves the realm of biophysics (or physical biochemistry) by utilizing NMR. By studying the lipid region of the ^{1}H NMR spectrum it investigates a side-effect of the cancer process - the change in the plasma membrane profile of the cell. As to what initiates changes in cellular metabolism resulting in the altered plasma membrane is a question for another field - probably molecular biology, to examine alterations at the genetic level within the nucleus, wherein lies the blueprint for the whole cell. The level at which intervention will successfully curb the cancer process, i.e. genetic,

metabolic, immunologic, etc., is yet to be determined. A combination of approaches may be necessary.

Before delving into the work of this thesis, an overview of NMR in the study of cancer and a summary of the preliminary work leading to our clinical study will be presented.

Nuclear Magnetic Resonance originated in the realm of Physics, where its theoretical base and first spectrometers were built. The chemists adopted NMR for characterizing the structures of their molecules. Only relatively recently have the biomedical sciences (biochemistry included) acquainted themselves with the applications of NMR. Today it is a rapidly expanding field exploring new horizons, among them cancer research.

The low- and high-energy phosphates are observable by ^{31}P NMR spectroscopy. In vivo NMR spectroscopy applied to tumours is relatively new, and provides biochemical information on metabolism and bioenergetics, state of oxygenation, and intra- and extra-cellular pH. NMR imaging, which defines the spatial distribution of a specific nucleus, provides anatomical information, the location of a tumour, for example, but is limited in the amount of biochemistry it can reveal. A combination of the two modalities is the ideal.

^{31}P NMR spectroscopy was used *in vivo* to monitor tumours subcutaneously implanted in mice (Ng et al. 1982).

Figure 1-1. Monitoring the unretarded growth of a tumour by ^{31}P NMR spectroscopy, in vivo.

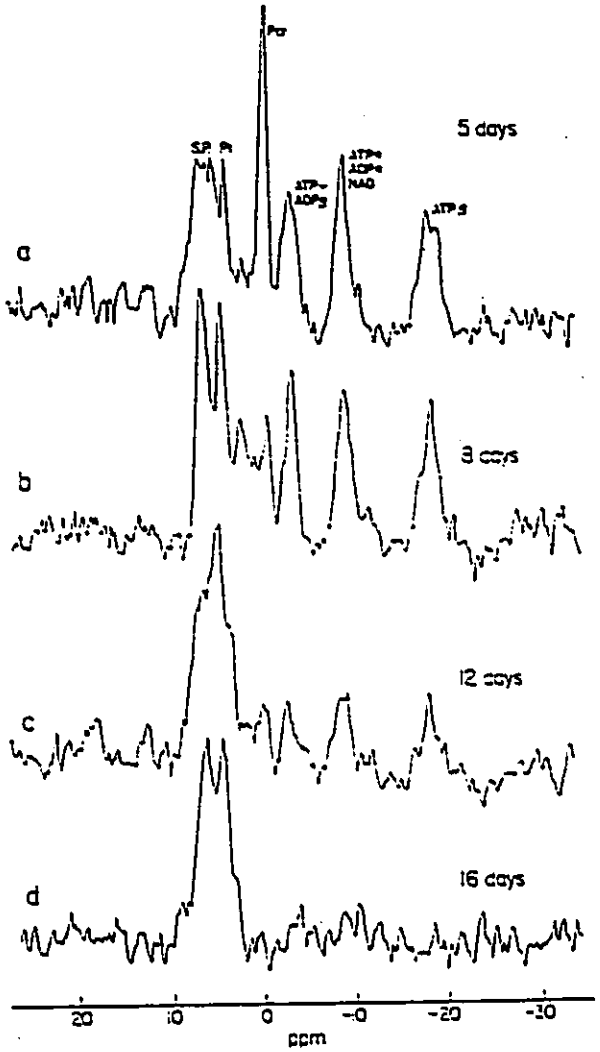

Abbreviations : PCr - phosphocreatine
P_i - inorganic phosphate
S.P.- sugar phosphates
ATP - adenosine triphosphate
ADP - adenosine diphosphate
NAD - nicotinamide adenine dinucleotide

The spectra are of a growing, untreated MOPC 104E myeloma subcutaneously implanted in mouse.

from Ng, T.C. et al. (1982) J. Mag. Res. 49, 271-86.

Metabolic changes could be monitored for untreated tumour growth, and in the treatment of tumours by chemo- and radiotherapy and hyperthermia. The changes induced by hyperthermia were the most striking and most rapidly detected. The changes were mostly qualitative, evidenced by changes in peak heights in the ^{31}P spectrum. The peaks due to phosphocreatine (PCr) and adenosine triphosphate (ATP) decreased in height with tumour growth, and the sugar phosphate and inorganic phosphate (P_i) peaks grew, indicating a decrease in aerobic metabolic activity (see Fig.1-1). The tumour on the back of a patient's hand was compared with that of a normal hand (Griffiths et al. 1983) and a decrease in the PCr peak was noted with unsuccessful therapy. The response to chemotherapy of human tumour-containing kidneys, excised and perfused, was monitored via ^{31}P NMR (Ross et al. 1984). Changes in the β-ATP peak and a resonance peculiar to renal tumours, which the authors speculated to be due to P_i, were noted. The precise biochemical processes leading to these observed changes remain to be elucidated.

Perhaps the most impressive study to date is the investigation of neuroblastoma in human liver <u>in vivo</u> (Maris et al. 1985). It was found that the phosphomonoester (PME) to β-ATP peak intensity ratio increased with tumour progression and decreased with tumour regression, as the infant concerned was given chemo- and radiotherapy (see

Figure 1-2. Monitoring the decline of the PME peak with chemotherapy in a neuroblastoma in human liver by ^{31}P NMR, in vivo.

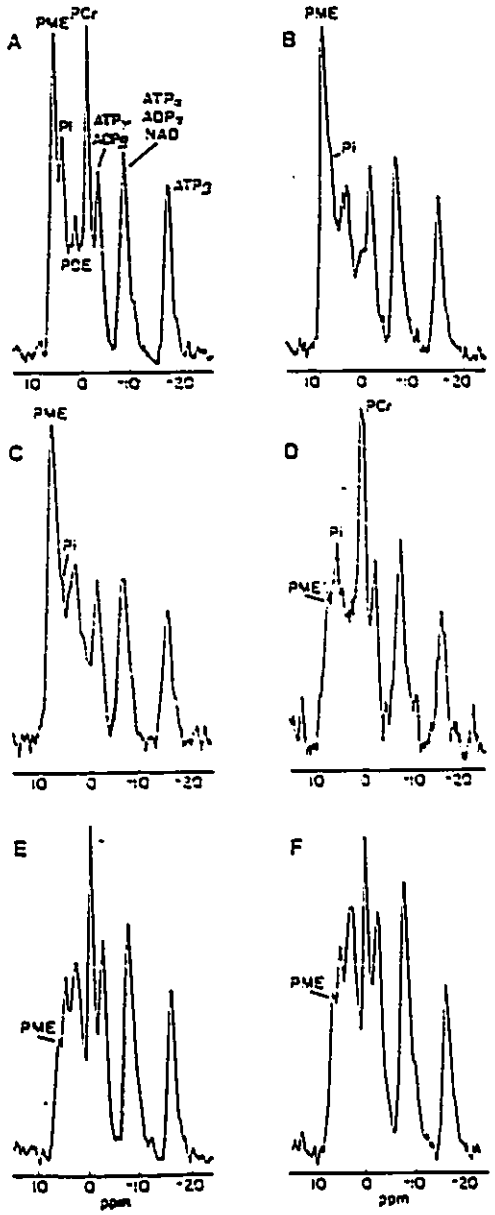

Abbreviations same as in Fig. 1-1, plus
PME - phosphomonoester
PDE - phosphodiester

A - initial study B - 4 weeks later C - 8 weeks later
D - 16 weeks later E & F - 24 weeks later, E at edge of liver
F anterolateral to edge of liver

from Maris, J.M. et al.(1985)The New Eng. J.Med. Vol 312 No.23: 1500-05.

Fig.1-2). Neonatal brain is the only other tissue studied where the PME/β-ATP ratio is greater than 1. The authors concluded that ^{31}P NMR can be used to detect tumours in situ and to monitor their response to treatment. Evanochko et al. (1984) wrote an excellent review of the application of ^{31}P NMR spectroscopy to cancer. They caution that monitoring the response of a tumour to various therapeutic modalities is based on the premise that the state of oxygenation of the tumour can be deduced from its ^{31}P NMR spectrum. It is necessary to test this by correlating changes in the NMR spectrum of the tumour with independent oximetric measurements. NMR can eventually be used in vivo to optimize the therapeutic protocol, and to measure the toxic effects of anti-neoplastic agents on vital normal tissues. They also state that there is "little evidence supporting the use of in vivo NMR in the clinical diagnosis of cancer". They refer to ^{31}P NMR spectroscopy, where the tumour-distinguishing characteristics manifest themselves in later stages of tumour growth. Imaging rather than spectroscopy will be the more useful technique for initial detection and diagnosis.

Fluorine (^{19}F) is a component of various anti-cancer drugs, such as 5-fluorouracil. ^{19}F NMR has been used to study the metabolism of this drug in vivo in mice (Hull et al. 1986). Direct monitoring in vivo of patients undergoing chemotherapy with 5-fluorouracil is shown to be feasible as

a result of this work.

Hydrogen is the most sensitive nucleus for NMR study. Since most of the hydrogen in biological tissues is in the form of water (the water peak, in fact, drowns out other resonances in the NMR spectrum unless specific measures are taken to minimize its massive overlap), almost all the proton NMR of tissue to date has involved relaxation studies of the water resonance. Bottomley et al. have aided this author's literature search immensely by writing two thorough reviews of ^{1}H NMR relaxation studies of water, one for normal and the other for pathological tissue. Their findings, recommendations and conclusions will be summarized.

Longitudinal (T_1) and transverse (T_2) relaxation times (see Chapter 2) can be used to characterize the level of molecular organization in biological systems. Relaxation times are vital for NMR imaging where they are used to enhance the contrast between various tissues. They underlie the selection of timing parameters in imaging pulse sequences. Bottomley et al. (1984) have published an extensive review of the hundreds of investigations of T_1 and T_2 values for normal tissues since the late 1950's in order to establish the normal range of relaxation times for NMR imaging purposes, and also to examine their dependence on tissue type, NMR frequency, temperature, species, time after excision, and age of the donor.

No significant differences in T_1 and T_2 values were found between species and time after excision of samples. Age of the donor was often neglected in the studies, but a drastic elevation in relaxation times was universal for neonatal or immature tissue samples. The effect of temperature was examined between 0° and 40°C - at higher temperatures the physiological relevance is negated. An increase in T_1 was roughly linear with the reciprocal of absolute temperature (1/T). The hydrogen exchange process was cited as a relaxation mechanism for T_2, and as the exchange rate slowed with decreased temperature, the T_2 relaxation time became longer initially, but decreased with further decrease in temperature, as all molecular processes slowed.

T_1 relaxation values were found to be single component, and dependent on NMR frequency. The relationship

$$T_1 = Av^B$$

where v is the NMR frequency and A and B are tissue dependent constants, was found to hold for all data examined. The constant A ranged from 0.000455 for skeletal muscle to 0.0113 for adipose tissue. B was approximately equal to 1/3, ranging from 0.1743 for adipose tissue to 0.4203 for skeletal muscle. T_2 values were multicomponent, and independent of NMR frequency. Both T_1 and T_2 depended on tissue type.

Most publications failed to interpret the physical

mechanisms responsible for tissue relaxation. Many attempts were made to correlate relaxation with tissue water content. Bottomley et al. emphasize that relaxation times measure structure and motion at the molecular level, and thus depend on the organization and composition of the tissue, rather than on content alone. There is one basic tissue relaxation mechanism proposed for water, the fast exchange two state (FETS) model. This refers to rapid exchange, relative to the NMR time scale, between a large free-water compartment and a bound-water compartment, hydrogen-bonded to macromolecules or hydration layers. T_1 is determined by intermolecular interactions between macromolecules and a single bound hydration layer. On the T_1 time scale the free and bound states cannot be resolved, so a one component relaxation time is observed. T_2 is governed by exchange diffusion of water between a bound layer and the free-water phase. T_2 measures the low frequency and static components of molecular motion, and can discriminate between free and bound phases. The bound phase has a T_2 of about 5 ms whereas the free phase, with greater mobility, has a T_2 of approximately 40 ms. The T_2 is always less than T_1, owing to the exchange diffusion relaxation mechanism, which is tissue dependent, for T_2. A very short (20 us) T_2 component is attributable to rigid membrane or protein structures, whereas a very long (140ms) T_2 results from the highly mobile protons on fatty acids, which have no hydration

layer.

Bottomley et al. recommend testing tissue in as natural a state as possible, which points to in vivo examination. For the large scatter of relaxation times obtained in their overview of the literature, they cite the actual measurement of relaxation times as the variable open to most doubt, especially the two-point determination used in NMR imaging. The method used in examining tissue in its natural state has the least desirable measurement of relaxation times. As pointed out later in their review of pathological tissue (1987), however, NMR imaging does not rely on quantitative relaxation time measurements for generating image intensities but rather uses the NMR signal amplitude from the pulse sequences used. Aside from its weakness in relaxation time measurement, important morphological information is obtained by imaging. The patient serves as his/her own control, supplying both normal and pathological tissue for study. Both studies by Bottomley et al. are slanted towards imaging as the preferred clinical modality of the future.

The review of pathological tissue relaxation times is impressive, having collected, collated and analyzed the abundant T_1 and T_2 values in the literature. The purpose of the undertaking is the same as for normal tissue, with one important addition : to determine the diagnostic value of T_1 and T_2 relaxation times for the water peak in the ^1H NMR

spectrum.

The observation by Damadian (1971) that the T_1 and T_2 values of excised cancerous rat tissue were twice that of normal or benign tissue initiated the studies of pathological tissue relaxation times, notably T_1's. In the ensuing literature, however, there was considerable overlap between cancerous and normal tissue, and tissues of other pathologies. Prospects for successful cancer diagnosis appeared doubtful. T_2 seemed more promising, and a malignancy index was established by Goldsmith, Koutcher and Damadian (1977) combining T_1 and T_2 measurements :

$$MI = \frac{T_1 \text{ sample}}{T_1} + \frac{T_2 \text{ sample}}{T_2}$$

where

$T_1 = T_1$ mean for normal tissue
$T_2 = T_2$ mean for normal tissue

This proved successful for differentiating 90-100% of tumour samples from normal samples, but there was significant overlap with other pathologies in studies of breast tissues and with benign tumour samples. Bottomley et al. suggest calling it a pathology index, rather than a malignancy index.

The literature abounded with conflicting results. Increases in sodium and potassium concentrations, water content, and T_1 and T_2 values were noted in both cancerous and normal tissue from a tumour-bearing host relative to normal autopsy tissue. Relaxation times were found to be proportional to the growth rate of tissue, and T_1 was

elevated in regenerating rat liver following partial hepatectomy, but the same increase was also produced by trauma in sham-operated rats.

In pathological tissue studies, as in studies of normal tissues, T_1 was found to increase with increasing frequency. A maximum in tissue contrast, i.e. (T_1 tumour - T_1 normal)/T_1 normal, was found at 10 MHz, and this frequency value is therefore suggested for whole-body imaging. T_2 was frequency independent for 1-100 MHz.

Several mechanisms for relaxation are cited, with a view to explaining the differences observed for normal and pathological tissue. Paramagnetic ions could cause differences in tissue water relaxation if they are bound to macromolecules or membranes in normal tissue and unbound in tumours. The correlation of tissue water content with relaxation time measurements was often conflicting, and water content is therefore ruled out as the determining factor for T_1 and T_2 values. As for normal tissue, the favoured explanation is the FETS model of water-macromolecular interactions.

The chief sources of data scatter in T_1 and T_2 values are inherent tissue heterogeneity, NMR measurement techniques arising from static or radiofrequency field inhomogeneity and 2-point sampling in imaging, and the existence of multiple component relaxation times whereas usually only one value is reported. Bottomley et al. state

that the lack of information on multiple component relaxation implies that multiple components are rarely observed in pathological tissue and hence do not significantly affect data scatter. Multiple components for T_2's are indicated in normal tissue studies, however, so the existence of pathological multiple T_2 components cannot be dismissed. Due to all these uncertainties in relaxation data (whether inherent or systematic) their diagnostic value is questionable. In general, the mean pathological tissue relaxation time is greater than that for normal tissue. But because of the large data scatter, resulting in overlap and lack of specificity of T_1's and T_2's, Bottomley et al. conclude that quantitative T_1 and T_2 measurements alone cannot at present be confidently used for diagnosis based on differences between normal and pathological tissue. The one exception is liver hepatoma, which can be reliably discriminated from normal liver tissue with one T_1 measurement. The authors soften the blow by stating that since the scatter in data is the cause, the problem may be overcome by the establishment of guidelines for reproducible measurement of tissue NMR relaxation.

The foregoing discussion and conclusion, i.e. the lack of diagnostic reliability of T_1 and T_2, relates to the water peak only, overwhelming though it may be, in the ^1H NMR spectrum.

In 1973 Block and Maxwell claimed to be the first to

Figure 1-3. Study of the upfield region in the ^1H NMR spectrum of EL-4 tumor and normal spleen cells in mouse.

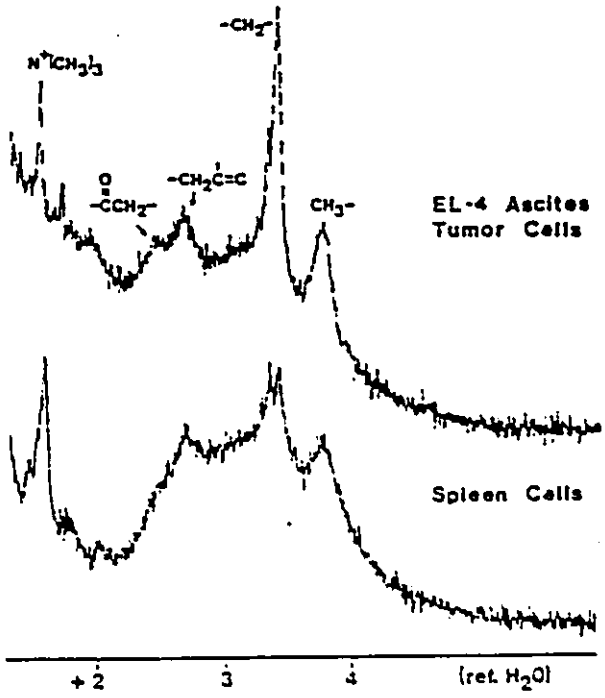

EL-4 Membrane

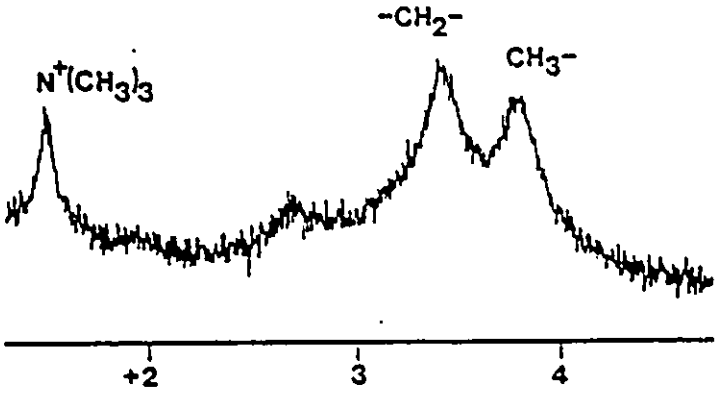

Spectra were obtained by a Varian HA-100D-15 spectrometer operating at 100 MHz.

from Block,R.E. and Maxwell,G.P.(1974)In: Membrane Transformations in Neoplasia (Academic Press)

report NMR studies of membranes from tumour cells. They used normal spleen cells and EL-4 tumour cells from mouse, and made their observations on peaks attributable to lipids. It had been shown earlier in an egg lecithin model system and sarcoplasmic reticulum membranes that only about 20% of the lipid chain protons have sufficient mobility to give rise to a high resolution spectrum of approximately 20 Hz which is superimposed on a broad spectral contribution with linewidth of about 500 Hz from lipid chains with very restricted mobility. Block and Maxwell note that the tumour cell resonances are much sharper and better resolved than those in the spleen cell spectrum (see Fig.1-3). A similarity between the spectra of intact cancer cells and isolated plasma membrane preparations was apparent, suggesting that at least part of the lipid signals originate from the plasma membrane. Phenomena which are known to involve cell surface components would affect resonances arising from plasma membrane components. Concanavalin A (Con A) treated EL-4 cells showed differential broadening of the methylene (CH_2) peak as compared to the N-trimethyl ($N^+(CH_3)_3$) peak. This was attributed to decreased mobility of the lipid chains resulting from the Con A treatment, a substance known to interact with cell surface sites. Today more detail is known about Con A, namely that it binds with carbohydrate chains containing certain sugar residues. The binding of the lectin would slow the overall motion of the

lipids containing the chains.

Four years later Block et al. (1977) studied NMR spectral characteristics of water, lipid and protein signals from normal mouse spleen, EL-4 ascites tumour cells and normal mouse erythrocytes. The major non-water resonances of the spleen and leukocyte cells resembled those of lipid extracts (as shown in 1973) whereas those of the red blood cells resembled resonances from hemoglobin solutions (i.e. a broad protein spectrum). The investigators seem mainly interested in water proton relaxation times and its correlation with total sample water content (later proved to be inconclusive diagnostically in Bottomley et al.'s extensive review). Of relevance to this thesis, however, is their observation that small, but observable non-water proton signals exist, and of paramount importance, that "the non-water PMR (Proton Magnetic Resonance) signals from tissues might reflect some pathological changes in the tissues".

In the original fluid mosaic model by Singer and Nicholson (1972), the lipids are relegated to the role of structural support for the more dynamic members of the membrane, the proteins. Upon NMR analysis, however, the proteins appear to be the more stationary components, yielding very broad lines from relatively rigid molecules, whereas mobile lipid molecules yield narrow resonances, indicating much greater ranges of motion. With the

Figure 1-4. Changes in normal human peripheral B lymphocytes upon transformation - a ^1H NMR study.

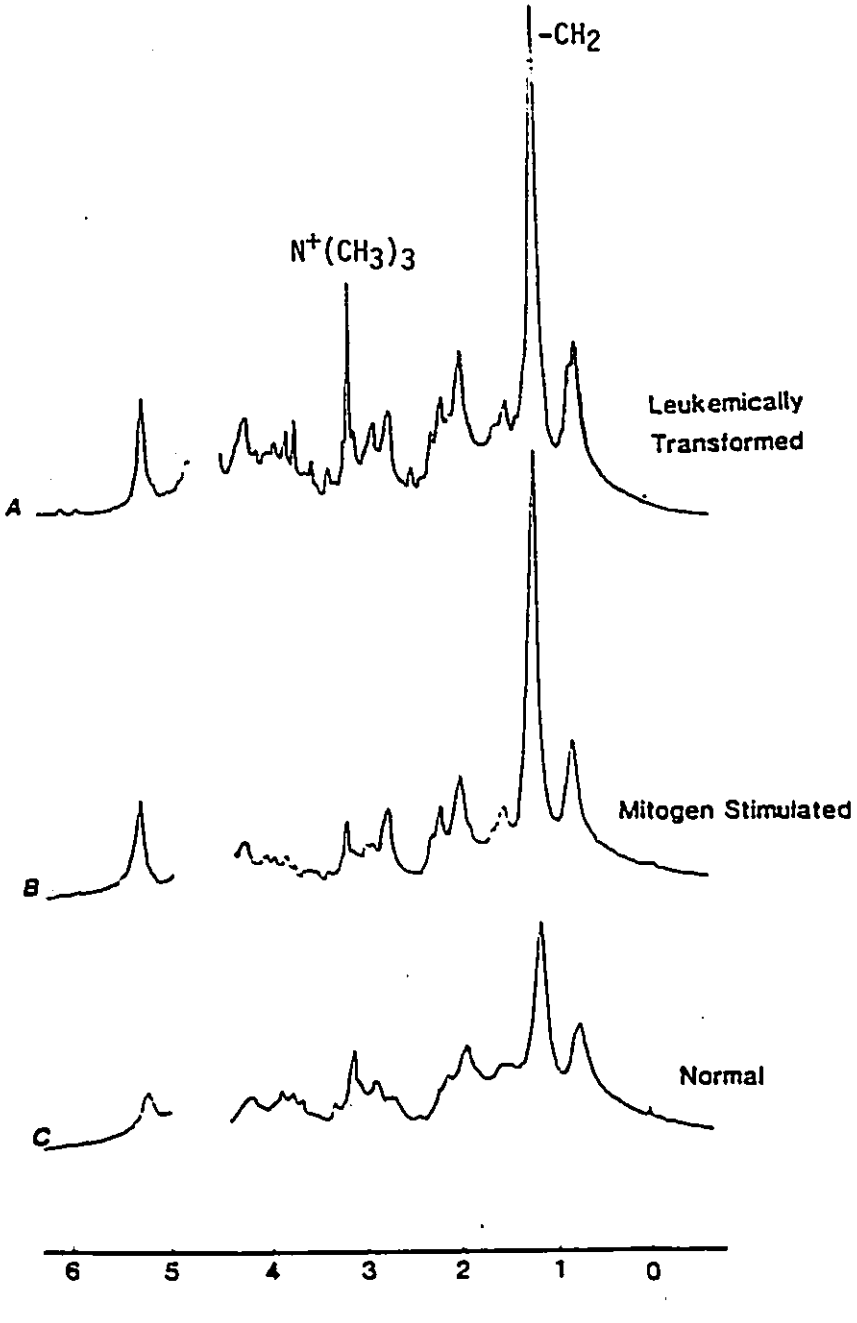

Spectra recorded at 37°C on a Bruker WM-400 MHz spectrometer. Cells ($5x10^7$ - $1x10^8$) suspended in PBS/D_2O.
A - ALL (acute lymphoblastic leukemia) B-cell line BALM
B - normal peripheral blood B lymphocytes after exposure to pokeweed mitogen (PWM) for five days
C - normal peripheral blood B lymphocytes

from Mountford, C.E. et al.(1982) Cancer Res. Vol.42:2270-6.

discovery of the phosphatidylinositol (PI) cycle in membranes, a signalling process for the cell, the role of the lipid bilayer as more than a structural scaffolding was confirmed.

Block et al. resumed their studies of the water signal, and Mountford et al. took up the lipid challenge.

Mountford et al. (1982) characterized transformed cells and tumours by ^1H NMR, observing the lipid region of the spectrum. They found that the spectral differences reflected the stage of differentiation and type of transformation of the cells, with the spectra themselves reflecting the molecular motions of the membrane. Upon stimulation of B lymphocytes with pokeweed mitogen (PWM), the intensity of the CH_2 peak increased (see Fig.1-4). In leukemic B cells, the intensities of both the CH_2 and $N^+(CH_3)_3$ (choline) peaks increased. The spectra of T lymphocytes were lumpier (not as well resolved) than those of the B cells, but upon transformation by PWM and in leukemic T cells, the changes were similar to those of B cells. With transformation, all the peak linewidths narrowed, but most notably those of the $N^+(CH_3)_3$ and CH_2 peaks. They isolated the plasma membranes of the EBV cell line and found that the spectrum was similar to the whole cell spectrum, suggesting, as in the experiments of Block et al., that the lipid resonances arose from the plasma membrane. Mountford et al. showed that the signal was indeed

localized to the plasma membrane by radioisotope labelling and NMR spectral broadening experiments using gadolinium (Gd^{3+}) and manganese (Mn^{2+}) ions. ^{54}Mn was found both inside and outside the cells, while ^{153}Gd was localized almost exclusively to the plasma membrane. Gd^{3+} affected mostly the choline resonance (a phospholipid head group on the cell surface) and the methylene peak also whereas Mn^{2+} broadened all resonances non-selectively. In 1984 Mountford et al. published a ^{1}H NMR study of two rat mammary adenocarcinoma cell lines, one metastatic (13762), and the other malignant but non-metastatic (J-clone). The metastatic cell line had an increased cholesterol/phospholipid ratio, and much increased plasma-membrane-bound cholesterol ester, as well as slightly increased triglycerides, as compared to the non-metastatic cell line. The role of the plasma membrane in metastasis was addressed. Poste and Nicolson (1980) had successfully transferred metastatic potential to previously non-metastatic cells via transfer of plasma membrane vesicles. They proposed that membrane-bound proteins were the source of metastatic potential. Mountford et al., on the other hand, proposed that lipid molecules were the key - by altering phase transition properties of the membrane, membrane-bound proteins were activated. Transverse relaxation times (T_2's) were obtained for the methylene peak of both cell lines. The non-metastatic J-clone cells yielded a 2-component T_2 profile with the

Figure 1-5. Resolution enhancement of resonances under the methylene (CH_2) peak of two rat mammary adenocarcinoma cell lines.

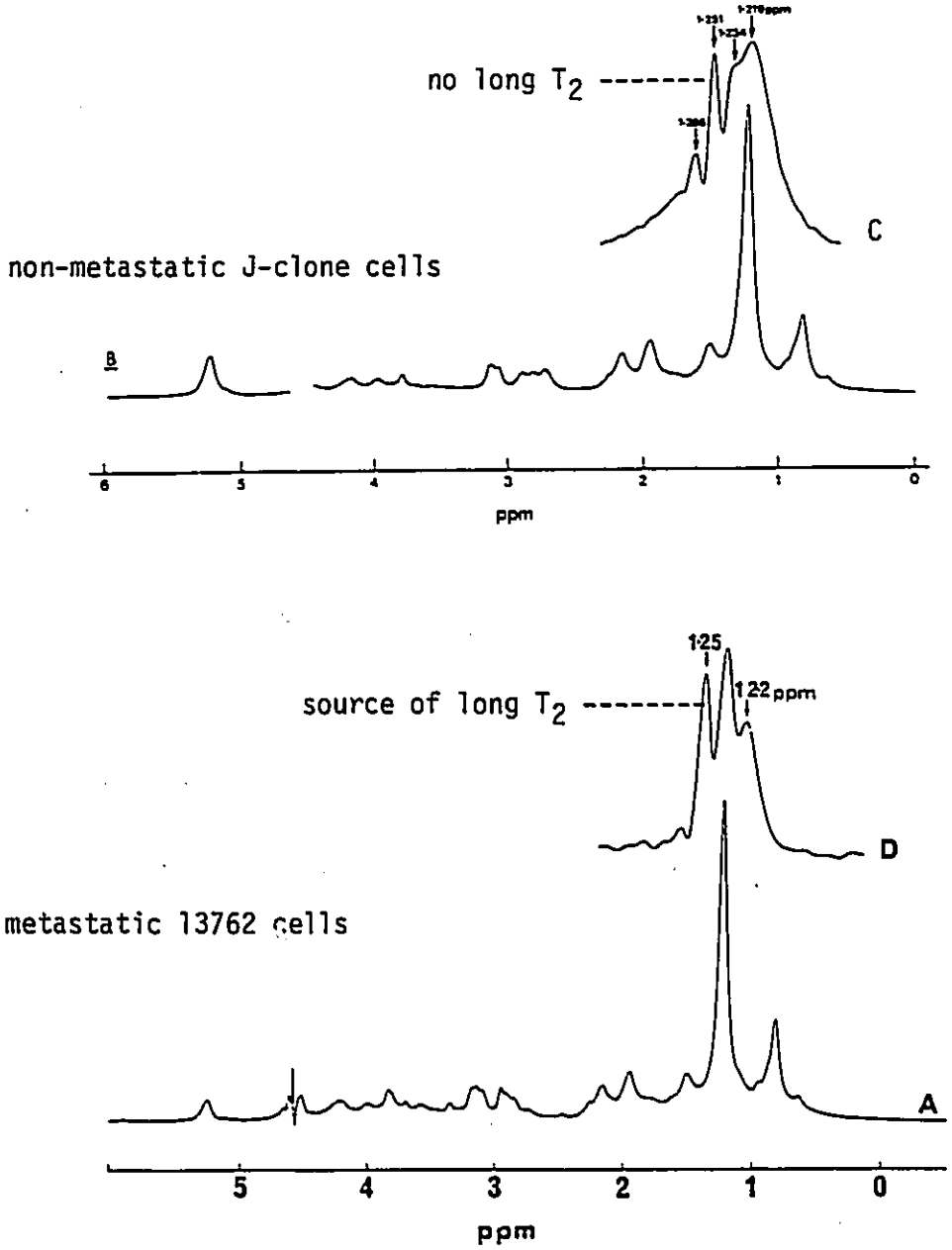

A and B are 400 MHz spectra of $1x10^8$ cells suspended in PBS/D_2O. The free induction decay was multiplied by an exponential function before Fourier transformation to resolve the resonances (C and D).

from Mountford, C.E. et al.(1986b)In: Progress in Clinical Biochemistry and Medicine Vol.3 (Springer-Verlag) pp 73-112.

longest T_2 value in the lipid range (154 ms), while the metastatic 13762 cells had a 3-component T_2 decay, with a very long T_2 value (772 ms) for the third component. The CH_2 peak is a composite peak made up of many resonances, some from different fatty acyl chain compositions. Upon resolution enhancement, whereby the methylene peak is decomposed or deconvoluted into several separate resonances, it was found that one particular resonance (at 1.25 ppm) gave rise to the long T_2 value (see Fig.1-5). In a mixture of the two cell types, a 20% composition of the 13762 cells was detectable by NMR via the 3-component profile containing the long T_2 value. The long T_2 is attributed to the increase in cholesterol ester in the plasma membrane. Triglycerides with a small amount of free cholesterol are deemed responsible for small, mobile membrane domains giving rise to the high resolution NMR signal. The presence of triglycerides and cholesterol esters in the plasma membrane was considered unusual. In lipoprotein studies it had been found that in the presence of triglyceride, cholesterol esters change from the cholesteric to the smectic phase. In other words, smaller membrane domains of various orientations are unified into a larger domain with one orientation, a more uniform membrane profile. The phase behaviour of cholesterol esters is influenced by their fatty acid composition. Thus, Mountford et al. proposed, an increase in cholesterol esters or alterations in their fatty

acid chains could change the phase transition of the small membrane domains, which would in turn affect the activation of membrane-bound proteins and enzymes, as well as the permeability and overall stability of the membrane.

Mountford et al. (1984b) next investigated membranes by 2-dimensional NMR, the COSY experiment. This experiment indicates coupling between adjacent protons by the presence of cross peaks at the intersection of the chemical shifts of the protons concerned, and will be explained in Chapters 2 and 5. The 2-D spectrum of the J-clone cells is comparable to that from phospholipid, i.e. arising from lipid acyl chain protons. They show the feasibility of 2-D studies on cells and possibly excised tissue, provided that the sample is in a metabolically steady state, and its T_2 relaxation is sufficiently slow. The COSY experiment takes longer than a simple T_2 experiment, and if the sample relaxation time is too fast, the NMR signal is lost.

The similarity of the cancer cell plasma membrane to the four major classes of lipoproteins (chylomicrons, VLDL, LDL, and HDL) are next explored (Williams et al. 1985). It had been shown that many cancer patients had elevated levels of VLDL (Dilman et al. 1981). The spectra of chylomicrons and VLDL are found to be similar to those of cancer cells - none exhibit diffusive exchange, as shown by selective and non-selective T_1 experiments (in the presence of diffusive exchange, the T_1 values in the two experiments would

Figure 1-6. ^{1}H NMR 2-D COSY study showing similarity between J-clone cells and chylomicra and VLDL in their 2-D spectra.

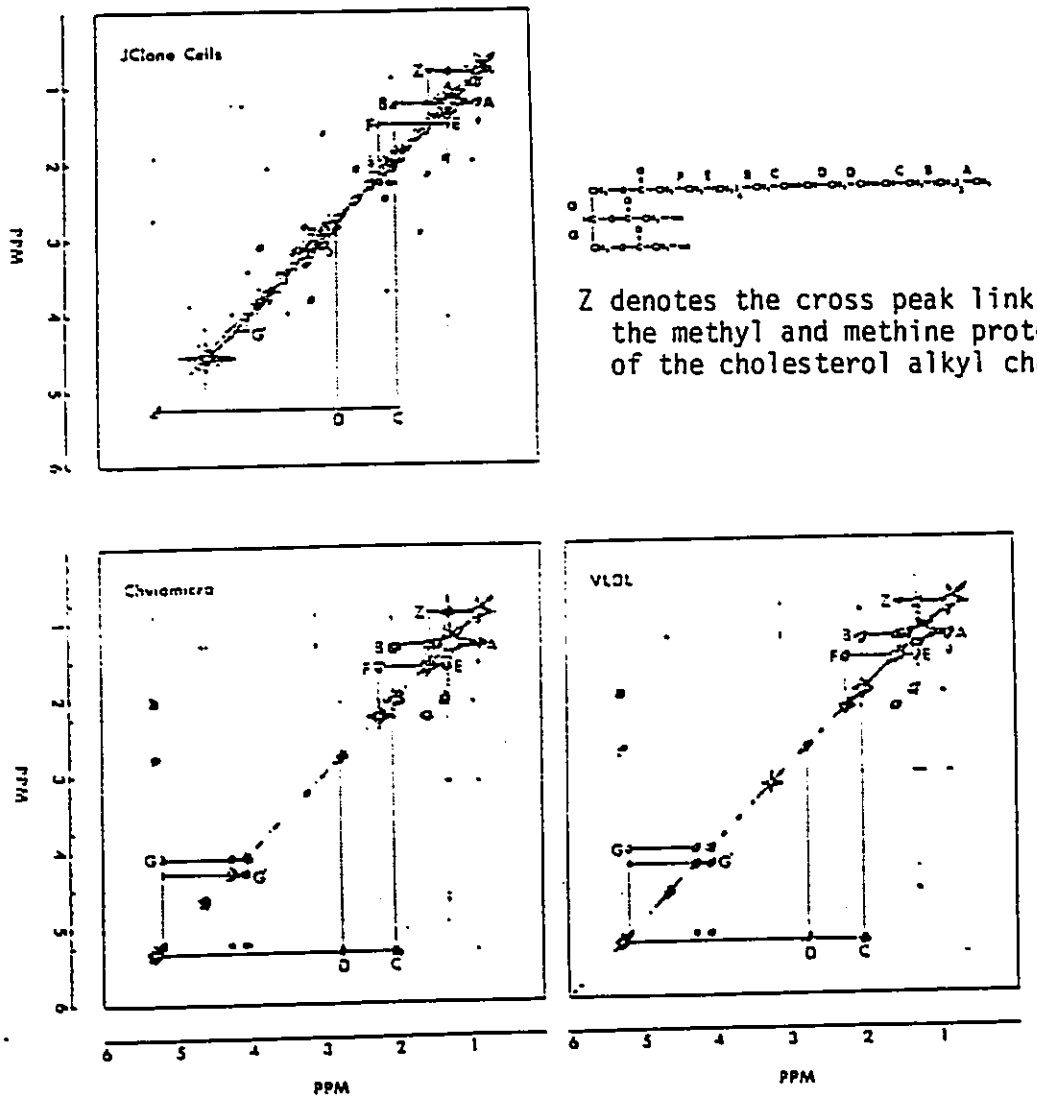

Z denotes the cross peak linking the methyl and methine protons of the cholesterol alkyl chain

Symmetrised COSY spectra were recorded at 37°C with a Bruker WM-400 MHz spectrometer.

from Williams, P.G. et al.(1985) FEBS Lett. Vol.192 No.1 Nov. pp 159-64.

differ). In the 2-D COSY spectra also, chylomicrons and VLDL are similar to cancer cells and tumours (see Fig.1-6). All three contain cross peaks specific to triglycerides. In contrast to the cancer samples, however, no lipoprotein class had a T_2 value exceeding 250 ms.

The source of the CH_2 peak in embryonic and transformed cells is subsequently narrowed down to plasma membrane triglycerides, the major component of VLDL (May et al. 1986). To summarize, the source of the CH_2 peak is from lipids, in or attached to the plasma membrane, which tumble isotropically and are in domains not in diffusive exchange with other lipids in the membrane (i.e. the mobile domains retain their integrity). The 2-D spectrum of the 13762 cells is similar to that of VLDL and cellular metabolites. Since the neutral lipid domain in the plasma membrane appears to be from lipoprotein, it is suggested that protein conformational changes may account for the long T_2 value observed in the metastatic 13762 cells. It seems highly unlikely, however, that a large protein molecule embedded in the lipid monolayer coat of a lipoprotein would possess the mobility necessary to yield a long T_2 value.

"High Resolution Proton NMR Detects Metastatic Potential" (Mountford et al. 1986a) heralded the entry of this thesis study. There was currently no method available to determine if a malignant tumour had the capacity to metastasize. All patients operated on for malignant growths

were subsequently given chemo- and/or radiotherapy, just in case. T_2 values had been successful in the rat model system as an indicator of metastasis. A clinical study was needed to correlate the T_2 values of biopsy samples with patient follow-up data. With cooperation from the Pathology Department of the Ottawa Civic Hospital, the active collaboration of the Molecular Biophysics group at the National Research Council under the direction of Dr. Ian C.P. Smith with the group at the Ludwig Cancer Institute under the direction of Dr. C.E. Mountford came into being. This thesis project began in May 1985. If metastatic potential could be reliably diagnosed, many patients could be spared the unnecessary trauma of further therapy. Thus our study was undertaken partly for humanitarian reasons. From a scientific basis, it was also a good opportunity to test further the applicability of NMR, a physical tool, to the study of biomedical problems. The lipid region of the ^1H NMR spectrum had not been investigated before in an extensive clinical study. This was a study to be performed in vitro, but if successful, in vivo investigation could possibly follow to exploit the true power of NMR - non-invasive study.

From this point onwards, the two teams worked in tandem. Animal and tissue culture studies, and the bulk of traditional biochemical work, such as lipid analysis, was performed by the Australians, whereas the work with human

tumour biopsies, notably NMR analysis, was our contribution.

After a brief explanation of NMR and relaxation times, this thesis will present the results of all the investigations carried out on human tumour biopsy and placenta samples.

References :

Bottomley,P.A., Foster,T.H., Argersinger,R.E. and Pfeifer,L.M. (1984) A review of normal tissue hydrogen NMR relaxation times and relaxation mechanisms from 1-100 MHz: Dependence on tissue type, NMR frequency, temperature, species, excision, and age. Med. Phys. 11(4), Jul/Aug.:425-48.

Bottomley,P.A., Hardy,C.J., Argersinger,R.E. and Allen-Moore,G. (1987) A Review of ^{1}H NMR Relaxation in Pathology : Are T_1 and T_2 Diagnostic? Med. Phys. 14(1) Jan./Feb.

Block,R.E. and Maxwell,G.P. (1974) Nuclear Magnetic Resonance Studies of Membranes of Normal and Cancer Cells. In: Membrane Transformations in Neoplasia (Schultz,J. and Block,R.E. Eds.) Proceedings of the Miami Winter Symposis, Jan. 17-18, 1974, Vol. B.:253-74.

Block,R.E., Maxwell,G.P., Prudhomme,D.L. and Hudson,J.L. (1977) High Resolution Proton Magnetic Resonance Spectral Characteristics of Water, Lipid, and Protein Signals From Three Mouse Cell Populations. J. Natl. Cancer Inst. Vol.58 No.1 Jan.:151-6.

Cross,K.J., Holmes,K.T., Mountford,C.E. and Wright,P.E. (1984) Assignment of Acyl Chain Resonances from Membranes of Mammelian Cells by Two-Dimensional NMR Methods. Biochem. Vol.23 No.25 Dec.4:5895-7.

Damadian,R. (1971) Tumor Detection by Nuclear Magnetic Resonance. Science 171 : 1151-3.

Dilman,V.M., Berstein,L.M., Ostroumova,M.N., Tsyrlina,Y.V. and Golubev,A.G. (1981) Peculiarities of Hyperlipidaemia in Tumour Patients. Br. J. Cancer 43:637-43.

Evanochko,W.T., Ng,T.C. and Glickson,J.D. (1984) Application of in Vivo NMR Spectroscopy to Cancer. Mag. Res. in Med. 1,

508-34.

Goldsmith,M., Koutcher,J.A. and Damadian,R. (1977) Nuclear Magnetic Resonance in Cancer,XII:Application of NMR Malignancy Index to Human Lung Tumours. Br. J. Cancer 36:235-42.

Griffiths,J.R., Cady,E., Edwards,R.H.T.,McCready,V.R., Wilkie,D.R. and Wiltshaw,E. (1983) ^{31}P NMR Studies of a Human Tumour in Situ. The Lancet, June 25:1435-6.

Hull,W.E., Port,R., Osswald,H. and Kunz,W. (1986) In-vivo ^{19}F-NMR Study of 5-Fluorouracil Metabolism in Liver and Implanted Tumors of the Mouse. Fifth Annual Meeting of Society of Magnetic Resonance in Medicine, Aug.19-22, 1986, Montreal, Quebec, Canada. Vol.3:594-5.

Maris,J.M., Evans,A.E., McLaughlin,A.C.,D'Angio,G.J., Bolinger,L., Manos,H. and Chance,B. (1985) ^{31}P Nuclear Magnetic Resonance Spectroscopic Investigation of Human Neuroblastoma in Situ. The New England J. Med. Vol.312 No.23:1500-05.

May,G.L., Wright,L.C., Holmes,K.T., Williams, P.G., Smith,I.C.P., Wright,P.E., Fox,R.M. and Mountford,C.E. (1986) Assignment of Methylene Proton Resonances in NMR Spectra of Embryonic and Transformed Cells to Plasma Membrane Triglyceride. J. Biol. Chem. Vol.261 No.7 Mar.5:3048-53.

Mountford,C.E., Grossman,G., Reid,G. and Fox,R.M. (1982) Characterization of Transformed Cells and Tumors by Proton Nuclear Magnetic Resonance Spectroscopy. Cancer Res. Vol.42:2270-6.

Mountford,C.E., Wright,L.C., Holmes,K.T., Mackinnon, W.B., Gregory,P. and Fox, R.M. (1984) High Resolution Proton Nuclear Magnetic Resonance Analysis of Metastatic Cancer Cells. Science Vol.226 Dec.21:1415-8.

Mountford,C.E., Holmes,K.T., Wright,L.C., May,G.L., Williams, P.G. and Smith,I.C.P. (1986a) High Resolution Proton NMR Detects Metastatic Potential. Mag. Res. in Cancer; International Conference, Banff, Alberta, Canada, Apr.30-May 4, 1985. Pergamon Press Inc. pp.111-8.

Mountford,C.E., Holmes,K.T. and Smith,I.C.P. (1986b) NMR Analysis of Cancer Cells. In: Progress in Clinical Biochemistry and Medicine, Vol.3 Springer-Verlag Berlin Heidelberg 1986. pp.73-112.

Mountford,C.E. and Tattersall,M.H.N. (1986) Proton Magnetic

Resonance Spectroscopy and Tumour Detection. Cancer Surveys Dec. 1986.

Ng,T.C., Evanochko,W.T., Hiramoto,R.N., Ghanta,V.K., Lilly,M.B., Lawson,A.J., Corbett,T.H., Durant,J.R. and Glickson,J.D. (1982) ^{31}P NMR Spectroscopy of in Vivo Tumors. J. Mag. Res. 49, 271-86.

Poste,G. and Nicolson,G.L. (1980) Arrest and metastasis of blood-borne tumor cells are modified by fusion of plasma membrane vesicles from highly metastatic cells. Proc.Natl.Acad.Sci.USA Vol.77 No.1: 399-403.

Ross,B., Marshall,V., Smith,M., Bartlett,S. and Freeman,D. (1984) Monitoring Response to Chemotherapy of Intact Human Tumours by ^{31}P Nuclear Magnetic Resonance. The Lancet Mar.24 :641-6.

Williams,P.G., Helmer,M.A., Wright,L.C., Dyne,M., Fox,R.M., Holmes,K.T., May,G.L. and Mountford,C.E. (1985) Lipid domain in cancer cell plasma membrane shown by ^{1}H NMR to be similar to a lipoprotein. FEBS Letters Vol.192 No.1 Nov.:159-64.

CHAPTER 2

NMR AND RELAXATION TIMES

Nuclear Magnetic Resonance (NMR) is the spectroscopic tool we have employed to gain information about tumour biopsy samples in order to discern what makes tumours different from normal tissue. NMR uses energy in the radiofrequency (rf) range, the megaherz (MHz) range, which corresponds to wavelengths of 1 to 5 metres, just longer than those of microwaves. Compared to other spectroscopic methods, NMR thus uses relatively low frequencies, and hence energies (energy being proportional to frequency), to cause nuclear spin transitions. As mentioned in the Introduction to this thesis, its greatest advantage is its non-invasiveness. With a superconducting magnet providing a high field and an adequate amount of sample to compensate for its relative insensitivity, NMR can provide a great amount of information. Let us now examine the basis of the NMR phenomenon.

All charged particles possess an electric field, and because of their motion, an induced magnetic field. Atoms with an odd mass or odd atomic number have a net magnetic moment or "spin", and angular momentum associated with their nuclei. When placed in a static magnetic field, the nuclear spins, by the principles of quantum mechanics, are allowed to take 2I+1 orientations with respect to the field, where I is the spin quantum number. For hydrogen nuclei, with I=1/2,

the spins can exist in two states : one parallel to, or aligned with, the magnetic field, the +1/2 α state, and the other antiparallel, or aligned against, the field, the -1/2 β state. The spins aligned antiparallel have a higher energy state. The separation of the two states in terms of energy is proportional to the strength of the magnetic field H_0 :

$$\begin{aligned} \Delta E &= h\nu \\ &= \hbar w \\ &= \hbar \gamma H_0 \end{aligned}$$

where

- ΔE is the energy difference between the two spin states
- h is Planck's constant $\hbar = h/2\pi$
- ν is frequency
- w is angular frequency ($2\pi\nu$)
- γ is the gyromagnetic ratio, specific for a certain nucleus, and is the constant of proportionality between the magnetic moment of a nucleus and its angular momentum ($\mu = \gamma \hbar I$)
- H_0 is the magnetic field strength

The distribution of the spins into the two populations α and β is given by the Boltzmann distribution :

$$\begin{aligned} \frac{n_\alpha}{n_\beta} &= e^{(\Delta E/kT)} \\ &= e^{(\hbar \gamma H_0/kT)} \\ &= 1 + \hbar \gamma H_0/kT \end{aligned}$$

where

- n_α is the number of spins in the α state
- n_β " " " " " " " β "
- k is Boltzmann's constant
- T is the absolute temperature

At room temperature, the population difference between the two states is small, differing from unity by only 10^{-5} or

Figure 2-1. Precession of the nuclear magnetic moment about a static magnetic field.

Abbreviations :

μ - nuclear magnetic moment
H_o - static magnetic field
θ - angle between u and H
H_1 - small magnetic field rotating about H_o

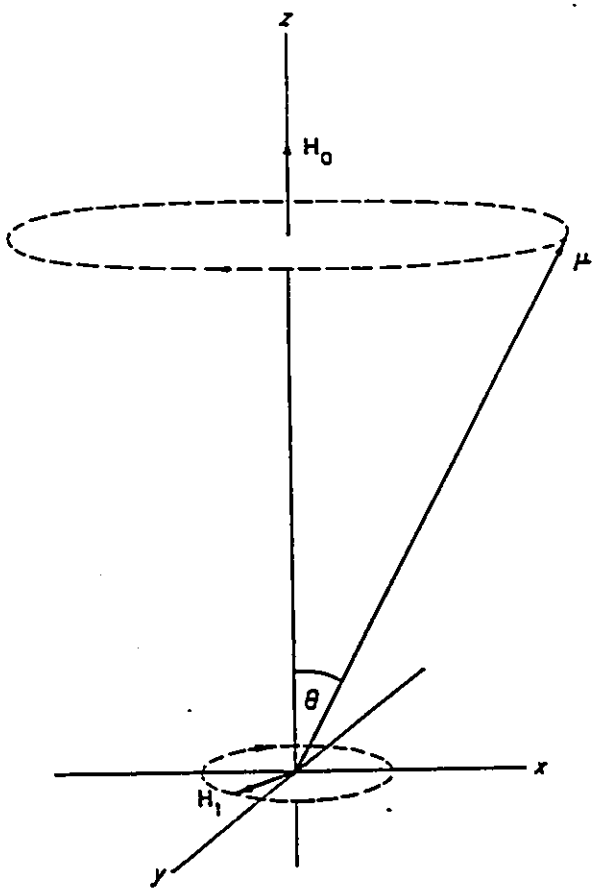

The magnetic interaction between μ and H_o generates a torque which causes the precession of μ about H_o. Energy is absorbed from H_1 into the spin system in a resonance phenomenon with the natural nuclear precession frequency.

from Becker, E.D. High Resolution NMR Theory and Chemical Applications (Academic Press Inc. N.Y. 1969)

10^{-6}, yet this difference is sufficient for the nuclei to provide a net magnetization.

The interaction between a magnetic field H_0 and the magnetic moments of the nuclei generates torque which, because of the angular momenta of the nuclei, causes them to precess around the magnetic field (see Fig.2-1), just as a spinning top precesses around the earth's gravitational field. The frequency of precession is proportional to the magnetic field and depends on the gyromagnetic ratio of the nucleus :

$$w_L = \gamma H_0$$

This is called the Larmor equation with w_L being the Larmor frequency.

If all the hydrogen nuclei in a sample experienced the same magnetic field, they would all precess at the Larmor frequency. We would then obtain one spectral line for the sample, which would be relatively uninformative. Because of the differences in their chemical environments, however, the various hydrogen nuclei experience slightly different net magnetic fields. The valence electrons of nuclei near the hydrogen atom in question (as well as its own valence electron) have their own magnetic fields (because they are moving charged particles), and the presence of these neighbouring fields influences the magnetic field actually "felt" by the hydrogen nucleus. For example, a relatively large electron cloud "shields" the nucleus, causing it to

resonate at a higher magnetic field value, while a neighbouring strongly electronegative nucleus (oxygen e.g.) "deshields" the nucleus by pulling the electron cloud to itself, leaving the hydrogen nucleus relatively bare of electrons and causing it to resonate at a lower magnetic field strength. Because of these shielding and deshielding effects, the frequency of precession of hydrogen nuclei in different molecular configurations varies from that of the Larmor frequency. This results in the chemical shift (δ) of the hydrogen nuclei, given in terms of parts per million (ppm) from a reference compound, tetramethylsilane (TMS). The chemical shift values of other protons are downfield from the very shielded methyl protons of TMS (δ=0), with δ ranging to 12 ppm. The term ppm came about in order to compare results from one spectrometer to another, since the term, by definition, is independent of magnetic field strength. The shift in Hz from TMS for a proton depends on magnetic field strength, but the ratio of this shift in Hz to the spectrometer operating frequency in MHz is a constant. Because of their different chemical shifts, one can differentiate between protons in different chemical environments. For example, the chemical shift of protons in CH_2 groups from lipid acyl chains occurs at 1.3 ppm, that of their terminal CH_3 groups at 0.9 ppm and that of $N^+(CH_3)_3$ groups from the choline head group of phospholipids at 3.25 ppm. These ppm values are constant for the respective

entities regardless of the spectrometer used to obtain the spectrum.

Spin-spin interactions also influence the net magnetic field felt by a proton. These occur because of the bonding of atoms through their electron orbitals. Information about the spin of one nucleus (A) is transmitted to another nucleus (B) via their bonding electrons - the nuclei are said to be coupled to each other (they can "talk" to each other). If the spins of the two nuclei are antiparallel, the energy of transition of A will be slightly lower than in the absence of B, whereas if the spins are parallel, the energy state of A will be slightly higher. Since there is equal probability for the two states, there is a splitting of A's energy level into two, and two spectral lines will result instead of the one that would be present if B had no influence on A. The situation is reciprocal, and there will also be two energy levels for B. The difference in frequency of the two spectral lines, measured in Hz and termed the coupling constant J, is proportional to the energy of interaction between A and B. This energy depends on their molecular orientation, and not on the strength of the external magnetic field. For protons the coupling constant J is in the range of 0 to 20 Hz. J is the same for nucleus A and B. By measuring the splitting in Hz of spectral lines, it can be determined which protons are coupled to one another. This is of relevance to our 2-D NMR COSY

experiments (see Chapter 5) which show the coupling between adjacent protons to a distance of 2 to 3 bonds. Spin-spin interactions both in 1-D and 2-D spectra can be used to elucidate the molecular structure of the compound under examination.

The energy levels of the spin states thus reflect the net magnetic field felt by the nucleus. It is the difference in population of the two spin states allowed for each proton that gives rise to a net longitudinal magnetization M_Z in the direction of the field (corresponding to the lower energy levels). If energy is now supplied to the system in the form of electromagnetic radiation with magnetic field vector perpendicular to the static field, nuclei whose spin energy level separation matches that of the incoming wave's energy will absorb that energy - this matching of energy required with energy supplied is resonance - and transitions between the two spin states will be induced. This leads to an equalization in population of the two states, and $M_Z=0$. Meanwhile, the rf field causes the spins to precess in phase, resulting in a transverse magnetization $M_\perp$ in a plane perpendicular to the field H_0. This magnetization rotates in the x-y plane at the Larmor frequency and induces a detectable signal in a receiver coil oriented perpendicularly to the transmitter coil. This signal is a sinusoidal wave decaying exponentially in time, which is termed a free induction decay (FID). This signal is

Figure 2-2. Vectorial representation of an NMR experiment.

a - equilibrium state - nuclear spins distributed according to the Boltzmann distribution
- net magnetization (M_Z) in +z direction

b - resonance condition - population of spin energy levels equalized and spins precess in phase with Larmor frequency
- net magnetization ($M_\perp$) in x-y plane, $M_Z = 0$

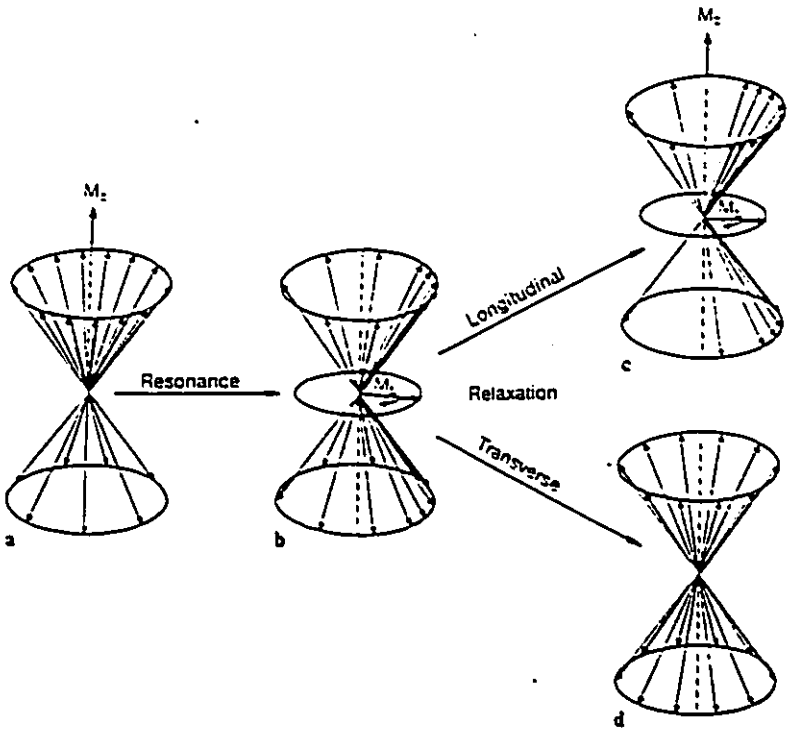

c - longitudinal relaxation restores equilibrium spin distribution
return of M_Z to original position

d - transverse relaxation - phase coherence of spins is lost
- $M_\perp = 0$

(c and d occur simultaneously)

from Paul, H.-H. et al.(1983) In: Biophysics (Springer-Verlag) pp 190-206.

amplified and digitized to be stored in the spectrometer's computer. The FID is then fourier transformed to yield the familiar NMR frequency spectrum.

When the rf field is shut off, two processes occur simultaneously, by means of which the nuclei rid themselves of their acquired excess energy in order to return to their previous equilibrium state. That is, the nuclei "relax" (see Fig.2-2). The first process involves the restoration of the longitudinal magnetization M_z by the excited spins giving up their energy to their surroundings, or lattice. The time for this to occur is called the longitudinal or spin-lattice relaxation time T_1. The second process involves the loss of phase coherence of the spins through various spin interactions as well as field inhomogeneity, which leads to different Larmor frequencies of individual spins. This transverse relaxation process leads to the net $M_\perp = 0$. The energy is transferred throughout the spin system, and is not lost to the surroundings. The time constant for this process is termed the transverse or spin-spin relaxation time T_2. It is the T_2 relaxation time that will concern us in this thesis.

There are various mechanisms by which nuclei can relax, nuclear magnetic dipole interactions being one of them. The magnetic dipole field associated with a magnetic nucleus fluctuates in magnitude and direction with motion of the molecule containing the nucleus. The effectiveness of this

Figure 2-3. The variation of T_1 and T_2 with correlation time τ_c.

T_1 - spin-lattice relaxation time

T_2 - spin-spin relaxation time

τ_c - correlation time, related to speed of molecular motion

ν_0 - Larmor frequency of nucleus (natural precession frequency)

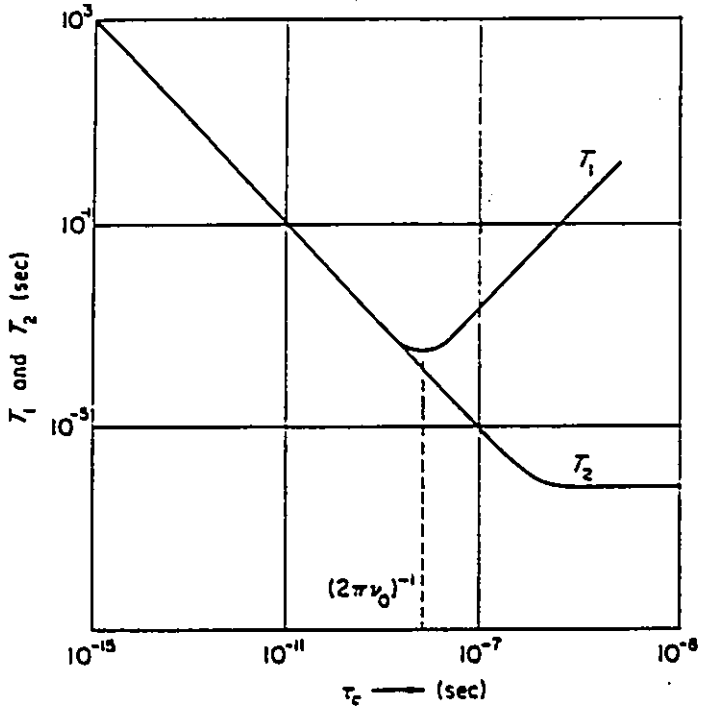

$\tau_c = \frac{1}{2\pi\nu_0}$ gives the most effective T_1 relaxation

$\tau_c \ll \frac{1}{2\pi\nu_0}$ is indicative of rapid molecular motion

$\tau_c \gg \frac{1}{2\pi\nu_0}$ arises from very slow motion

from Becker, E.D. High Resolution NMR Theory and Chemical Applications (Academic Press Inc. N.Y. 1969)

field in relaxing other nuclei depends on the magnitudes of the nuclear moments, the distance between the two nuclei, and the frequency distribution of the molecular motion. Protons have large magnetic moments and thus dipole-dipole interactions are an effective relaxation mechanism for these nuclei when they are a short distance apart. Only the components of motion at the Larmor frequency of the relaxing nucleus are able to receive its energy, again a resonance phenomenon. Molecular motion is related to the relaxation times T_1 and T_2 through a correlation time τ_c, which indicates the average time that two nuclei remain in a given relative orientation. For molecular rotation, related to intramolecular relaxation, it is the length of time that the molecule requires to rotate through a solid angle of one radian. For translation, related to intermolecular relaxation, the correlation time is the time it takes the molecule to move one molecular diameter. The variation of T_1 and T_2 with τ_c is shown in Fig.2-3. At $\tau_c = 1/2\pi\nu_0$ $(=1/w)$, the most effective spin-lattice relaxation is observed, with T_1 increasing for shorter or longer τ_c. At shorter τ_c $(<1/w)$, i.e. for rapid molecular motion, T_2 coincides with T_1, and at longer τ_c $(>1/w)$, i.e. for slow molecular motion, T_2 decreases drastically with respect to T_1. A long τ_c permits dipole-dipole interactions to lead to broad lines in the spectrum, and hence short T_2 values, since the linewidth at half-height is proportional to $1/\pi T_2$. The T_2 value thus

Figure 2-4. Measurement of T_1 relaxation time - the inversion recovery experiment.

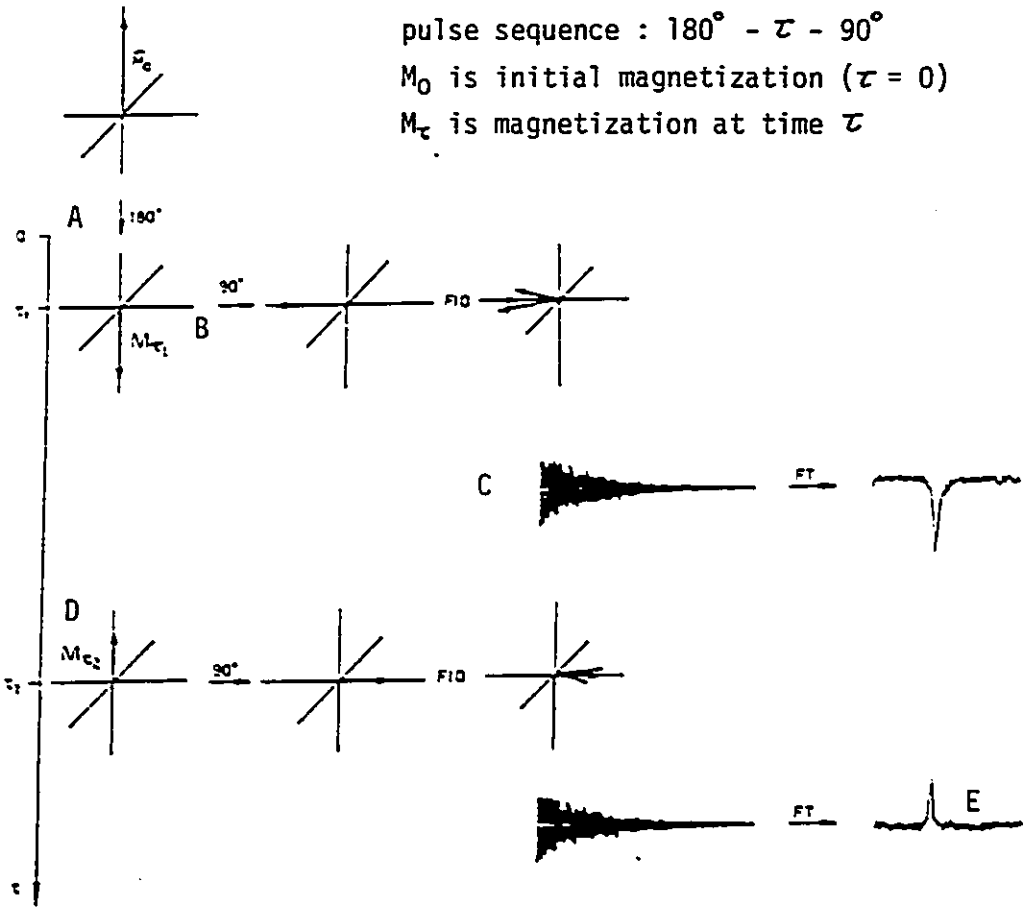

A - inversion of magnetization M_0 by a 180° pulse
B - after time τ_1, magnetization decays to M_{τ_1}, and a 90° pulse brings it into the x-y plane
C - free induction decay (FID) is recorded
D - sequence is repeated for τ_2
E - calculation of T_1 :

$$\frac{dM}{dt} = -\frac{M_0 - M_\tau}{T_1}$$

$$\ln (M_0 - M_\tau) - \ln 2M_0 = -1/T_1$$

$\ln(M_0 - M_\tau)$ is plotted vs. τ and the slope is $-1/T_1$

from Paul, H.-H. et al.(1983) In: Biophysics (Springer-Verlag) pp 190-206.

Figure 2-5. The Carr-Purcell-Meiboom-Gill (CPMG) pulse sequence for measurement of T_2 relaxation time.

A $90^\circ_x(\tau - 180^\circ_{\pm y} - \tau)_n$ - acquire pulse sequence is used.

The 180° pulses are phase shifted by 90° from the initial 90° pulse.

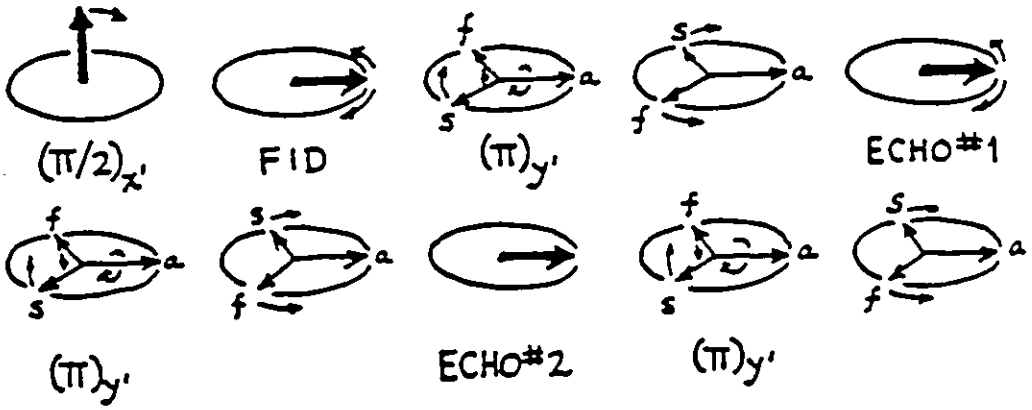

from Fukushima, E. and Roeder, S.B.W. Experimental Pulse NMR A Nuts and Bolts Approach (Addison-Wesley Publishing Co. Inc. 1981)

reflects the rate of molecular motion, and rapid molecular motion is required for a long T_2 value.

There are various methods for measuring relaxation times, utilizing various pulse sequences. These involve "gymnastics" with the net magnetization components M_z and $M_\perp$, represented as arrows or vectors in the accompanying diagrams. The most common method for T_1 determination is termed inversion recovery (see Fig.2-4). A 180° pulse flips the positive longitudinal magnetization into the negative z axis. A 90° pulse then tips the magnetization vector into the x-y plane, where a signal can be picked up in the receiver coil. By varying the time from the 180° pulse to the 90° pulse and acquisition, the relaxation of the M_z vector back to its original positive z axis value can be monitored, and the T_1 value for a certain peak calculated.

The Carr-Purcell-Meiboom-Gill (CPMG) pulse sequence (Meiboom and Gill 1958) is used to measure long T_2 relaxation times (see Fig.2-5). If a 90_x° pulse is used to tip the magnetization vector into the x-y plane, a signal is received in the receiver coil which decays with a time constant T_2^*, the "effective" relaxation time which is a result of T_2 as well as magnetic field inhomogeneity. The CPMG sequence removes the effects of magnetic field inhomogeneity by a $(\tau - 180_{\pm y}° - \tau)$ echo sequence following the initial 90_x° pulse. For a time τ = 1 ms, the spins are allowed to dephase. The 180° pulse causes the spins to

Figure 2-6. Complete proton NMR spectrum of rat mammary adenocarcinoma 13762 cells.

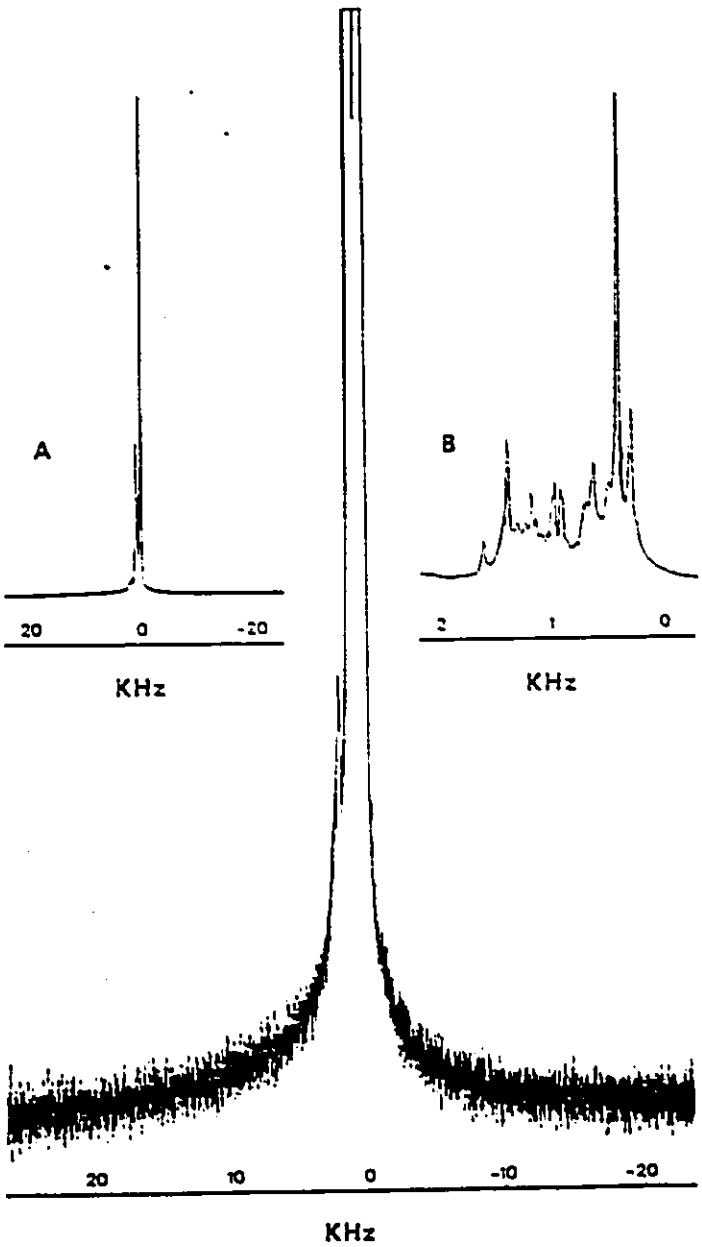

The spectrum ($1x10^8$ cells) was obtained at 37°C on a Bruker CXP-300 spectrometer. A - spectrum plotted with reduced gain. B - horizontal expansion of the central part of the spectrum.

from Bloom, M. et al.(1986) J. Mag. Res. 69: 73-91.

refocus after another time τ, by refocussing the effects of chemical shift. The echo sequence is repeated n times, and the whole process for several values of n. The 180° pulse, alternated in phase each time between the +y and -y direction, is thus applied at τ, 3τ, 5τ... and FID's are acquired at 2τ, 4τ, 6τ... intervals, from the trailing edge of the n^{th} echo. By alternating the phase of the 180° refocussing pulse, the effects due to field inhomogeneity cancel. Since the signal is now decaying under the influence of T_2 only, monitoring the decay in intensity of a certain peak in the spectrum with increasing time before acquisition will yield the T_2 value. The actual calculation process will be further explained in Chapter 3.

We have measured the T_2 relaxation time for the methylene (CH_2) peak in the high resolution proton spectrum of tumour biopsy samples. The fact that the spectrum is high resolution indicates relatively long relaxation times of molecules in rapid motion. As mentioned in the Introduction (Chapter 1), it is unusual to obtain a high resolution spectrum for cells. Bloom et al. (1986) have analyzed the complete proton spectrum for the metastatic 13762 rat mammary adenocarcinoma cell line, and estimated the contributions from various cell components to the spectrum. Most of the spectrum is broadline (see Fig.2-6) from relatively rigid membrane lipids and proteins. Local domains, associated with the plasma membrane, of mobile

lipids (neutral lipids such as triglycerides and cholesterol esters) which can move fast enough to eliminate dipolar broadening give rise to a high resolution spectrum sitting on top of the broadline component. Flexible parts of cytoplasmic proteins with rapid internal motions also contribute to the high resolution part. The high resolution spectrum was calculated to arise from 35% of the protons in the cells. The methylene peak at 1.3 ppm contained 7.3% of all the protons in the cells, and a fraction of this gives rise to the metastatic marker of interest to us. In general, the area under the methylene resonance reflects the proportion of protons in neutral lipid acyl chains (Holmes et al. 1987). The correlation was not perfect, however, indicating that not all protons resonating at 1.3 ppm derive from acyl chains. There are other entities under the peak, and rightly so, because even mobile acyl chains do not yield T_2 values in excess of 200 ms.

We will thus examine a small part of the whole cell spectrum, the high resolution component arising from the dynamic cell membrane. We will use NMR, notably its T_2 relaxation time parameter, to characterize human tumour biopsy specimens.

References

Becker,E.D. High Resolution NMR Theory and Chemical Applications. Academic Press, Inc. New York. 1969.

Bloom,M., Holmes,K.T., Mountford,C.E. and Williams,P.G.

(1986) Complete Proton Resonance in Whole Cells. J. Mag. Res. 69: 73-91.

Fukushima,E. and Roeder,S.B.W. Experimental Pulse NMR A Nuts and Bolts Approach. Addison-Wesley Publishing Co. Inc. 1981.

Holmes,K.T., Williams,P.G., King,N.J.C., May,G.L., Dyne,M., Bloom,M. and Mountford,C.E. (1987) A Comparison of the Chemical Analyses of Cell Lipids with Their Complete Proton NMR Spectrum. Mag. Res. in Med. 4: 567-74.

Meiboom, S. and Gill, D. (1958)Modified spin-echo method for measuring nuclear relaxation times. Rev. Sci. Instrum. 29, 688-91.

Mountford,C.E., Mackinnon,W.B., Bloom,M., Burnell,E.E. and Smith,I.C.P. (1984) NMR methods for characterizing the state of the surfaces of complex mammalian cells. J. Biochem. Biophys. Methods 9:323-30.

Paul,H-H., Penka,V. and Lohmann,W. (1983) Nuclear Magnetic Resonance Spectroscopy In: Biophysics Eds.: Hoppe,W., Lohmann,W., Markl,H. and Ziegler,H. (Springer-Verlag 1983) pp.190-206.

Pavia,D.L., Lampman,G.M. and Kriz,G.S.Jr. (1979) Introduction to Spectroscopy. W.B. Saunders Co. 1979.

CHAPTER 3

THE HUMAN TUMOUR DATA BASE IN SEARCH OF A CORRELATION BETWEEN T_2, MALIGNANCY AND METASTASIS

Introduction

There have been many ^1H NMR studies on the T_1's and T_2's of the water peak in normal relative to malignant tissue (Bottomley 1986). The results have been inconclusive, except for studies on liver (Hollis et al. 1975) and a study (Bronskill et al. 1986) using a combination of T_1 and T_2 to discriminate between cancerous and non-cancerous breast tissue. Block (1977) was the first to indicate that "the non-water PMR (proton magnetic resonance) signals from tissues might reflect some pathological changes in the tissues". Then, with the discovery by Mountford et al. (1984) that the T_2 of the methylene (CH2) peak was a useful index for the metastatic potential of cancer cells in a rat mammary adenocarcinoma model, came the hope that the rat-tested hypothesis might also hold for human tumours. If the T_2 relaxation time could predict the potential for metastasis of a biopsy sample, some patients could be spared the adjuvant chemo- or radiotherapy routinely given after the removal of a primary tumour.

Thus the present study came into being : an extensive clinical ^1H NMR study of breast, colon and lymph tumour biopsies and their respective T_2 relaxation times. This involved the cooperation and coordination of many people. A

large data base was amassed, and histograms were prepared for easier visualization of the results than from columns of numbers in tables. The present chapter will describe in detail the steps leading up to, and the analysis of, the resulting histograms.

Materials and Methods

Tumour Biopsy Samples

Because of the heterogeneity inherent in biological specimens, it was decided to limit the types of tumours examined. In order to amass a sufficiently large data base in a reasonable amount of time, samples from common types of tumours were requested. Colon (n=130), breast (n=58), and lymph (n=20) biopsy specimens were obtained from the Ottawa Civic Hospital Pathology Laboratory. "Normal" specimens from sections of colon uninvolved with cancer were received with 12 tumour samples. All samples used in the study were primary tumours and the patients had received no previous medical intervention.

Immediately after surgery, the samples for NMR were put into a test-tube containing physiological (pH 7.4) phosphate-buffered saline (PBS, Dulbecco 1954) in heavy water (D_2O). The sample was kept at room temperature and transported to the NRC laboratory on Sussex Drive. It was prepared for NMR in a Class B Biohood.

The breast samples usually consisted of small white

chunks of firm tissue, which cut like celery, often interlaced with bright yellow adipose tissue. The colon samples ranged from firm, greyish-white pieces, not as clean-looking as breast, to extremely soft, pulpy-looking greyish-pink, with an abundance of vasculature. Adipose tissue was often present, but not throughout the sample, as with the breast tissue. Lymph tissue was of medium consistency, which cut like soft bacon, and resembled the greyish-white colon samples, with patches of vasculature. A razor-blade was used to trim excess adipose tissue and vasculature from each specimen, which was then further cut into pieces small enough to fit into a 5mm NMR tube. From speciment #187 onwards, one or two small pieces were taken from the sample for lactate analysis, pre- and post-NMR. This will be described in detail in Chapter 6.

Great care was taken in handling the tumour specimens. Double gloves were worn, and all tools, containers, and wastes were treated with CIDEX (a glutaraldehyde-based disinfectant against viruses, bacteria, and fungi) obtained from the Civic Hospital. All waste was autoclaved before discard. Excess tissue pieces were immediately placed into a jar containing a 10% formalin solution, and labelled with the NMR sample number, type of tissue, hospital number for the patient, and the date received.

The time between excision of the biopsy specimen from the patient and the NMR experiment ranged from 2 to 6 hours.

The T_2 value of the specimen was found to be stable for 12 hours.

After the NMR experiment, each sample was removed from its NMR tube by means of a thin wire twisted into a corkscrew at one end and dropped into its previously labelled jar of formalin. Any liquid remaining in the tube was pipetted into the jar also. The fixed NMR samples were subsequently returned to the Civic Hospital Pathology Laboratory for analysis post-NMR. This report, as well as the routine histological examination performed on every biopsy sample, was received for each NMR sample, well after the NMR experiment and T_2 calculations were completed.

All tools were washed with CIDEX and ethanol, and the long pasteur pipette rinsed with fresh formalin between samples. On conclusion, all tools and NMR tubes were treated with CIDEX for 15 minutes. Tools were rinsed with ethanol, and the razor blade and tweezers used were stored in a jar of 95% ethanol. All wastes were autoclaved.

The NMR Experiment

The earlier samples (May 1985 - May 1986) were run on a Bruker CXP 300 MHz spectrometer, and later ones on a Bruker AM 360 MHz. All samples were run at 37°C. Water was saturated to minimize its resonance using a gated irradiation sequence at the frequency of the water peak in the sample (for automated sequence PRESAT.AUR with typical

run parameters, see Appendix A). A Carr-Purcell-Meiboom-Gill pulse sequence ($90°-(\tau-180°-\tau)n$) was used (for automated sequence CPMGHG.AU with typical run parameters, see Appendix A). A τ value of 1 ms was used, and n varied from 4 to 480 for a 30 experiment run (a listing of values for n is included in Appendix A). The total delay time before acquisition of a free induction decay (FID) thus ranged from 8ms to 960 ms. At times 35 or 60 experiments were run, extending the longest delay time to 1280 ms for 35 experiments, and to 1348 ms for 60 experiments. In this way more points were obtained for the initial and terminal sections of the decay curve. However, it was found that the extra points made no significant difference in the T_2 values obtained by our calculation method. The 30 experiment run was therefore used for most samples to minimize the always precious and scarce NMR machine time. Generally 24 scans were used for each of the 30 experiments. Given the usually good signal-to-noise ratio obtained for the tumour samples, the number of scans was sometimes reduced to 16 or 8, when NMR machine time necessitated.

Calculation of T_2 Values

The CXP 300 experimental data were processed after acquisition on the CXP spectrometer, with spectra printed out on a Nicolet computer. Once the Bruker AM 360 was operational, all processing was done on its accompanying

Figure 3-1. Typical NMR spectra of tumour samples.

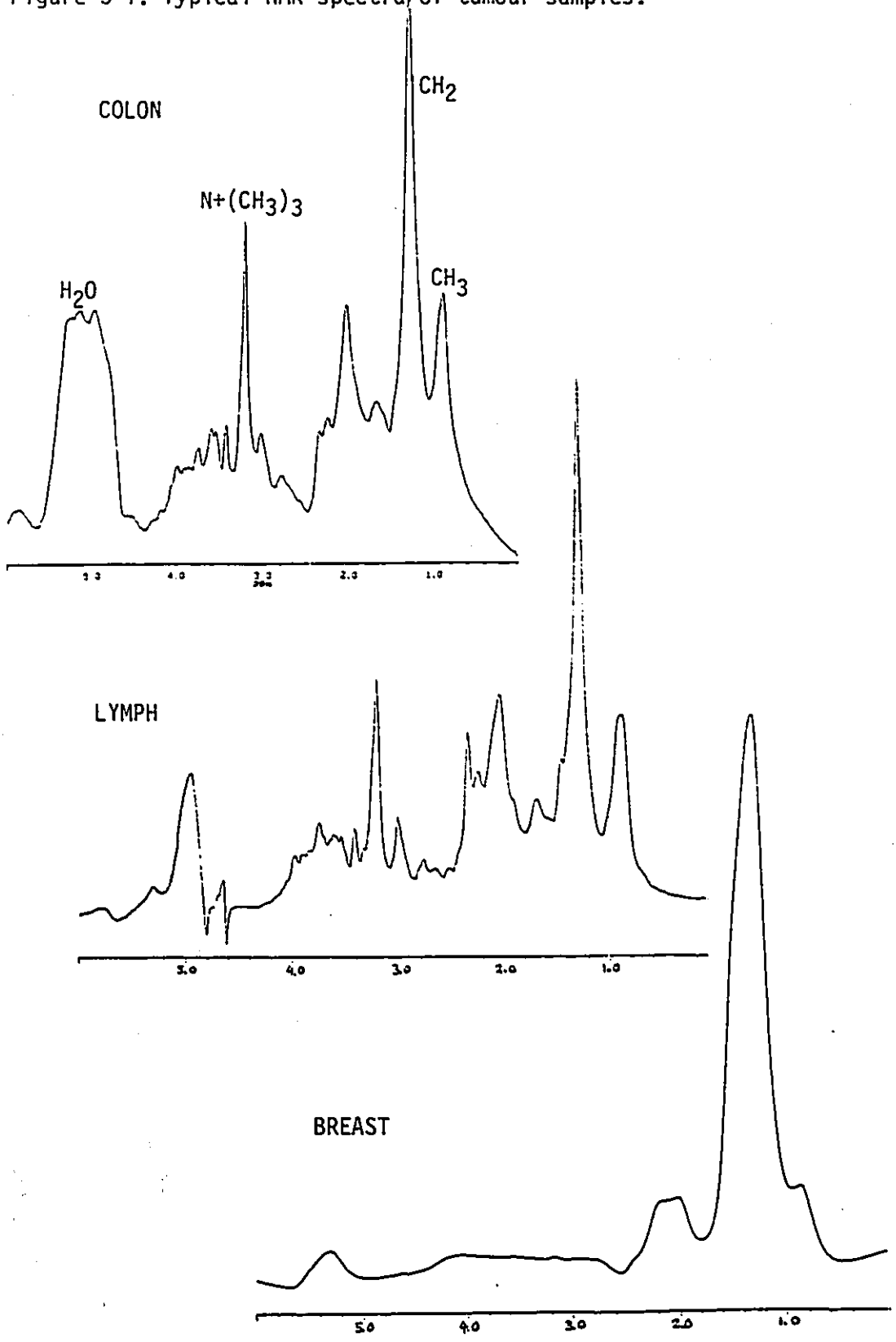

Figure 3-2. Listing of Intensity vs. Delay Time τ values.

TAU	CURSOR	FREQ	PPM	INTEGRAL	INTENSITY
.0080	1705	468.175	1.300	72.862	91.548
.6080	1705	468.175	1.300	4.668	7.771
.2240	1705	468.175	1.300	20.026	28.137
.4800	1705	468.175	1.300	7.295	11.498
.9600	1702	474.035	1.316	1.904	3.602
.8000	1701	474.035	1.316	2.434	4.925
.7680	1702	474.035	1.316	1.202	5.091
.0960	1706	466.222	1.295	35.659	47.686
.3640	1704	470.123	1.305	2.235	4.063
.1600	1707	464.269	1.289	25.982	36.915
.9280	1703	472.082	1.311	.905	3.572
.4000	1705	468.175	1.300	9.496	14.522
.7040	1703	472.082	1.311	3.690	6.337
.2560	1707	464.269	1.289	14.294	21.690
.5440	1705	468.175	1.300	5.755	9.566
.0160	1705	468.175	1.300	66.944	82.357
.3520	1706	466.222	1.295	11.452	17.268
.8960	1704	470.123	1.305	1.915	3.964
.6400	1703	472.082	1.311	4.485	7.670
.0640	1706	466.222	1.295	44.953	60.018
.6720	1705	468.175	1.300	4.226	6.817
.5760	1705	468.175	1.300	5.392	8.997
.4320	1705	468.175	1.300	8.748	13.409
.8320	1703	472.082	1.311	1.117	4.331
.1920	1705	468.175	1.300	23.106	32.786
.7360	1704	470.123	1.305	2.777	5.697
.1280	1706	466.222	1.295	28.300	43.110
.2560	1705	468.175	1.300	16.704	25.011
.5120	1706	466.222	1.295	6.335	10.495
.3200	1705	468.175	1.300	12.978	19.515

Figure 3-3. Semi-log plot to determine T_2 values.

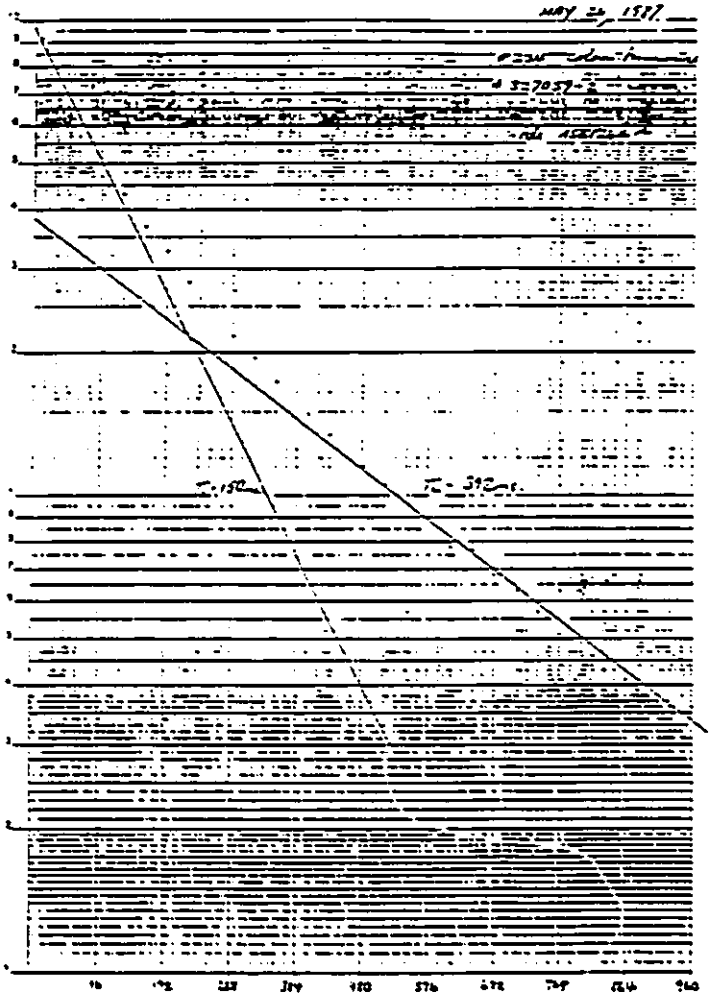

Decay of intensity vs. time :

$$I = e^{-t/T_2}$$

$$\ln I = -t/T_2$$

$$\ln I_1 = -t_1/T_2$$

$$\ln I_2 = -t_2/T_2$$

$$\ln I_1 - \ln I_2 = (t_2 - t_1)/T_2$$

$$T_2 = \frac{t_2 - t_1}{\ln I_1 - \ln I_2}$$

$$(\ln I = 2.3 \log_{10} I)$$

$$T_2 = \frac{t_2 - t_1}{2.3(\log_{10} I_1 - \log_{10} I_2)}$$

If we choose I_1 to be 2.7 (e) and I_2 to be 1.0,

$$T_2 = (t_2 - t_1)/(\ln e - \ln 1.0)$$

$$T_2 = t_2 - t_1$$

Data Staticn. The data were stored in the form of FID's on magnetic tape.

The first file (8ms FID) of each experiment was Fourier transformed to an NMR frequency spectrum using a line broadening of 3 Hz (Fig.3-1). This increases the signal-to-noise ratio at the expense of resolution, in effect smoothing out the spectrum. The spectrum was then phased (lineshapes adjusted to be purely absorptive) and the always prominent methylene (CH_2) peak was set to 1.3 ppm, as our chemical shift reference. No internal reference standard was used. The remaining FID's of the experiment were then processed according to the settings of the first one. Once all the spectra were obtained, the decay in intensity of the CH_2 peak with increasing delay times was monitored using a Bruker T_2 calculation program, which produced a listing of intensity values vs. delay time tau (Fig.3-2). These values were plotted by hand on semi-log paper to determine roughly the number and values of the major T_2 relaxation components for the sample (Fig.3-3).

The intensity and tau values were then fed into a non-linear least squares fitting program (Marquardt 1963) modelled to fit a one, two, or three exponential relaxation curve of the form

$$I = \Sigma\alpha_n e(-t/T_{2n})$$

where α_n - pre-exponential component (where line extrapolates through y-axis)

Figure 3-4. T_2 Multiexponential Fitting computer plots.
E3 is the better fit.

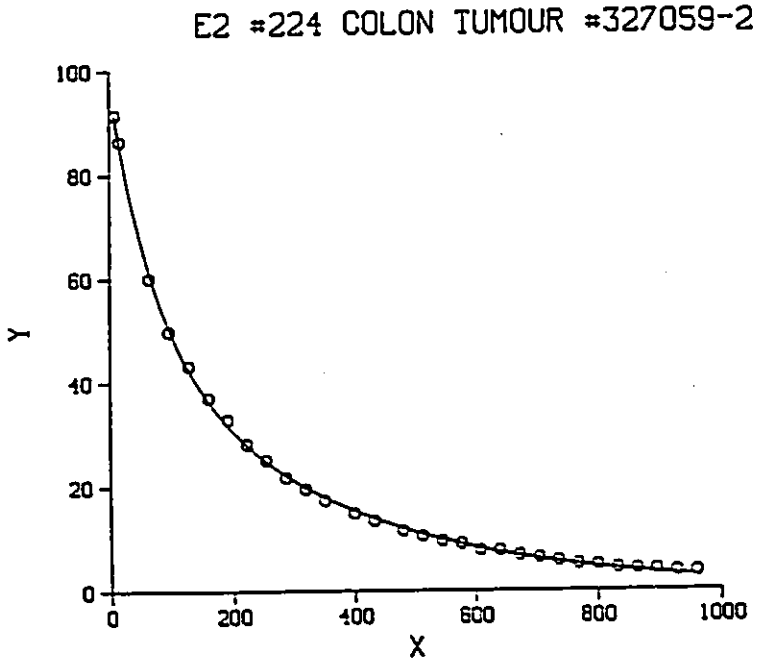

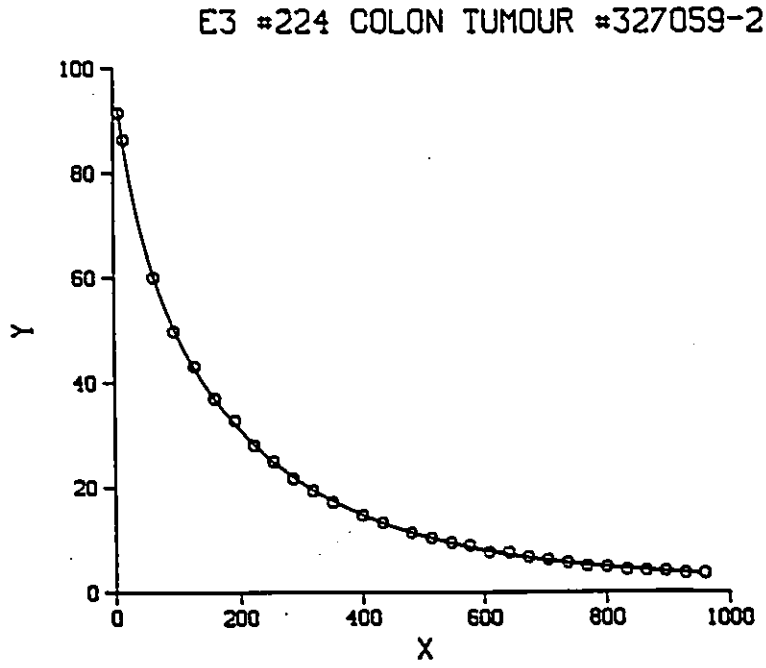

t - time

T_{2n} - T_2 relaxation time of the n^{th} term

The two exponential fit was usually tried first, and depending on the results obtained, a 1 or 3 exponential was then run on the data. To determine which fit gave the best result, a simple F-test was used :

$$F = \left[\frac{(SSRES(a) - SSRES(b))/ DF}{SSRES(b)/DF(b)} \right]$$

where SSRES(a) - sum of squares of residuals of the lower exponential fit

SSRES(b) - sum of squares of residuals of the higher exponential fit

DF - the difference in degrees of freedom between the two fits. This equals 2, in going from 2 to 3, or 1 to 2 exponentials.

DF(b) - degrees of freedom of the higher exponential

At times even though the F-test indicated that the higher exponential was the better fit to the data, the errors were so large in the results produced (indicating an unresolvable n^{th} term), that the lower exponential was chosen. Other parameters were also examined to determine goodness of fit for the data. A plot produced for each exponential fit indicated how well the experimental data points fitted the curve (Fig.3-4). The SVR (sum of variance

of residuals), with an ideal value of 2 for a perfect fit, was also examined, as well as the scatterplot of the sums of squares of residuals. From all these parameters, a decision was made as to the best T_2 value(s) with their corresponding pre-exponential (α) components. Most tumour samples gave 2 or 3 T_2 relaxation components, while the normal samples yielded 1 or 2 components.

Tabulation of T_2 Values, Histograms

The longest T_2 value obtained for each sample was used for the histograms. There are many resonances under the CH_2 peak, the major one from mobile fatty acyl chains of lipids. The T_2 corresponding to lipid is always less than 300 ms, as verified when we measured T_2 at 1.3 ppm for mouse fat. The metastatic marker of interest to our experiments (which we believe to be fucose, see Chapters 4 and 5) has a T_2 in the range of 600 to 700 ms, while lactate, also a resonance under the CH_2 peak, possesses a T_2 value greater than 1 second. Thus our long T_2 is a composite of several relaxation components under the methylene peak. A long T_2 value was the criterion for metastasis in the rat model system. We assumed the same to be true for the human situation - that a certain entity in the tumour samples giving a long T_2 component would distinguish those tumours with metastatic potential.

Tables were constructed of sample identification, type

Figure 3-5. Tabulation of tumour data.

SAMPLE NUMBER	HOSPITAL NUMBER	DATE	TUMOUR TYPE	T_1 VALUES (PLOTTED BY HAND)	T_2 VALUES (COMPUTER FITTING)	HISTOLOGICAL REPORT METASTASES PRESENT?
110 3M	647215-3	Feb. 17, 1986	breast	152, 272, 384	49, 301	N
111 3N	656458-7	Feb. 20, 1986	rectum colon	176, 360, 944	102, 934	N
112 3O	657606-0	Feb. 24, 1986	breast	232, 328	28, 207, 532	Y
113 3P, 3S	431173-8	Mar. 3, 1986	breast	256, 368	131, 341	Y
114 3Q, 3T	328419-7	"	colon	136, 280, 536	72, 534	N
115 3U	658406-4	Mar. 4, 1986	rectum colon	64, 296, 544	13, 369	N
116 3V	376963-5	Mar. 6, 1986	breast	176, 316, 664	115, 577	N
117 3W	659073-1	"	lymph	204, 344, 392	71, 371	no lymphoma
118 3X	656967-7	Mar. 10, 1986	breast	264, 376	234, 812	N
119 3Y, 3Z	452622-4	"	colon	304, 752	157, 1071 3Z	Y
120 4A	476060-5	Mar. 12, 1986	breast	136, 224, 424	16, 133, 445	Y
121 4B	655090-9	Mar. 13, 1986	breast	256, 432	164, 409	Benign fibrocystic disease
122 4C	660818-6	Mar. 18, 1986	lymph	288, 404	265, 1667	malig. lymphoma
123 4D	371424-3	"	colon	904	14, 148, 958	Y
124 4E	455070-0	"	colon	208, 376, 688	122, 630	N
125 4H	660651-2	Mar. 19, 1986	breast	264, 384	178, 401	Y
126 4I, 5I	412259-4	"	colon	116, 300, 520	12, 155, 509	Y

of tissue, T_2 values, and indication of metastasis from the hospital histology reports. An example of this is given in Fig.3-5. From these data histograms were drawn on an H7221C plotter using the TELLAGRAF programming package on the NRC's IBM computer. The spread of T_2 values for all tissue types was first plotted in ranges of 50 ms, then histograms of T_2 values vs. metastasis for each tissue type.

To determine if any significant difference in the distribution of T_2's could be discerned for samples with metastasis present, and for those without, the breast and colon data sets were each split into two populations. The Wilcoxon Rank Sum statistical test was applied. The test was run on the NRC's IBM computer using the NRWRST program from IMSL (International Mathematical Society Library). For each population, the number of actual samples in each 50 ms T_2 range are ranked in order of increasing numbers. The two ranked populations are then merged, and the sum of the ranks for the first population is obtained and compared to the mean value for the two populations. The initial hypothesis is that the two populations are the same. In this case the Rank Sum of the first population will be high, and not much different from the mean. If the two populations are very different, the Rank Sum for the first population will be low and quite different from the mean value. A probability is calculated for obtaining a rank sum less than or equal to the rank sum from the first data set if the two populations

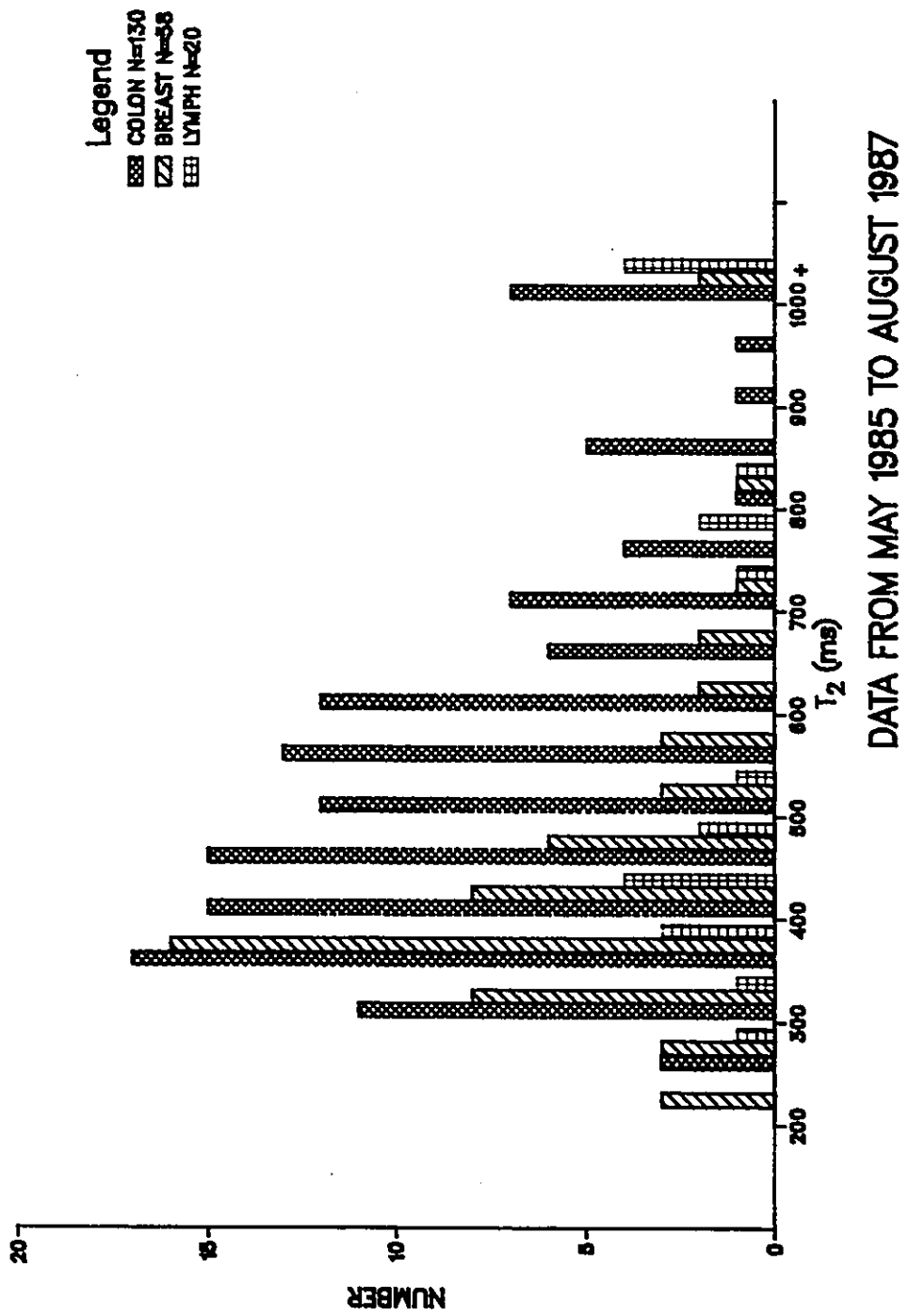
HISTOGRAM OF T_2 VALUES FOR BREAST, COLON AND LYMPH TUMOURS
Legend
COLON N=130
BREAST N=35
LYMPH N=20
NUMBER
0
5
10
15
20
200
300
400
500
600
700
800
900
1000 +
T_2 (ms)
DATA FROM MAY 1985 TO AUGUST 1987

Figure 3-6.

are the same. A probability less than or equal to 5% (giving a 95% confidence interval) indicates that the two populations are significantly different, disproving the initial hypothesis that they are identical.

Patient Follow-up Data

Questionnaires were sent out in May 1987 requesting follow-up data on patients studied from May 1985 until May 1986. This information is vital for the conclusiveness of our study, in order to see if any of the patients with long T_2 values, and no indication of metastasis at the time of biopsy, would later develop metastasis within this two year period. It is also of interest to this study if histologically borderline cases (such as polyps) with long T_2's subsequently develop cancer.

Results

Histogram of T_2 Values for Breast, Colon and Lymph Tumours (Fig.3-6)

In this histogram can be seen the spread of T_2 values for the whole tumour data base. The number of samples of each tumour type are plotted versus T_2, which ranges from 200 ms to greater than 1 sec. The colon tumours possess the widest-shaped distribution of T_2 values, with the bulk of the samples falling between 300 and 650ms. The values peak at 350-450 ms. The breast samples form a sharper, narrower distribution around 350-400 ms, with most lying between 300

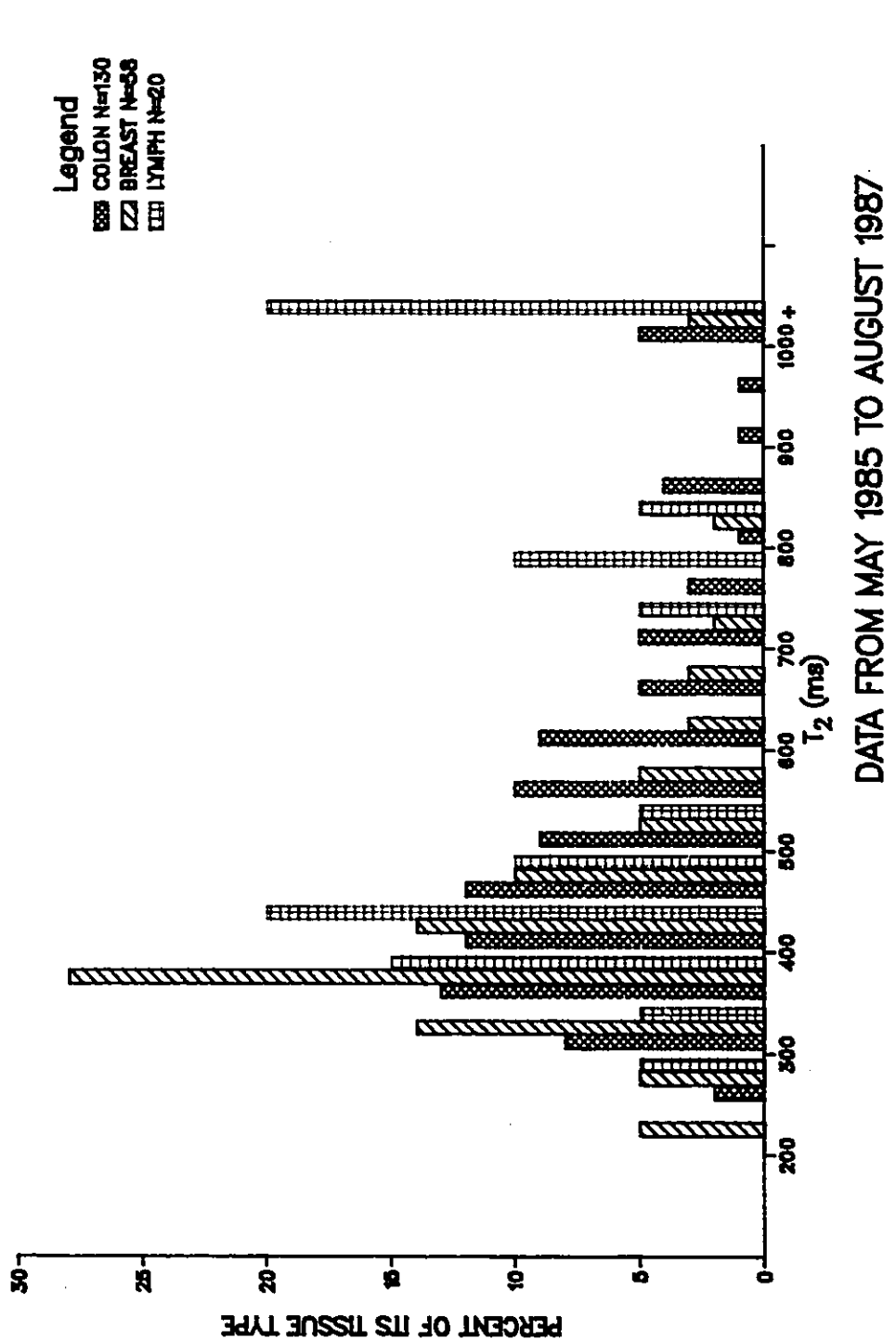
HISTOGRAM OF T_2 VALUES FOR BREAST, COLON AND LYMPH TUMOURS -- NORMALIZED
Legend
COLON N=130
BREAST N=58
LYMPH N=20
PERCENT OF ITS TISSUE TYPE
0
5
10
20
25
30
200
300
400
500
600
700
800
900
1000+
T_2 (ms)
DATA FROM MAY 1985 TO AUGUST 1987

Figure 3-7.

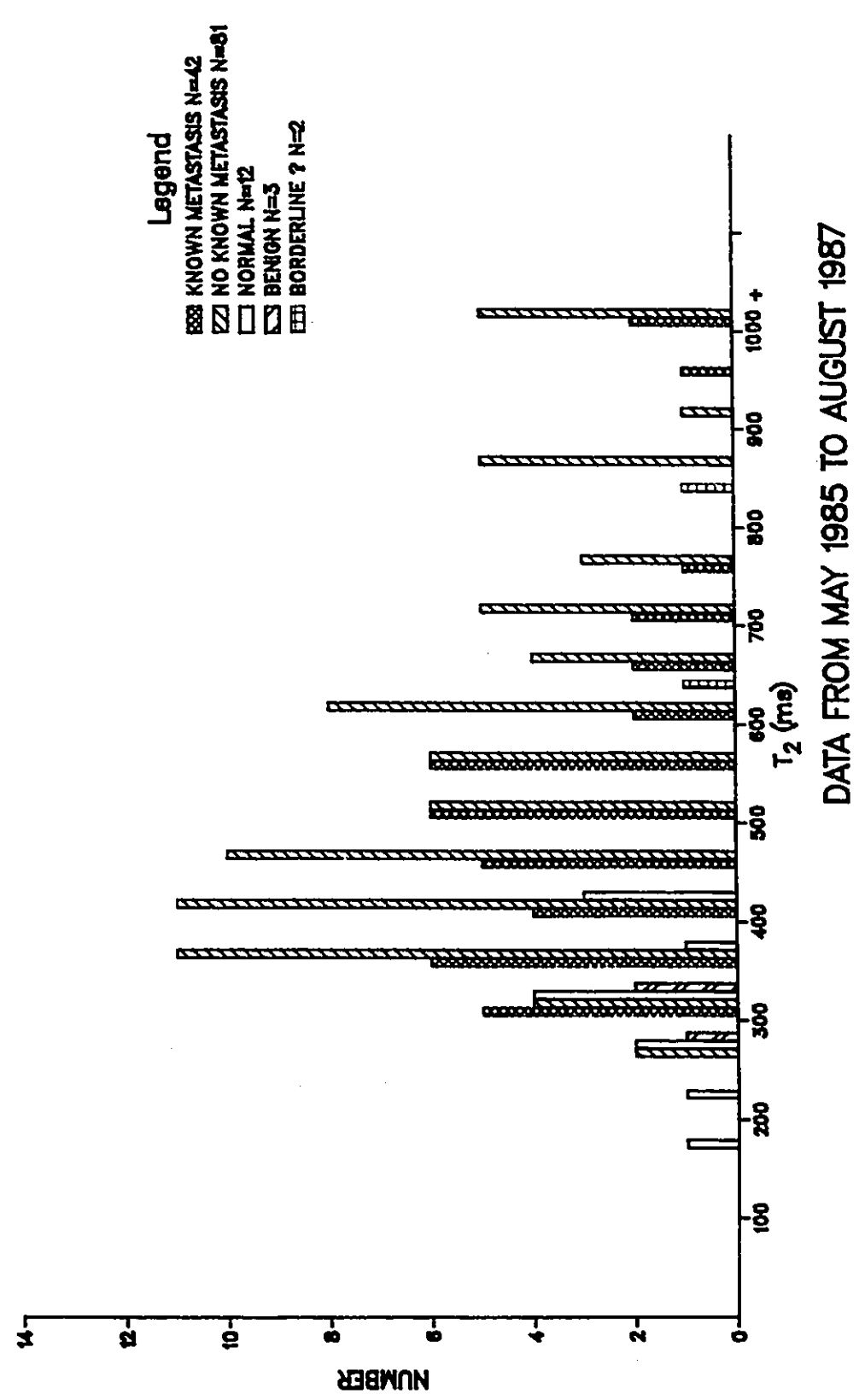
HISTOGRAM OF T_2 VALUES FOR COLON TUMOURS AND NORMALS
Legend
KNOWN METASTASIS N=42
NO KNOWN METASTASIS N=61
NORMAL N=12
BENIGN N=3
BORDERLINE ? N=2
NUMBER
0
2
4
6
8
10
12
14
100
200
300
400
500
600
700
800
900
1000 +
T_2 (ms)
DATA FROM MAY 1985 TO AUGUST 1987

Figure 3-8.

and 450 ms. Less than 25% have a T_2 greater than 500 ms, whereas almost 50% of the colon samples fall in this range. The lymph samples, though small in number, peak at three different T_2's : 400-450 ms, 750-800 ms, and 1000+ ms. More than 50% are centered about the first peak. Just as the tissue composition of the three types varies, so does the distribution of their T_2 values.

Fig.3-7 presents the same data, but with the populations of samples normalized. The number of samples of each tissue type in each T_2 range were divided by the total number of samples for that type. This was done to compare better the three types, because of the great variation in the number of samples. One can compare the percent of each type that falls into a certain T_2 range. The trends remain unaltered, only the perspective is varied slightly.

Histogram of T_2 Values for Colon Tumours and "Normals" (Fig.3-8)

The colon data base was divided into five groups to determine correlation between T_2 values and the grouping. The 12 "normal" samples yielded T_2's betweem 198 ms and 450 ms. Two benign tumour specimens were within this range, at 250-350 ms. Of the malignant tumour samples, 66% have T_2's greater than 450 ms, and 33% lie below 450 ms, overlapping the region of "normal" and benign samples. Two samples have been classed as borderline, because the usual pathological examination, which is subjective, gave no clear indication

Figure 3-9.

NORMALIZED HISTOGRAM OF T_2 VALUES FOR COLON TUMOURS – METASTASIS FOUND

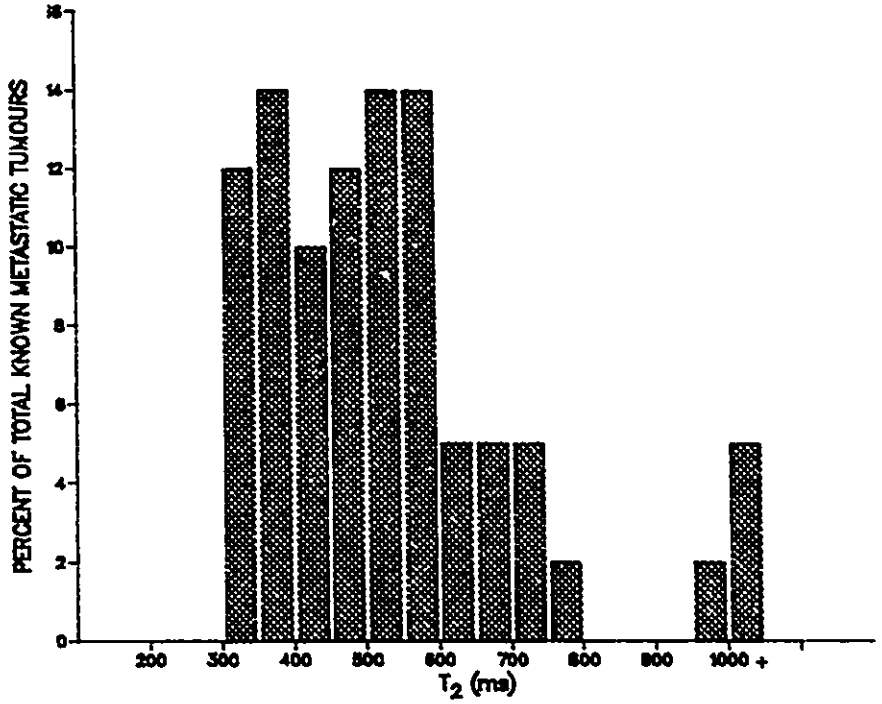

DATA FROM MAY 1985 TO AUGUST 1987

NORMALIZED HISTOGRAM OF T_2 VALUES FOR COLON TUMOURS – METASTASIS NOT YET FOUND

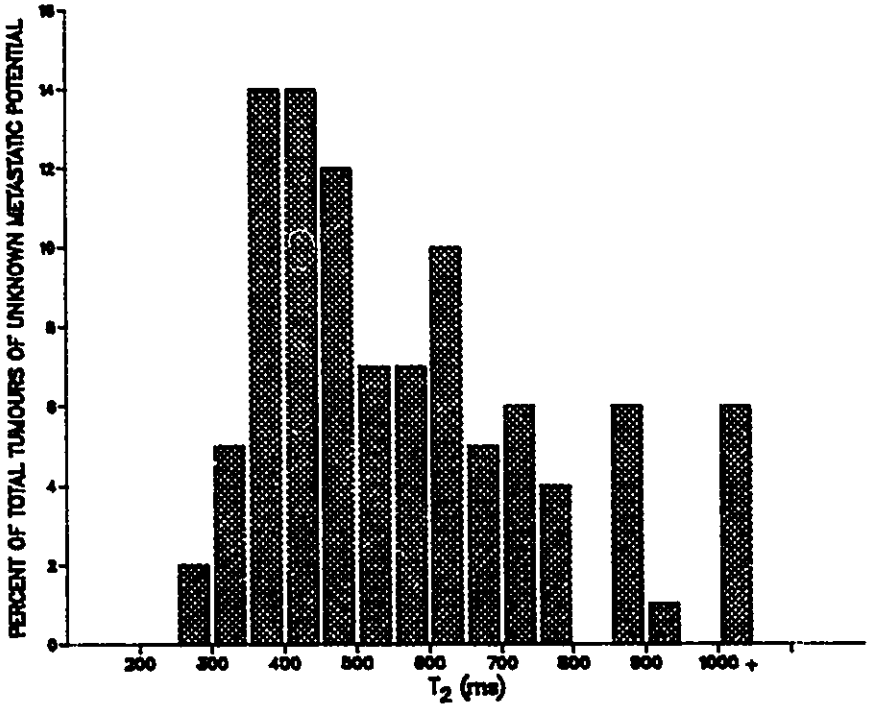

DATA FROM MAY 1985 TO AUGUST 1987

of malignancy. One of the samples was classed as high grade dysplasia, which is an abnormal change in the cells very close to a cancerous state, and the distinction between the two states can be very difficult to make. Yet the T_2 values for these two borderline specimens were very long - 650 and 850 ms - well above the normal range. The second sample, with no indication of malignancy, was from a patient who had a colostomy years previously. When a microscopic re-examination was requested for these two samples, along with other samples, a different pathologist classed the high grade dysplasia as definitely malignant. It would be a true confirmation of the diagnostic value of T_2 for malignancy, if these two patients later presented with cancer.

The pathologically malignant tumour tissues were divided into two groups, those with clinically evident metastasis (spread of the cancer to the lymph nodes surrounding the section of colon involved with tumour), and those with no metastasis evident at the time of surgery. In order to discern differences in T_2 distributions between these two groups, each group was normalized, and plotted separately (Fig.3-9). Although the shapes of the two distributions vary somewhat, the range of T_2 values encompassed does not seem to differ except for an extra 50 ms range at the low T_2 end for colon tumours with no evidence of metastasis. The Wilcoxon Rank Sum Test run on the two distributions of T_2 values verified this initial surmise, giving no

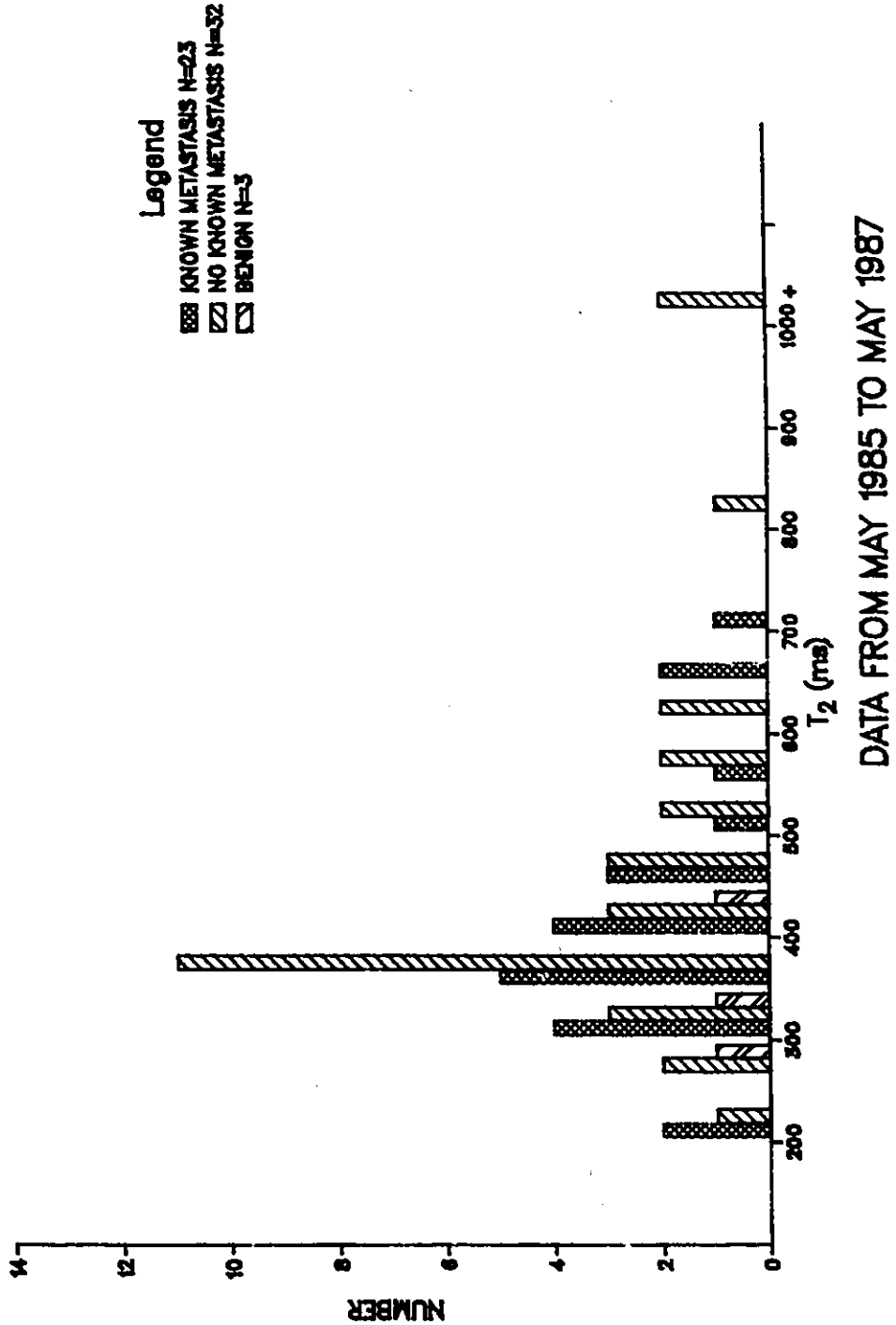
HISTOGRAM OF T_2 VALUES FOR BREAST TUMOURS
Legend
KNOWN METASTASIS N=23
NO KNOWN METASTASIS N=32
BENIGN N=3
NUMBER
0
2
4
6
8
10
12
14
200
300
400
500
600
700
800
900
1000 +
T_2 (ms)
DATA FROM MAY 1985 TO MAY 1987

Figure 3-10.

Figure 3-11.

NORMALIZED HISTOGRAM OF T_2 VALUES FOR BREAST TUMOURS – METASTASIS FOUND

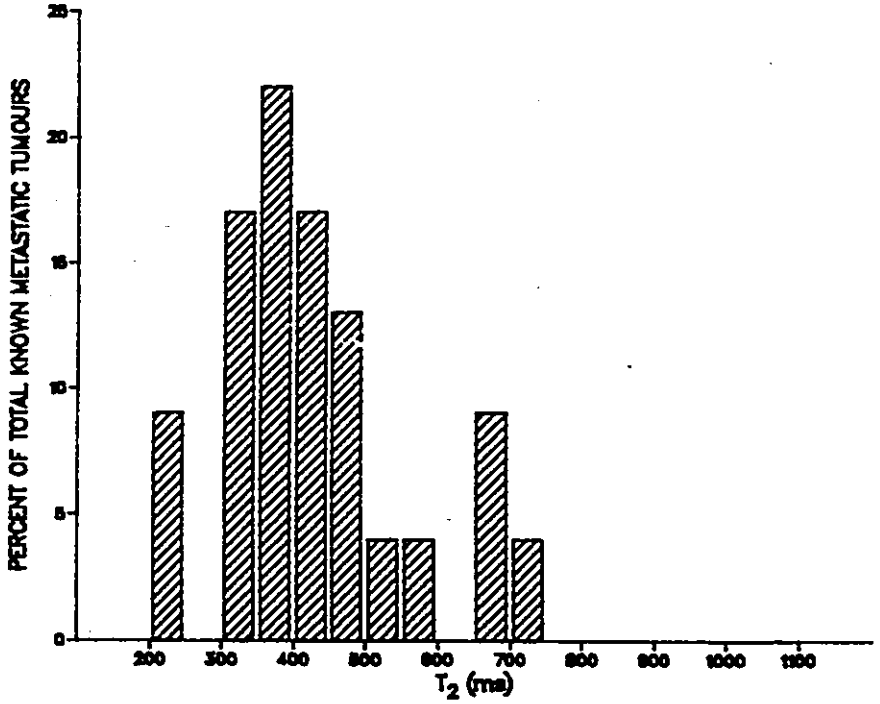

DATA FROM MAY 1985 TO MAY 1987

NORMALIZED HISTOGRAM OF T_2 VALUES FOR BREAST TUMOURS – METASTASIS NOT YET FOUND

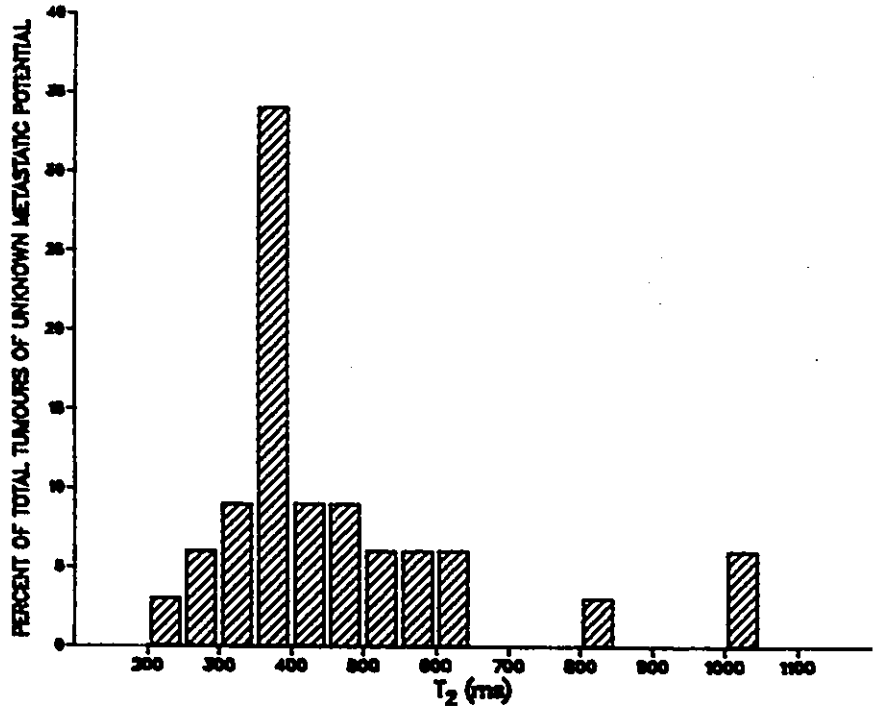

DATA FROM MAY 1985 TO MAY 1987

statistically significant evidence of a difference between the two populations. From replies to the follow-up questionnaires received to date, 3 tumour cases with long T_2's from the metastasis-not-yet-found population have since developed metastases. A change in but 3 samples from one population to the other is not enough to alter the distributions. A longer time span is necessary for such a study.

Histogram of T_2 Values for Breast Tumours (Fig.3-10)

The T_2's of the three benign breast samples range from 250 to 450 ms. The bulk (67%) of the malignant tumours from breast, having T_2's from 200 to 450 ms, fall into the range of benign tissue. We received no samples of normal breast tissue, and thus have no knowledge of its T_2 range by our method. Of the malignant samples 33% have T_2's greater than 450 ms, above the range of the benign samples.

Fig.3-11 shows the two normalized populations of metastasis found/ metastasis not yet found for the breast tumours. As for the colon tumours, the Wilcoxon Rank Sum Test verified that there is no statistically significant difference in the distribution of T_2 values for the two populations. From the follow-up questionnaires, 3 cases with no metastasis at the time of surgery have since developed metastases. Again, this change is insufficient to alter the statistics.

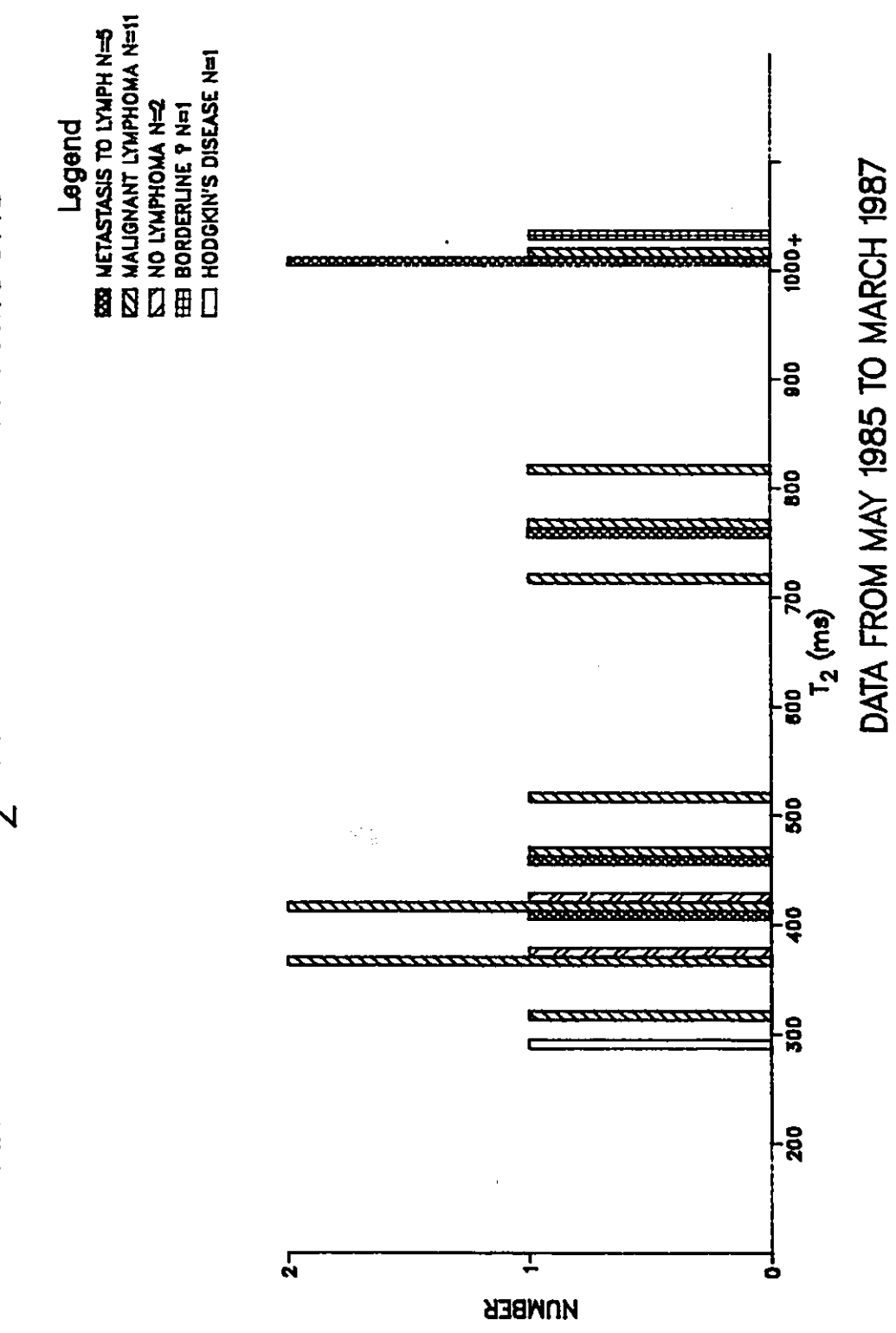
HISTOGRAM OF T_2 VALUES FOR LYMPH TUMOURS
Legend
METASTASIS TO LYMPH N=5
MALIGNANT LYMPHOMA N=11
NO LYMPHOMA N=2
BORDERLINE ? N=1
HODGKIN'S DISEASE N=1
NUMBER
0
1
2
200
300
400
500
600
700
800
900
1000+
T_2 (ms)
DATA FROM MAY 1985 TO MARCH 1987

Figure 3-12.

Histogram of T_2 Values for Lymph Tumours (Fig.3-12)

The sample from a patient with Hodgkin's Disease gave a very low T_2 value (200 ms). Interestingly, serum samples from Hodgkin's Disease patients yield large Fossel numbers, indicative of normal serum. The Fossel number is an NMR parameter using linewidth at half-height as an index for malignancy, and will be addressed in Chapter 4. The Hodgkin's Disease biopsy was one of the samples for which histological re-examination was requested. The pathologist's report stated that a very large percent of the sample examined by NMR was comprised of normal cells. The two benign specimens received had T_2's in the range 350-450 ms. Of the malignant lymph samples 35% overlap in the range of the two benign samples and the "normal" sample from the Hodgkin's Disease patient. Sixty-five percent of the malignant samples have T_2's greater than 450 ms. One sample was classed as borderline where the pathological diagnosis fell short of malignancy, but was definitely abnormal. Its T_2 was long.

Discussion

Spread of T_2 Values as a Diagnostic Indicator of Malignancy and Metastasis

The rat model system did not address the question of malignancy, a normal cell line was not included for

comparison. For all three human tumour tissue types, no benign sample gave a T_2 greater than 450 ms. Thus a T_2 value greater than 450 ms would indicate malignancy in a human tissue sample. For values less than 450 ms the diagnosis is questionable on the basis of T_2 alone. For malignant tumours received, 67% of breast, 33% of colon, and 37% of lymph samples had T_2's less than 450 ms. For colons, "normal" samples were all within this range. Since no normal samples for breast or lymph tissues were received, and because it would be unwise to extrapolate from one tissue type to another, we cannot say what the normal range for these tissues would be. Benign samples, which are encapsulated abnormal growths, are certainly not the same as normal. Some could actually be premalignant, meaning that at some point in time the progression to malignancy could occur.

As noted previously in the Materials and Methods section, breast tissue contains a large amount of adipose tissue, which has a T_2 less than 300 ms. The large proportion of lipid in these samples could well account for the large amount of breast tumours with T_2's less than 450 ms. An increase in lipid content could also lower the effective T_2 values of colon and lymph tumours by masking the long T_2 component of low relative population. This will be discussed in greater detail, specifically for colons, in Chapter 4. The borderline cases are of utmost interest to this study, but only time will tell if the prediction of

malignancy-to-come is fulfilled. Parameters other than T_2 will be investigated for colons in the next chapter. T_2 as the sole criterion for malignancy appears to be too narrow. Often in the course of research new avenues are opened, and our whole outlook on the problem is broadened in the search for the truth.

No colon or lymph samples with a short T_2 (less than 300 ms) have yielded metastases. Breast samples, which have given T_2 values in the 200 ms range, appear to be in a class of their own. Further investigation would have to be done on the breast data base, probably expansion, as well as examining the unique characteristics of breast tissue. The verdict on T_2 vs. metastasis must await more follow-up data on the patients, possibly until five years post-biopsy.

Difficulties in a Human Clinical Study

In the rat model system two relatively homogeneous mammary adenocarcinoma cell lines were used : the non-metastatic J-clone line and the metastatic 13762 line. These were injected into rats bred from the same line. Thus the time of inception of the tumour was known, and the tumours could be excised, or the rats sacrificed to check for metastatic deposits in lungs at any point in time. The rate of growth of the primary tumour could be easily monitored, if desired, as well as the time of appearance of metastatic deposits. The time span of the system involved

Figure 3-13.
PER CENT TUMOUR CELLS IN COLON TUMOUR SAMPLES VS. T_2 VALUES

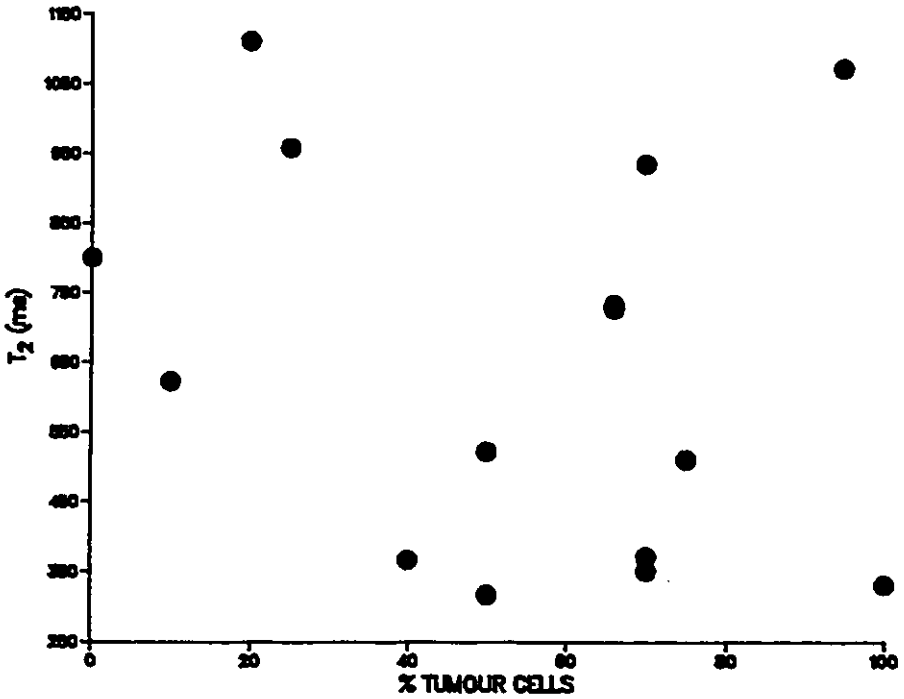

PER CENT TUMOUR CELLS IN COLON TUMOUR SAMPLES VS. T_2 PRE-EXPONENTIALS (α)

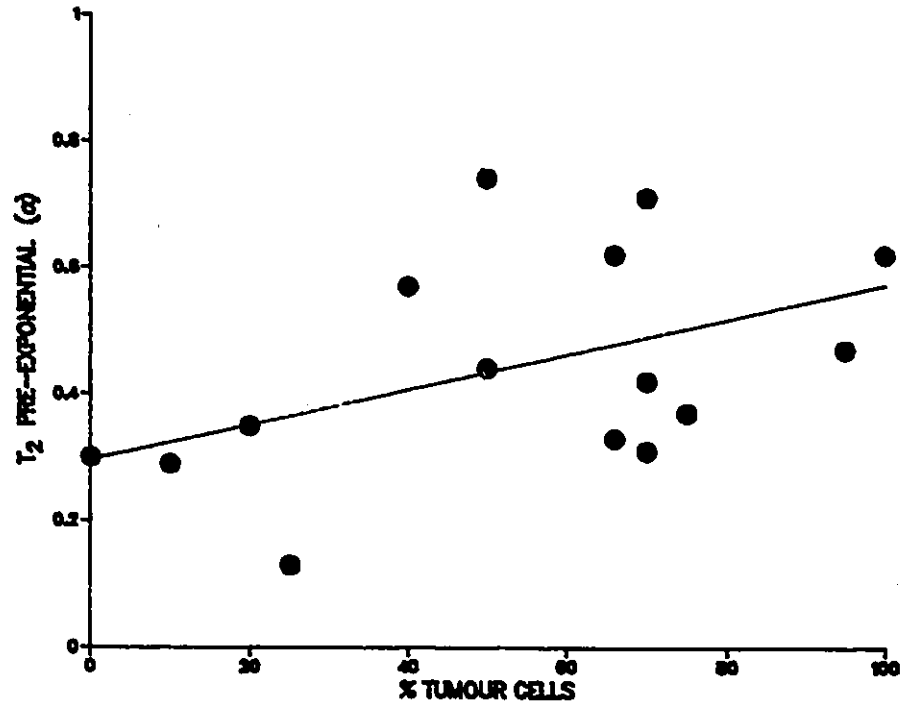

days or weeks. In short, the whole system was relatively clean and well-controlled, as much as could be expected for a living biological system.

A human clinical study, where each patient is unique, is quite another matter. There are two basic problems - heterogeneity of samples and the time element. The tumour lines dealt with are certainly not well-established and cultured cell lines, in fact we do not know how diverse a spectrum of tumour cells we are studying with NMR.

Histological re-examination of several of the samples studied by NMR was requested for the purpose of correlating the percentage of tumour cells with the longest T_2 obtained and its corresponding pre-exponential (α) value. The results for the colon samples examined are shown in Fig.3-13. There is a general increase in the proportion of the longest T_2, given by the α-value, with an increase in tumour cell content. The actual T_2 value does not appear to depend on the % of tumour cells within the sample. The relevant parameter is possibly not the amount, but the type of tumour cell present, i.e. that containing a certain cell surface component. The T_2 obtained is a composite of all the relaxation components within the tissue, which depends on the molecular species contained therein.

The colon sample with a long T_2 (800 ms) and 0% tumour cells was a benign polyp. For breast and lymph, benign samples with 0% tumour cells did not yield a long T_2 (data

not shown). This is interesting, for it implies that NMR is sensitive to a premalignant change in the membrane profile of a polyp that is undetectable by histological examination. Polyps will be further discussed in Chapter 4.

It is believed that only a small percentage of tumour cells within a tumour possess the capacity to metastasize,and of these, only a small percent again succeed in forming metastatic deposits (Fidler and Kripke 1977, Fidler and Hart 1982). We are looking at a very small, but potent amount of something that determines metastatic potential. At the same time, we are observing parameters indicative of the malignant prototype of human tissue.

With the heterogeneity inherent in human tumour samples, it is no surprise that it is difficult to obtain an answer as clear-cut as in the rat model system.

In an attempt to eliminate this heterogeneity, experiments were planned to isolate cells containing the sugar fucose on cell surface carbohydrate antigens. Several studies link fucose with cancer (see Chapter 5), notably experiments by Kaizu et al. (1986) and Nudelman et al. (1986) which led to the production of an antibody binding to a cell surface antigen containing fucose present in all colon cancers studied. 2-D NMR (Chapter 5) also shows fucose to be a major contender for the source of the long T_2 value associated with cancer. Our cell isolation experiments were stopped, however, due to several technical difficulties, but

the possibility for this type of approach to the problem of heterogeneity exists nonetheless. Biochemical analysis for fucose of one tumour and a "normal" sample from the same patient showed equivalent amounts of fucose for both samples. The difference could lie, however, in the conformation of fucose on the cell surface. It is known that fucose expressed on normal cells is cryptic or hidden, not free to interact with other cells or move unimpeded.

The second problem in a human clinical study is the element of time. We have no idea of the time of inception of the primary tumour in question, and how long, in years, it took to grow to its present size. There is no question of monitoring these tumours, or the production of metastatic deposits by the means available for ethical reasons. We get one look at the patient, frozen in time, while the disease process has been steadily progressing to this point. One day, when Medical Resonance Imaging has progressed sufficiently in its sensitivity for lipids, the growth of a tumour could be monitored noninvasively. For now, the best that can be done is to look at follow-up data for the patients in the study, to see if events predicted by our T_2 values come to pass. Any medical intervention can alter the natural disease progression, so that patients not receiving any chemo- or radiotherapy after the initial surgery are choice candidates for follow-up. Colon cancer patients usually fall into this category, since their tumours are

Figure 3-14. Lognormal Distribution.

$$g(t) \propto t^{-1} e^{-[\log(t/T_2)]^2/\gamma^2}$$

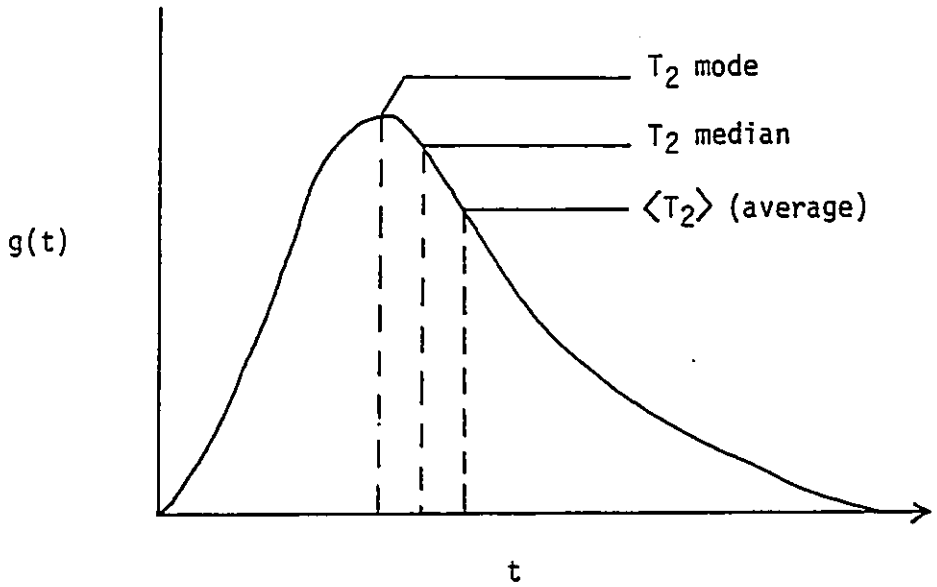

T_2 mode is the maximum T_2 value

T_2 median divides the distribution into 2 equal parts

$\langle T_2 \rangle$ is the average T_2 value

γ is a mathematical expression characterizing the broadening of the distribution, and is related to the standard deviation (σ) of the distribution :

$$\sigma = T_2 \sqrt{e^{\gamma^2/2}(e^{\gamma^2/2} - 1)}$$

here, that the experimental data must fit to a predetermined number of exponentials. The data determine the number and character of the components.

One method is to examine the relaxation parameters as a lognormal distribution. Fig.3-14 gives an example of such a distribution, with its relevant parameters. The lognormal distribution was fitted to some of our recent colon biopsy sample data values. Interestingly, the parameter for differentiating between malignant and "normal" tissue shifted from T_2 values to the γ value, which is the width of the lognormal distribution around a maximum T_2 value. Table 3-1 below summarizes the results for 2 samples.

Table 3-1. Parameters of Lognormal Distribution for 2 Sample Pairs.

Sample	T2 mode	<T2>	γ
#226 Tumour	37	223	1.53
#235 Tumour	75	184	1.07
#226 "Normal"	216	271	0.56
#235 "Normal"	182	265	0.71

The T_2 values of "normals" are higher than those of tumours (the opposite of our T_2 calculation model), but the better parameter is the γ value, being larger (indicating a wider distribution of T_2 values) for tumours than for "normals".

A second method, and one coming into vogue for biological experiments, uses a program developed by Provencher in 1982 called CONTIN - a constrained regularization method for inverting data represented by

linear algebraic or integral equations. The program finds the most acceptable solution, and the simplest, incorporating the principle of parsimony, which states that the most appropriate solutions are the simplest ones that reveal the least amount of detail or information that was not already known or expected, to the integral equation

$$y(t) = \int S(T)\exp(-t/T)dT + \beta$$

where

$y(t)$	is the data measured at time t
$\exp(-t/T)$	is the integral describing the data, i.e. exponential decay
$S(T)$	is a weighting distribution function
β	is a constant baseline term

The CONTIN program was run on the two sample pairs with 30 and 44 delay times. The results are shown in Table 3-2.

Table 3-2. Comparison of T_2 Values Obtained by Multiexponential Fitting and CONTIN.

Sample	30 Points		44 Points	
	Exp.Fit	CONTIN	Exp.Fit	CONTIN
#243 Tumour	306	307	314	315
#243 "Normal"	277	276	180,519	289
#244 Tumour	122,407	248	7,141,460	9,259
#244 "Normal"	283	284	203,451	287

There is good agreement between the Multiexponential Least-Squares Fitting and CONTIN when the usual 30 data points are taken, but for tumour #244. In general, CONTIN gives a shorter average T_2 value for the sample which is the weighted average (using the normalized value of the preexponential as the weighting factor) of the T_2 values

Figure 3-15a. CONTIN plot of T_2 relaxation data for lipid in colon tumour and "normal" biopsy sample.

ratio of areas under peaks :

"Normal" : 1:100

Tumour : 23:46

(diagram is misleading due to log scale of T_2 axis)

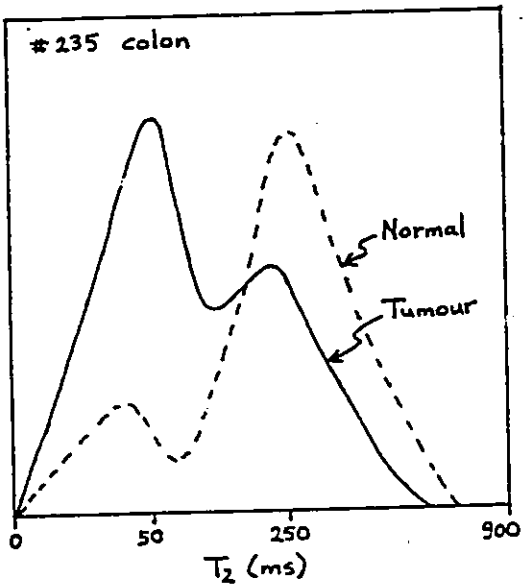

Figure 3-15b. CONTIN plot of T_2 relaxation data for water in normal mouse leg and leg with tumour growth.

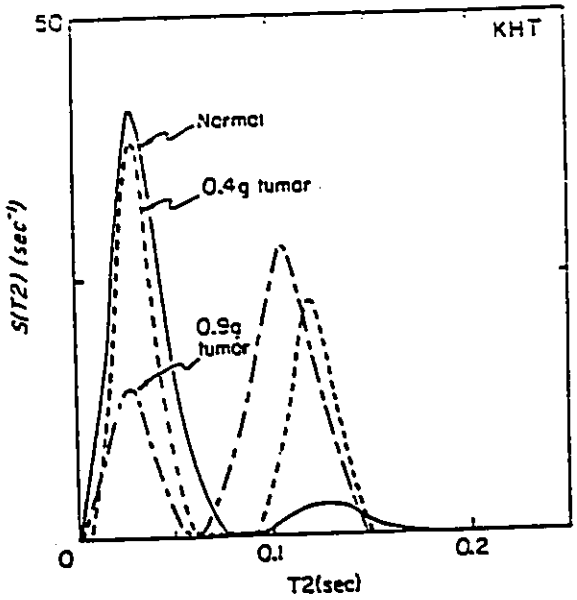

from Kroeker et al. (1985) Mag. Res. in Med. 2:1-13.

obtained by the multiexponential fitting program. With the addition of 14 points at the low and high acquisition times, differences from the fitting procedures emerge. A definite short T_2 lipid component is resolved by CONTIN for tumour #244, which is absent from "normal" #244. CONTIN runs for earlier tumour/"normal" sets indicate a shift to longer T_2 values for the "normal" samples (giving them a longer T_2 than for the tumours), and a dominance of the shorter T_2 peak for the tumours (see Fig.3-15a). This short T_2 peak could indicate a difference in lipid composition of the membrane for the tumour, and would perhaps be worthwhile investigating. For the ten tumour/"normal" sample pairs before #'s 243 and 244, however, there are insufficient data points at short delay times to properly resolve the short lipid component, so this would be a project for future samples.

Kroeker et al.(1985) used this method to analyze relaxation times for water in animal tumours. Fig.3-15b shows the peaks obtained in their T_2 experiments. With the growth of the tumour,the peak positions move only slightly toward longer times, but the relative contributions of the components change. Kroeker and Henkelman (1986) find that the method provides a more stable and accurate fit than discrete component models, in extensive analysis of biological NMR relaxation data. The method, however, cannot resolve components that differ by less than a factor of

four from each other. They state that the different peaks correspond to different tissue compartments for water, the nature and meaning of which has yet to be interpreted. Our studies involve differences in relaxation times for the lipid region of the spectrum, but the problem of resolving relaxation times for biological samples is universal.

There are several methods for fitting T_2 relaxation parameters, and probably more yet to come. The important point for analyzing data is consistency, in order to compare whatever relaxation parameter is used (T_2 in this study, γ in lognormal, relative peak areas and distributions in CONTIN) with histological data parameters. Providing a reasonable biological and physical interpretation can be made, and a significant difference between normal and malignant tissue can be shown, one method is as good as another. Each has its own advantages and limitations.

Conclusions

Despite all the limitations and difficulties encountered, the study gave a good preliminary assessment of the value of T_2 as a diagnostic criterion for malignancy. The method is indisputable for T_2 greater than 450 ms. For values less than 450 ms other parameters must be investigated for discrimination between tissues. Follow-up must be continued in order to discern the relationship between T_2 and the possibility of metastasis.

The following chapter will present a more in-depth look at the colon data base. A similar study could possibly be undertaken for the breast data; it is a question of discovering the right criteria and expanding the data base.

References

Block,R.E.,Maxwell,G.P.,Prudhomme,D.L.,and Hudson,J.L. (1977) High resolution Proton Magnetic Resonance spectral characteristics of water, lipid, and protein signals from three mouse cell populations. J. Natl. Cancer Instit. Vol.58 No.1 January 151-6.

Bottomley,P.A.,Hardy,C.J.,Argersinger,R.E. and Allen-Moore,G. (1986) A Review of ^{1}H NMR Relaxation in Pathology : Are T_1 and T_2 Diagnostic ? Med. Phys. 14(1) Jan./Feb.

Bronskill,M.J.,Brown,D.W.,Yafte,M.J.,Johns,P.C.,Foster,F.S. and D'Astous,F.T. (1985) Comparison of NMR with Ultrasound and X-Ray : Relaxation Time Measurements of Human Breast Tissue. Mag.Res. in Cancer International Conference, Banff, Alberta, Canada. Apr.30-May 4. (Pergamon Press 1985) pp 47-8.

Deslauriers,R.,Somorjai,R.L.,Geoffrion,Y.,Kroft,T.,Smith-,I.C.P., and Saunders,J.K. (1987) ^{1}H and ^{13}C NMR Studies of Tissue from Normal and Diseased Mice. Analysis of T_1 and T_2 Relaxation Profiles of Triglycerides in Liver. NMR in Biomed. Vol.1 No.1:32-43.

Fidler,I.J. (1985) Macrophages and Metastasis - A Biological Approach to Cancer Therapy : Presidential Address. Cancer Res. 45, 4714-2, Oct. 1985.

Fidler,I.J. and Hart, I.R. (1982) Biological Diversity in Metastatic Neoplasms : Origins and Implications. Science Vol. 217 10 Sept. 1982.

Fidler,I.J. and Kripke,M.L. (1977) Metastasis Results from Preexisting Variant Cells Within a Malignant Tumor. Science Vol. 197 26 Aug. 1977.

Hollis,D.P.,Saryan,L.A.,Eggleston,J.C. and Morris,H.P. (1975) Nuclear Magnetic Resonance Studies of Cancer. VI Relationships Among Spin-Lattice Relaxation Times,Growth Rate and Water Content of Morris Hepatomas. J.Natl.Cancer

Instit. Vol.54 No.6, June 1975.

Kaizu,T.,Lavery,S.B.,Nudelman,E.,Stenkamp,R.E., and Hakomori,S. (1986) Novel Fucolipids of Human Adenocarcinoma : Monoclonal Antibody Specific for Trifucosyl Le (III FucV FucVI FucnLc) and a Possible Three-dimensional Epitope Structure. J. Biol. Chem. Vol.261, No.24 Aug.25: 11254-58.

Kirikuta,I.,Bojan,O., and Munteanu,S. (1986) Biochemical markers in ovarian cancer. Arch.Geschwulstforsch. 56(1): 35-8.

Kroeker,R.M. and Henkelman,R.M. (1986) Analysis of Biological NMR Relaxation Data with Continuous Distributions of Relaxation Times. J. Mag. Res. 69, 218-35.

Kroeker,R.M.,Henkelman,R.M. and Bronskill,M.J. (1986) Continuous Distributions of Relaxation Times in Animal Tumours. Mag.Res. in Cancer; International Conference, Banff, Alberta, Canada, Apr.30-May 4. (Pergamon Press Inc. Editors Allen,P.S.,Boisvert,D.P.J. and Lentle,B.C.)

Kroeker,R.M.,McVeigh,E.R.,Hardy,P.,Bronskill,M.J. and Henkelman,R.M. (1985) In Vivo Measurements of NMR Relaxation Times. Mag.Res. in Medicine 2, 1-13.

Marquardt,D.W. (1963) An algorithm for least-squares estimation of non-linear parameters. J.Soc.Indust.Appl.Math. 11, 431-41.

Mountford,C.E.,Wright,L.C.,Holmes,K.T.,Mackinnon,W.B.,Gregory,P., and Fox,R.M. (1984) High Resolution Proton Magnetic Resonance Analysis of Metastatic Cancer Cells. Science Vol.226 21 Dec. 1984.

Nudelman,E.,Levery,S.B.,Kaizu,T., and Hakomori,S. (1986) Novel Fucolipids of Human Adenocarcinoma : Characterization of the Major Le Antigen of Human Adenocarcinoma as Trifucosylnonaosyl Le Glycolipid (III FucV FucVI Fucnl Lc). J.Biol.Chem. Vol.261 No.24 Aug.25 : 11247-53.

Provencher,S.W. (1982) A Constrained Regularization Method for Inverting Data Represented by Linear Algebraic or Integral Equations. Comp.Phys.Commun. 27(1982) 213-27.

Provencher,S.W. (1982) CONTIN : A General Purpose Constrained Regularization Program for Inverting Noisy Linear Algebraic and Integral Equations. Comp.Phys.Commun. 27(1982) 229-42.

Sokal,R.R. and Rohlf,F.J. (1973) Introduction to Biostatistics. (W.H. Freeman and Co., San Francisco).

CHAPTER 4

THE COLON DATA BASE

Introduction

In the previous chapter were presented the results of the study of the correlation between T_2 relaxation times and malignancy, and the metastatic potential of the malignancies. Although a clear distinction can be seen between normal and malignant tissue, the problem of predicting the metastatic potential of the tumours studied is not as easy to resolve. Follow-up questionnaires were sent out in May 1987 to obtain data on the patients studied between May 1985 and May 1986. From 40 questionnaires returned to date, three patients that had colon tumours with T_2 values greater than 600 ms (thereby possessing metastatic potential by our hypothesis) and no evidence of metastasis at time of surgery, did indeed develop metastasis within 2 years. No samples with short T_2 values have metastasized. Metastases may yet develop for the remaining tumours with long T_2's, in one or two years' time. Because of necessary medical intervention which alters the natural course of the disease, metastases may never occur. Some patients may die from causes other than their cancer.

Perhaps another parameter in the histology reports for each tumour studied, other than the presence or absence of metastasis at time of surgery, would correlate with the T_2 relaxation times obtained for that sample.

Figure 4-1. Intestinal polyp.

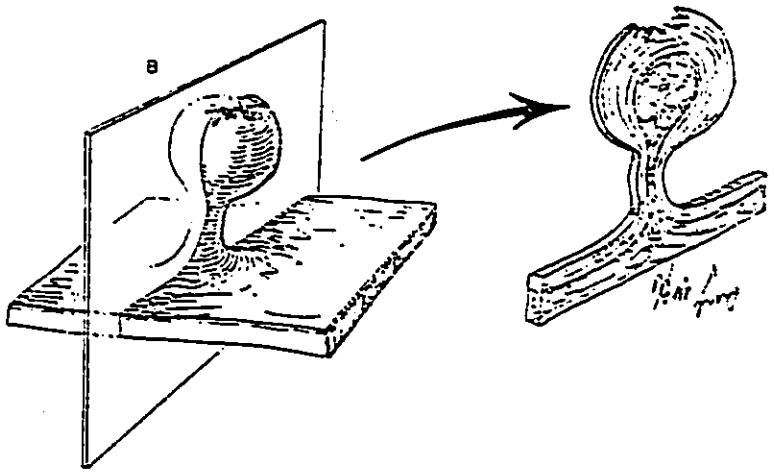

from Principles and Techniques of Surgical Pathology,
Schmidt, W. A., Addison-Wesley Pub. Co. 1983.

Since most of the specimens obtained were from colon, and since colon cancer is well documented and, unlike breast cancer, is not under the influence of steroid hormones, the colon data base was selected for more rigorous study.

As with other types of cancer, the cause of colon cancer is unknown, but the progression of the disease is well documented. Although infectious diseases can occur in the bowel, they almost never lead to cancer. Idiopathic inflammatory disease, however, particularly ulcerative colitis, leads to dysplasia and carcinoma in patients with long-term illness. We obtained only 1 tumour specimen from a patient with a chronic inflammatory ailment (Crohn's Disease). Premalignant changes can occur in the form of hyperplasia (an increase in number of one type of cell) or dysplasia (abnormal development or growth of cells), the latter usually in the form of a polyp (an outgrowth from the interior wall of the intestine - see Fig.4-1). Dysplasia ranges from low to high grade. Types near the low grade end of the spectrum can regress to normality, or they can progress toward high grade, in which case progression to malignancy is probable, but not inevitable. Malignancy indicates the invasive property of a tumour with the potential for metastasis, i.e. a cancerous state, whereas a benign tumour can grow in size, pushing on the tissue where it occurs, but it does not invade or infiltrate the host tissue. It is self-contained with no potential for

metastasis. Polyps can be either benign or malignant. The T_2 values measured in this study for both benign and malignant polyps are high (greater than 500 ms) and indeed, according to most pathologists, benign polyps can be considered premalignant. What is unknown is the length of time necessary for the progression to malignancy.

Once the progression to malignancy has occurred, there are two basic means of describing the state of malignancy : grading and staging. Grading has been defined as "an attempt to measure tumour aggressiveness, i.e. the capacity to spread, metastasize and ultimately kill...and is essentially a subjective composite appraisal of a number of discrete histopathological parameters." (Jass et al. 1983). The word "subjective" should be underlined, for all pathologists would agree that grading is in the eye of the beholder. Several parameters are examined to describe how the cells in question differ from their normal counterparts, and in the end the question of grading narrows down to the differentiation of the cells and how closely they resemble the natural architecture of the organ in which they arise. The cells of a well-differentiated tumour closely resemble the host cells whereas those of a poorly-differentiated tumour bear little resemblance to the normal cells amongst which they are growing. A poorly differentiated tumour has a poor prognosis (outlook for survival of the patient), and as the degree of differentiation increases, the prognosis

Figure 4-2. Dukes' Original Classification.

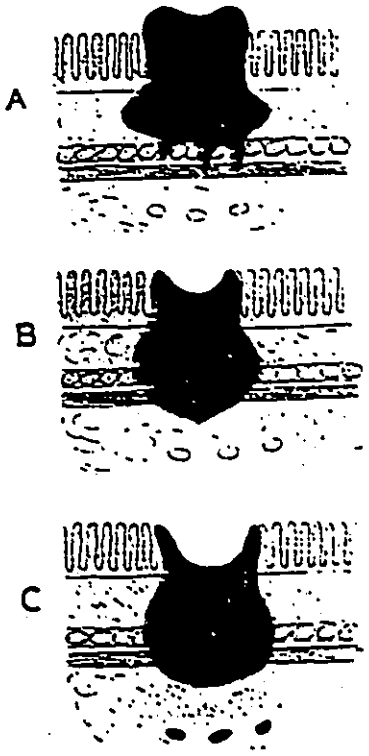

A. GROWTH LIMITED TO WALL OF RECTUM.
B. EXTENSION OF GROWTH TO EXTRA RECTAL TISSUES BUT NO METASTASES IN REGIONAL LYMPH NODES.
C. METASTASES IN REGIONAL LYMPH NODES

Extent of spread of cancer of rectum.

from Kyriakos, M. (1985) Arch. Pathol. Lab. Med. Vol.109 Dec.

improves. Cuthbert E. Dukes, the "father" of colonic staging, did not consider grading, to him a measure of the pace of growth, as important a parameter as staging. He looked at the character of the tumour growth as a whole, and the arrangement of the cells, rather than the amount of differentiation. Dukes and Bussey in 1958 published the grading of 2447 rectal cancers using a three grade system, but neglected to define the precise criteria which they used, and to this day confusion and subjectivity abound in the grading of colorectal cancer.

Whereas grading describes the type of cells present in a tumour, staging describes the invasiveness of the tumour at the time of biopsy, i.e. how far it has penetrated through the bowel wall. As mentioned above, Dukes was the first, in 1932, to describe a system of staging for colon tumours in his classic article "The Classification of Cancer of the Rectum" (see Fig.4-2). Despite many modifications by others to his original classification throughout the years (Zinkin 1983, Hutter and Sobin 1986, Jass et al. 1987), his system is still frequently used, and often misused.

Shortly after the present project was begun in May 1985, the President of the United States of America, Mr. Ronald Reagan, had a right hemicolectomy for a polyploid cecal tumour (an operation to remove a polyp from his intestine). Needless to say this was headline news, and a very interesting article by Kyriakos (1985) entitled "The

Figure 4-3. The Astler-Coller Classification.

Astler-Coller Modification of Dukes' Classification of Colonic Cancer

TYPE	DEFINITION	5 YR. SURVIVAL RATE
A	Lesion limited to the mucosa	84.0%
B_1	Lesions extending into the muscularis but not penetrating it, with negative nodes	66.0%
B_2	Lesions penetrating the muscularis but with negative nodes	63.9%
C_1	Tumor penetrating all layers, lower nodes positive but highest node negative	42.8%
C_2	Tumor penetrating all layers, lower nodes *and* highest node positive	22.8%

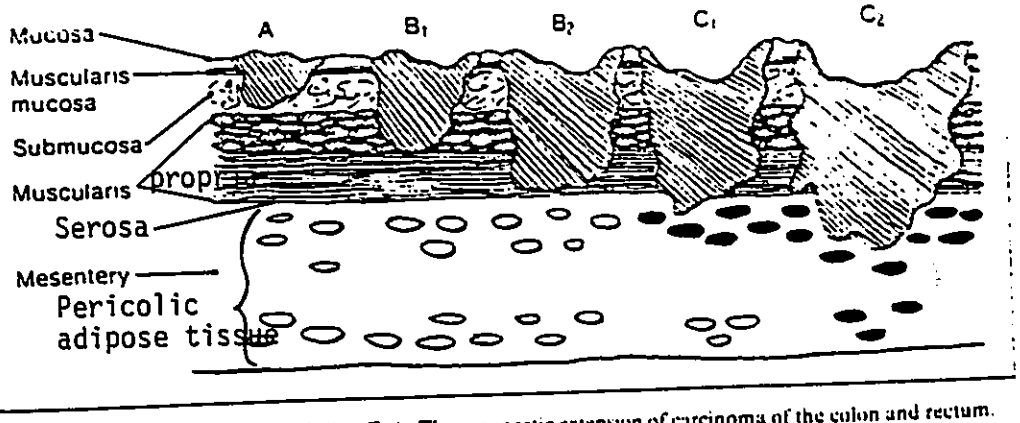

From Astler, V. B. and Coller, F. A. The prognostic extension of carcinoma of the colon and rectum. *Ann. Surg.*, 1954, 139:846.

from Principles and Techniques of Surgical Pathology,
Schmidt, W. A., Addison-Wesley Pub. Co. 1983.

President's Cancer, the Dukes Classification, and Confusion" commented strongly on the ensuing chaos from misdiagnosis of the President's tumour, a result of misuse of Dukes' original classification. The first reported diagnosis of a Dukes B tumour, with prognosis of a mere 50%, was later corrected to an Astler-Coller B1, a subcategory of Dukes A, with a prognosis greater than 50% but less than 85-90%, a much better outlook for Mr. Reagan and the world economy. To avoid further confusion, this thesis will clearly define the staging system used for the colon data in the results to follow.

The colonic wall can be divided into distinct layers, and staging indicates the layers through which the tumour has penetrated. Fig.4-2 shows the original Dukes Classification. Fig.4-3 illustrates the Astler-Coller modification frequently in use. The author has in turn modified the latter slightly, as described below :

Class A - tumour or lesion limited to mucosa and submucosa (Astler-Coller A)

Class B - tumour penetrating the muscularis to various depths, possibly through serosa to border of pericolic adipose tissue
- no lymph node involvement
B1 - tumours extending partway through muscularis
B2 - tumours extending through to the serosa (Astler-Coller B)

Class C - tumour extending through all layers of bowel wall, with tumour infiltrating at least one lymph node (Dukes C)

Class D - tumour metastasizing beyond lymph nodes, to other parts of body

(Dukes D)

Grading and staging are not the only parameters which can be used to describe colon tumours. Jass et al. (1983) did an extensive study in order to discover the best combination of parameters for prognosis. Various combinations of grade-related parameters such as lymphocytic infiltration at the tumour site and pattern of growth were tried, as well as stage-related parameters, and analyzed statistically. The best model for prognosis depended on the number of lymph nodes affected, the presence of lymphocytic infiltration and the extent of spread through the bowel wall. Wolmark et al. (1984) found that for Dukes C cancers, the significant variable for prognosis was depth of penetration, which was related to tumour size and the number of positive lymph nodes. But tumour size was not related to the number of positive lymph nodes. Dukes B and Astler-Coller C2 tumours were similar in size, yet Dukes B never involves the lymph nodes by definition, whereas C2 always does. The number of lymph nodes involved is the most important prognostic indicator in colon cancer, and since this bears no correlation to tumour size, the size of the primary tumour burden was excluded from the present study for a correlation with T_2 values.

In a recent article, Jass and Morson (1987) stressed the need for a universal system of classification in order to compare pathological findings and treatment results between

different hospitals. They extend their previous findings and propose a new system based on several parameters, as determined by multivariate regression analysis : the number of lymph nodes affected, the character of the invasive margin of the tumour, the presence of lymphocytic infiltration, and the extent of local spread of the tumour. Scoring of these four variables is translated into four prognosic groups. Although the 5-year survival figures for these four groups are similar to those for patients in the Dukes' stages A,B,C1 and C2, more patients are allocated to groups with a clear cut prognosis using the new method. It will be several years until the usefulness of this new system will be proven. With the numerous rival pathological staging systems presently in existence, one universally accepted system would aid tremendously (in the testing of new drugs, for example, in several treatment centres) in the overall treatment of colon cancer.

Materials and Methods

Colon Samples

The colon samples used for this extended analysis were the same samples as in the colon data base described in the previous chapter. All tumours included in the study were primary. The tumours or lesions are rounded and circular in shape, and the pieces cut for NMR studies were taken in cross-section from the centre to the outer edge, with the

bulk from the outer perimeter. At times greyish-green or yellowish necrotic portions would be included in the sample, but generally these would be excised along with the bright yellow adipose tissue and burgundy-coloured vasculature, in order to have as clean a sample as possible of viable tumour tissue. In cases where very little sample was received, the total was used for NMR, in order to have sufficient height (3 to 4 cm) of tissue in the NMR tube for the sample to fill the coil of the magnet. The samples were cut into pieces small enough to fit into a 5 mm NMR tube. The tumours received ranged from firm in texture (almost crunchy to cut), greyish-white in colour, to a soft and slimey consistency, pinkish-white in colour. Due to the differences in amount received and the great variability in tissue morphology, even to the naked eye, the samples for NMR were heterogeneous indeed. Yet all were colon tumours, originating from one type of body tissue.

"Normal" colon specimens from the same patient were received with some colon tumour samples. These consisted of a section of the colonic mucosa at the resection margins. This is part of the same length of colon that contained the tumour, but at a distance from the tumour, a part that is "clean", i.e. containing no evidence of disease by histological examination.

Histological Data

Figure 4-4. Colon sections taken for histological analysis.

Sections from small bowel

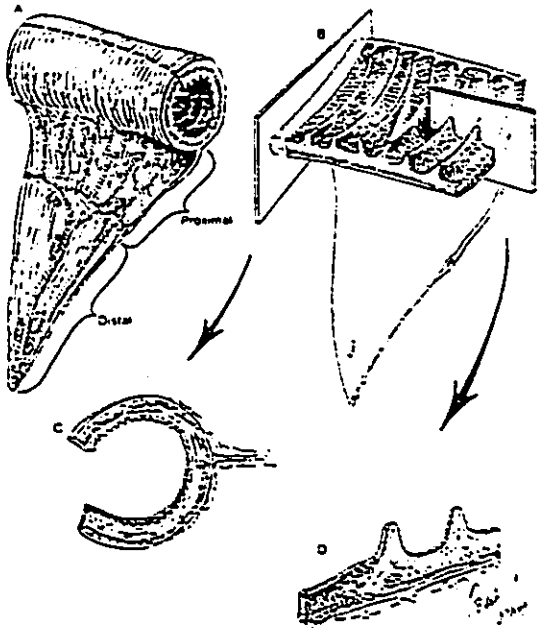

Sections from large bowel

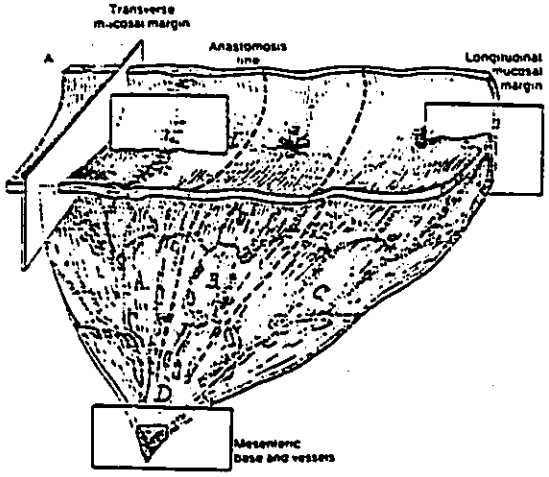

from Principles and Techniques of Surgical Pathology, Schmidt, W. A., Addison-Wesley Pub. Co. 1983.

Figure 4-5. Example of hospital pathology report.

OTTAWA CIVIC HOSPITAL

SURGICAL PATHOLOGY REPORT APR 10

NAME [redacted] SEX F DATE April 8, 1987 NO. S4716-87

WARD ES AGE 19-06-25 NATURE OF SPECIMEN RECTUM
MESENTERIC BIOPSY

HOSPITAL # 715 551 8 HISTORY Rectal bleeding - tumor easily palpable.
Biopsy confirmed carcinoma.
PRE & POST-OP DIAGNOSIS: Ca rectum.

SERVICE OF [redacted]
Box #42

GROSS
The specimen is received in two different containers labelled #1 "RECTUM", and #2 "MESENTERIC BIOPSY".
Specimen #1 consists of the rectum, anal verge, and the anus. It measures 28 x 4.5 cm in the widest dimensions. The external surface looks unremarkable with the exception of some areas of congestion and hemorrhage of the appendix epiploica. In the area of the anus there are fragments of striated muscle. The mucosa of the anus looks unremarkable with the exception of the presence of external hemorrhoics, however a large fungated and ulcerated tumor mass is seen arising right at the version of the anal verge and the rectum. The lesion measures 6 x 4 cm in its largest dimensions and 0.7 cm in the thickness of the wall and it is extending through the wall and into the serosa. The rest of the mucosa looks unremarkable with the exception of two small metaplastic polyps.
Specimen #2, mesenteric biopsy, consists of three small fragments of fibrofatty tissue which weigh 5 grams. They look grossly unremarkable with the exception of a small cyst cavity measuring 0.7 cm in its largest dimensions, filled with clear fluid.
The following sections are submitted: Cassette A and B - surgical resection margins.
MICROSCOPIC Cassette C, D, E, F and J - samples of the tumor, serosa and anal verge.
Cassette H, J, K - lymph nodes.
Specimen #2 - representative samples of the cyst submitted in cassette L. GO/mm

MICROSCOPIC:
Sections of the proximal colonic and distal anal resection margins show no evidence of malignancy. The sections of the tumour show an infiltrating adenocarcinoma which exhibits glandular differentiation in most areas. It is associated with a desmoplastic stromal response and chronic inflammation. Many sections show the tumour extending through the muscularis propria into the serosal fat. Focal necrosis is present. In some areas remnants of a villocubular adenoma can be seen. Sections of nine pericolic lymph nodes show no evidence of metastatic tumour.

The mesenteric biopsy shows a mature fatty tissue with no evidence of malignancy.

T	M	E	F

DIAGNOSIS
1. MODERATELY WELL DIFFERENTIATED ADENOCARCINOMA RISING IN VILLOTUBULAR ADENOMA AND EXTENDING THROUGH BOWEL WALL TO SEROSA - RECTUM.
2. NO PATHOLOGIC DIAGNOSIS - 9 PERICOLIC LYMPH NODES.
3. NO PATHOLOGIC DIAGNOSIS - MESENTERIC BIOPSY.

BB/dn
April 7/87

PATHOLOGIST _____ MD

Figure 4-6. Section of tabulated histological data for colon samples.

SAMPLE NUMBER	HOSPITAL NUMBER	METASTATIC STATUS	NO. OF LYMPH NODES INVOLVED	DUKE'S CLASSIFICATION	EXTENT OF SPREAD THRU BOWEL WALL	LYMPHOCYTIC INFILTRATION	TUMOUR GROWTH PATTERN	PRIMARY TUMOUR [illegible]	LONGEST T_1 (BY HAND)	LONGEST T_2 (COMPUTERIZED)	additional
107	570721-7	N		B	full thickness → to subserosal tissue	several dense foci		6 cm dia.	392	578	mod. well diff
108	654452-2	N	0	B	full thickness → [illegible]	mild infiltration by chronic inflam cells [illegible]	[illegible]	6 cm diameter	384	367	mod well diff.
109	543315-6	N		B	thru entire thick of bowel wall	chronic inflam cells	stroma	2.5 x 2.5 x [illegible]	496	705	mod well diff.
111	656458-7	N		B	→ [illegible]		infiltr.	6 cm dia	944	934	Colloid [illegible]
114	328419-7	N		B	→ [illegible]			5 x 3 cm.	648	876	mod [illegible] diff.
115	658406-4	N	C	B	deeply into muscularis propria		infiltrating	1.5 cm thick	544	534	mod. well diff.
119	452622-4	Y	2 (adj-)	C	thru wall → [illegible]			8 x 4 x .8 cm	752	1071	mod diff.
123	371424-3	Y	1	C	thru all layers of wall & [illegible]	mild to moderate	infiltrating	.7 cm thick 3.5 cm long	898/904	958	moderately well d
124	458070-0	N	C	E	→ [illegible]	moderate chronic [illegible]	infiltrating (bunching of cells)	6.3 cm wide	688	630	mod. well
126	412359-4	Y	2 (adj-)	C	→ pericolonic adipose	minimal lymphocytic response to tumour		3.5 cm dia.	520	509	mod well
127	645566	N	[illegible]	B	→ [illegible]	[illegible]	[illegible]	10 cm x (3) 2 cm thick thru wall 5 cm long	752	1153	mod well
130A	469649-8	N	0	B	→ [illegible]	chronic [illegible]	infiltrating	?	512	496	well
130B	"	N		B				[illegible]	368	506	
131	463079-4	N	0	B	thru entire thick → pericolonic adipose tissue	yes; colitis	infiltrating	5 cm dia.	794	643	well
137	664131-0	Y	6 (adj)	C	→ [illegible]	[illegible]	[illegible]	[illegible]	340	331	mod to poorly diff.
138	422534-8	Y	5 (adj)	C	full thick of muscularis propria			polypoid [illegible]	524	622	mod to poorly (diff.
138	"	Y		C	→ pericolonic tissue	focal chronic inflam. cells infiltrate		4.5 cm dia	364	331	
139	667699-3	N		B	thru bowel wall → [illegible]	focal areas of chronic inflam.		3 cm dia.	408	421	mod well
142	344042-7	Y	2 (adj)	C	into but not thru muscularis			3 cm dia.	608	592	mod well
143	515494-3	N	0	B	thru muscularis propria		infiltrating		588	638	mod well

Fig.4-4 shows the sections taken from small and large bowel samples for histological analysis. Both gross (as viewed by the unaided eye) and microscopic examination is routinely performed on all excised specimens. Photocopies of the original hospital pathology reports were received for each specimen studied by NMR. An example is shown in Fig.4-5. Relevant data from these reports were tabulated as shown in Fig.4-6. These were compared with the T_2 relaxation times observed for each sample.

T_2 Relaxation Times

The methylene (lipid) peak at 1.3 ppm is a composite peak comprised mainly of acyl chain resonances, as well as several other underlying resonances, those due to fucose and lactate among them. T_2 values for the peak at 1.3 ppm were obtained for each sample, as explained in detail in the previous chapter. As for the histograms, the longest T_2 value, that corresponding to the relaxation time of the proposed malignancy/metastasis marker fucose, was chosen for the analyses. The shorter T_2 components (less than 300 ms) are attributable to lipids, whereas any longer than 1 second are most likely influenced by the presence of lactate. The presence of these shorter and longer components can influence the magnitude of the relaxation component due to fucose, depending on the proportion of each in a tumour sample. The T_2 value used is thus a composite average from

Figure 4-7. Measurements of linewidth at half-height for the methylene peak and Fossel number.

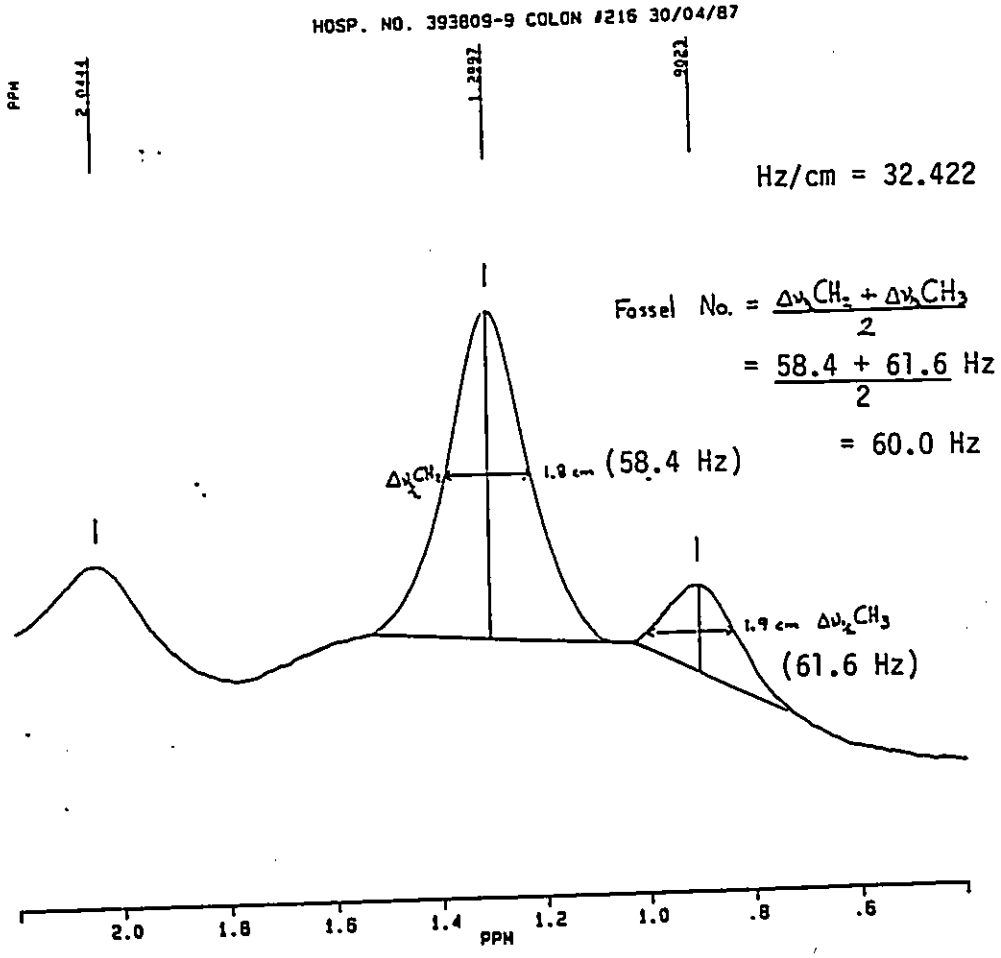

the molecular species present in the sample. It is difficult to extract the value due to fucose alone by the T_2 calculation method used.

Linewidth at Half-height of the Methylene Peak and Fossel Number

With the finding of Fossel et al. (1986) that the average of the linewidths at half-height of the methylene (CH_2) and methyl (CH_3) peaks in the ^1H NMR spectrum of plasma from cancer patients was significantly different from that of normal patients, it was decided to test this relationship for solid tumours. The spectra of "normal" colonic tissue, benign and malignant polyps, benign tumour, and the various stages of tumour progression were examined and measured for this purpose, as illustrated in Fig.4-7. Each spectrum was normalized to compensate for the different amounts of tissue used and the different NMR acquisition parameters, and plotted from 0.4 to 2.2 ppm to include the CH_2 and CH_3 peaks. One representative sample from each group was examined for initial comparison. Analysis of more samples was then undertaken to confirm the trend apparent in this cross-section of samples.

Presence of $N^+(CH_3)_3$ (Choline) Peak

It was observed by Mountford et al. (1982) that upon transformation of lymphocytes, the peak attributable to the choline head group of cell-surface phospholipids narrowed

Figure 4-8.

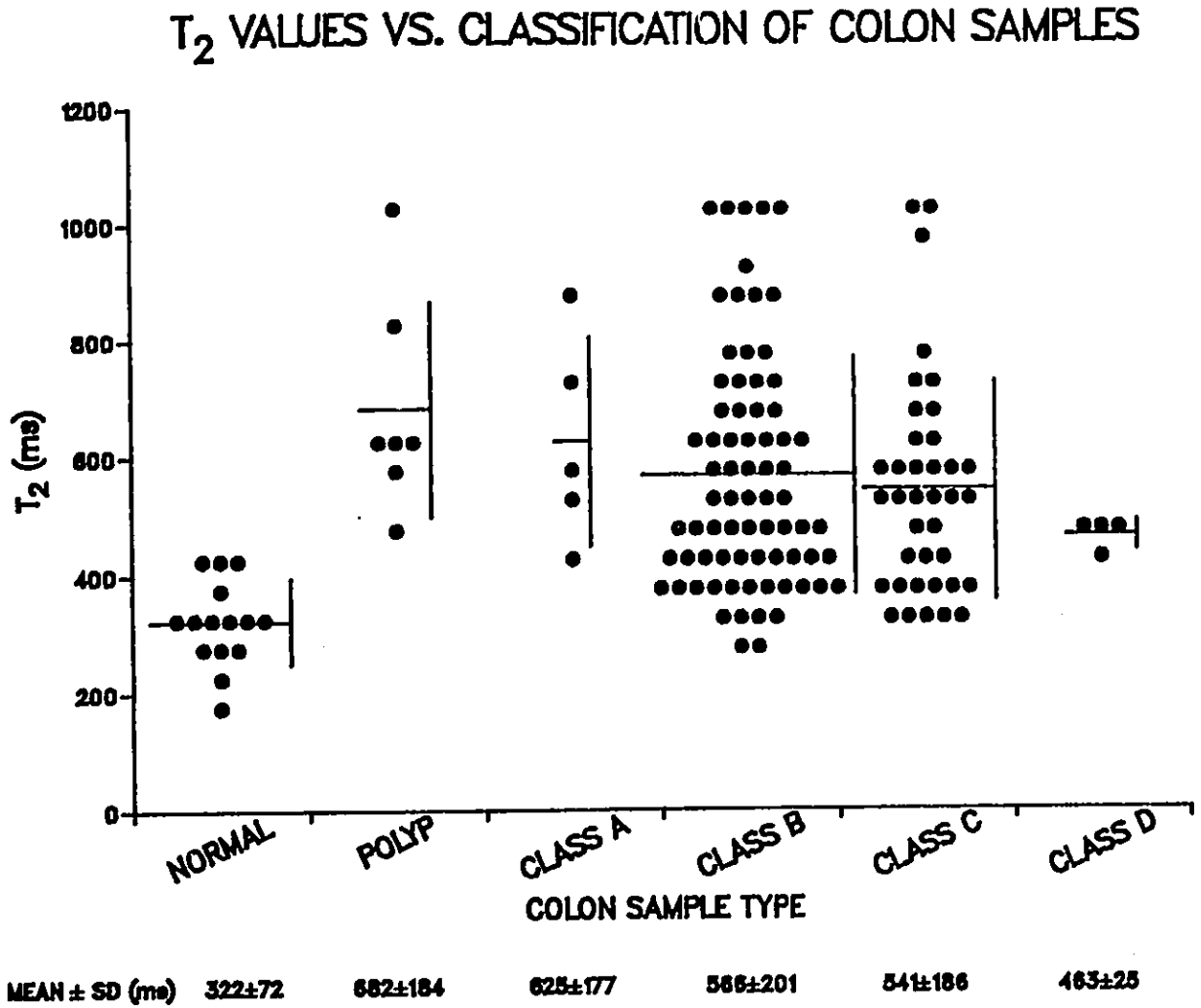
T2 VALUES VS. CLASSIFICATION OF COLON SAMPLES
T2 (ms)
1200
1000
800
600
400
200
0
NORMAL
POLYP
CLASS A
CLASS B
CLASS C
CLASS D
COLON SAMPLE TYPE
MEAN ± SD (ms) 322±72 682±184 625±177 566±201 541±186 463±25

and grew dramatically in intensity. Upon biochemical analysis of normal and transformed cells, it was found that the amount of choline did not differ significantly in the two cell types. The change observed in the peak was therefore attributed to an increase in mobility of the choline head group upon transformation. The presence and character of the $N_+(CH_3)_3$ peak was noted in the spectra of normal samples and tumour samples in various stages of cancer progression.

Results and Discussion

T_2 Values vs. Classification of Colon Samples (Fig.4-8)

T_2 values for "normal" colonic mucosa are always less than 450 ms. The single inflammatory polyp has a very short T_2. As a possible premalignant state, the other polyps, both "benign" and malignant, always have a T_2 greater than 450 ms, as do the Astler-Coller A tumours, which are limited to the mucosa and sub-mucosa. As the tumours progress further in their invasion through the colonic wall, becoming B's and C's, the range of T_2 values changes. Most of the T_2 values are above 450 ms, but a substantial number fall beneath this level, overlapping the range of "normal" values. The four Dukes D samples yield a narrow range of T_2's from 425 to 500 ms.

There is an excellent separation of T_2 values for "normal" colonic tissue (as well as the one inflammatory

polyp and two benign samples) and premalignant polyps and Class A tumours at the initial stage of cancer growth. This difference could prove very useful for diagnosis of malignancy by Magnetic Resonance Spectroscopy (MRS). Early detection of cancer would be the aim of any diagnostic procedure and this significant elevation in T_2 values at the initial stages of the disease could lead to earlier treatment and a better prognosis. These T_2 values were obtained from biopsies, meaning the patients presented with symptoms requiring surgery. It is not inconceivable that in the future, MRS using a whole body imager could provide T_2 values of sections of colon non-invasively, either as part of a routine medical check-up or as confirmation of the nature of a patient's symptoms. Magnetic Resonance Imaging (MRI) would localize tumours or polyps, while T_2 values of the lipid peak by MRS would indicate the stage of that section of colon. Perhaps some surgeries could be avoided.

Progressing to the B and C categories, these cancers are more established and aggressive. Most of the samples received turned out to be B's and C's, mainly because it is usually at these stages that patients develop symptoms. The shorter T_2 values (lying within the normal range) are not of concern at this stage for diagnostic purposes, for it is clearly evident that the patient has cancer by the usual pathological examination.

Two interpretations are possible for the shorter T_2

values with progression of colonic cancer. Firstly, it is possible that the MRS marker is in greater evidence at the initial stages of the disease, yielding longer T_2's. Two-dimensional NMR (next Chapter) indicates that the source of the long T_2 could likely be fucose, a sugar found at the terminus of cell-surface oligosaccharides (Mountford et al. 1987). One can speculate as to its function, whether it be to keep the immune system of the host at bay, or part of the immune response itself, strong initially and declining as the tumour gains a foothold and progresses, or whether it is part of the process for disseminating the cancer, one requirement for the process of metastasis, and decreases once its function is fulfilled. There is always pattern in nature, whether normal or pathological, and the tumour marker evidenced by NMR is part of the pattern of cancer.

The second interpretation is that the amount of the long T_2 -yielding entity does not change, but that the proportion of other molecular components changes, thus masking the presence of the MRS marker. Holmes et al. (1988) in their paper on the biochemical basis of the Fossel test disclose that the ^1H NMR linewidth of the CH_2 lipid peak decreases in cancer because of an increase in the amount of lipid present, notably triglycerides and cholester esters. Lipids have relatively short T_2 values, of the order of 200 to 300 ms, and as the proportion of mobile lipids increases, it can average the resultant T_2 relaxation time to a much lower

value than it would otherwise have. In the same manner, a large amount of lactate in the sample could give longer T_2 values (greater than 1 second) than normally found for fucose (600 to 700 ms - personal communication with Dr. Mountford). Lactate analysis was performed on 44 colon tumour samples. Lipid analysis was undertaken on only three samples due to lack of time and biohazard requirements for human tumour samples (the results of these analyses will be discussed in Chapter 6). Nonetheless, for the samples with low T_2 values and several with long T_2's, the relaxation component due to lipid was extrapolated to the X-axis on the semilog plots of Intensity vs. Delay Time in order to discern the amount of overlap in the fucose range. The overlap appears to come at the same place for tumours with short T_2's as for long T_2's, and the amount of lactate in the samples does not correlate with the resultant T_2 values (see Chapter 6). It is a very real problem with our present T_2 calculation procedure to isolate the relaxation component due to fucose, i.e. to eliminate the stronger components due to lipid and lactate. Yet their presence does not seem to influence in any logical way the resultant longest T_2 value. Perhaps the problem must await more lipid analysis, as well as lactate analysis on subsequent samples. Or perhaps the first interpretation is true, that the amount of the MRS marker decreases with progression of the disease.

Very few biopsy specimens were received from a Dukes D

Table 4-1. Depth of penetration vs. T_2 for Astler-Coller B tumours.

T_2 range	Astler-Coller*		through layers specifically		
	B_1	B_2	in muscularis propria	extending to serosa	extending to pericolic adipose
250-299		11		11	
300-349	11	11	11	11	
350-399	11	~~1111~~ 111	1	1111	~~1111~~
400-449		~~1111~~ 111		1	~~1111~~ 11
450-499	~~1111~~	1111	~~1111~~	11	11
500-549	1	111	11	1	1
550-599		~~1111~~		111	111
600-649		~~1111~~		111	111
650-699	1	111	1	11	1
700-749		111		11	1
750-799	1	111	1	11	1
800-849					
850-899	1	111	11	1	1
900-949		11		1	1
950-999					
1000+		111		11	1

*Astler-Coller Classification :

B_1 - tumour penetrates into muscularis propria, but not all the way through it

B_2 - tumour goes through muscularis propria, to serosa and beyond

tumour, where metastasis has occurred to other parts of the body. The disease is usually caught at the B or C stages. It is interesting that the T_2's of the four Dukes D's are just above normal range, but no higher than 500 ms. T_2 appears to decrease with the terminal stages of the disease.

The Wilcoxon Rank Sum Test was applied to test for statistical differences between the various stages of colon cancer and their respective spread of T_2 values. Polyps and Class A tumours effectively form one population as do Class B and C tumours, and both populations are significantly different from the "normal" population with respect to T_2 values, with a 99% confidence interval. There was an insufficient number of Dukes D tumours to form a statistical base.

Astler-Coller B's : Depth of Penetration vs. T_2 (Table 4-1)

Dukes C's all penetrate the entire bowel wall, and invade at least one lymph node, yet their T_2 values encompass the whole range from low to high. Here the T_2 -determining parameter is obviously not depth of penetration.

What of the Astler-Coller B tumours? Is there a correlation between depth of penetration and T_2 ? The B's were subdivided into B1's and B2's, B2's penetrating further than B1's, but no difference in range of T_2 values was found between the two groups. The B's were again subdivided

Figure 4-9.

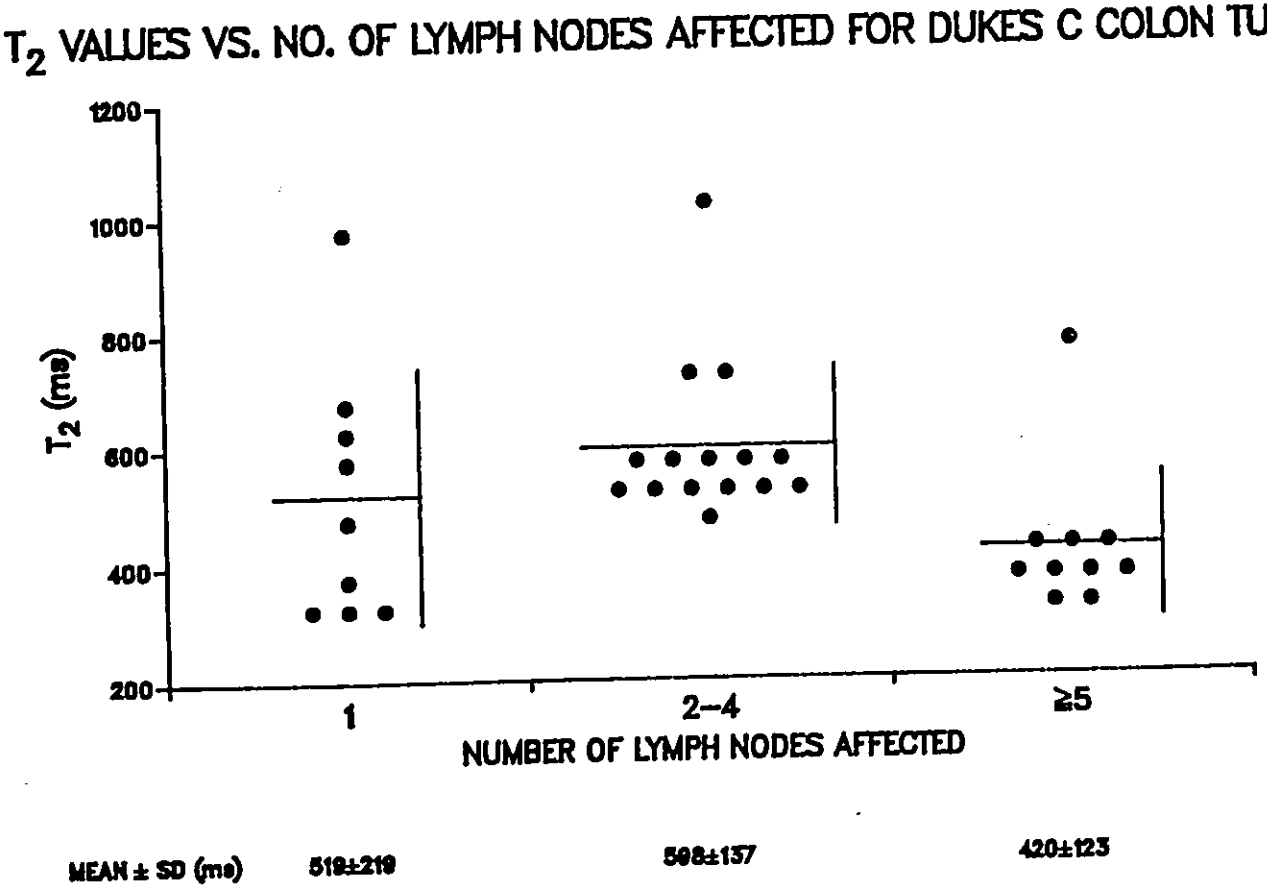
T_2 VALUES VS. NO. OF LYMPH NODES AFFECTED FOR DUKES C COLON TUMOURS
1200
1000
800
600
400
200
T_2 (ms)
1
2–4
≥5
NUMBER OF LYMPH NODES AFFECTED
MEAN ± SD (ms)
519±219
598±137
420±123

according to the specific layer reached by the tumour - involving only the muscularis propria, extending to the serosa, and penetrating through the serosa to the pericolic adipose tissue boundary. Once again, no correlation was found between T_2 and depth of penetration.

It would be interesting to see if a relationship exists between space (physical area invaded) and time (the length of time taken for this particular tumour to invade this space, i.e. aggressiveness) of tumour invasion and T_2. This we cannot measure for our samples, for we get a freeze-frame of the end result. It might be possible, however, to test this hypothesis using a small animal imaging machine such as the Bruker Medspec, to perform MRS/MRI experiments on tumours implanted in animals.

Perhaps a relationship will exist for T_2 value vs. metastatic potential for B tumours. Will only the B tumours with T_2's greater than 450 ms metastasize? Have the B tumours with T_2 less than 450 ms lost the capacity to metastasize, or, have they already metastasized, in keeping with the trend that T_2 decreases post-metastasis, but with metastases of insufficient size to be clinically evident? Only time, and results from the follow-up questionnaires can answer these questions.

T_2 Values vs. No. of Lymph Nodes Affected for Dukes C Colon Tumours (Fig.4-9)

The distribution of T_2 values depending on the number of

lymph nodes invaded for Dukes C tumours shows an interesting parabolic pattern. The T_2's are elevated as the number of lymph nodes affected increases from 1 to 2-4 and decrease as the degree of metastasis increases. The T_2's of the primary tumours which are very metastatic, i.e. greater than 5 lymph nodes involved, have decreased by approximately 200 ms from samples where 2-4 lymph nodes are affected. The Wilcoxon Rank Sum Test indeed shows a statistically significant difference (99% confidence interval) between these two populations. There is no statistically significant difference, however, in the spread of T_2 values between tumours with 1 lymph node affected and those with 2-4, nor between tumours with 1 lymph node affected and those with greater than 5. Whether the amount of the metastatic marker decreases as metastasis occurs in greater amount, or whether the amount of free lipid increases is yet to be resolved. Two-dimensional NMR could give an indication of this in the magnitude of a certain cross peak which is attributed to the MRS marker, as well as the width at half-height of the lipid peak in the one-dimensional spectrum obtained for each sample.

The T_2's of colon tumours were also examined with respect to degree of differentiation in the tumour. Five samples were received that were histologically diagnosed as poorly differentiated, which indicates a very poor prognosis. Four of these were Dukes C tumours, all with T_2's

less than 450 ms, reaffirming the observation that T_2 appears to decrease with worsening of the disease process. The fifth was a Dukes B, with a T_2 of 465 ms, a relatively low value in the malignancy range.

Linewidth at Half-height of the Methylene Peak and Fossel Number

There are several resonances under the prominent CH_2 peak, including that of the proposed marker fucose, and that of lactate, the metabolic by-product omnipresent in tissues, especially in tumour samples. There are probably many more resonances, but fortunately these do not show up in 2-D NMR COSY spectra (next Chapter). The major determining factor, however, for the width of the CH_2 peak is the type and amount of lipid present. If there are several types, each with slightly different resonance frequencies, the peak is broadened. An increase in any one type of lipid, on the other hand, results in peak narrowing.

Early experiments with gadolinium (Gd^{3+}), which does not penetrate the cellular plasma membrane, but broadens the CH_2 peak (Mountford et al. 1982), have shown that the lipids in question are associated with the plasma membrane. Wright et al. (1986) have proposed that special lipoprotein particles, malignancy-associated lipoproteins (MAL) on the cell surface give rise to the high resolution lipid peak observed. They suggest that these particles are shed from the cell at some point in the disease process, and are perhaps the same

particles observed in the blood of cancer patients (Wieczorek et al. 1986). Experiments by Rosi et al. (1987) indicate that lipoprotein particles are found in the supernatant of tumour cell membrane preparations.

In serum, the amount of VLDL increases with cancer (Dilman et al. 1981) as with hyperlipidemia (Holmes et al. 1988) and since VLDL particles contain a large amount of triglycerides, which are very mobile within the lipoprotein core, the lipid resonance centred at 1.3 ppm. narrows. An increase in molecular motion can also be responsible for the narrowing phenomenon.

In the foregoing discussion, serum, tumour cell suspensions, and solid tumours have been discussed interchangeably with respect to lipoprotein composition. What is their connection with each other?

Brown et al. (1975 - including the Nobel-prize-winning team of Goldstein and Brown for their work on the role of the LDL receptor in familial hypercholesterolemia) have shown that the free cholesterol and cholesterol ester levels in human fibroblasts grown in culture depend upon the presence of LDL in the surrounding medium. When supplying nonlipoprotein cholesterol to the cells, the need for the LDL receptor is bypassed, and an increase in free cholesterol is noted. The amount of cholesterol ester produced by the cells, however, is decreased when greater than 50 ug/ml of cholesterol is supplied. The authors do not

Figure 4-10. Change in linewidth at half-height of methylene peak (CH_2) with progression of colon cancer.

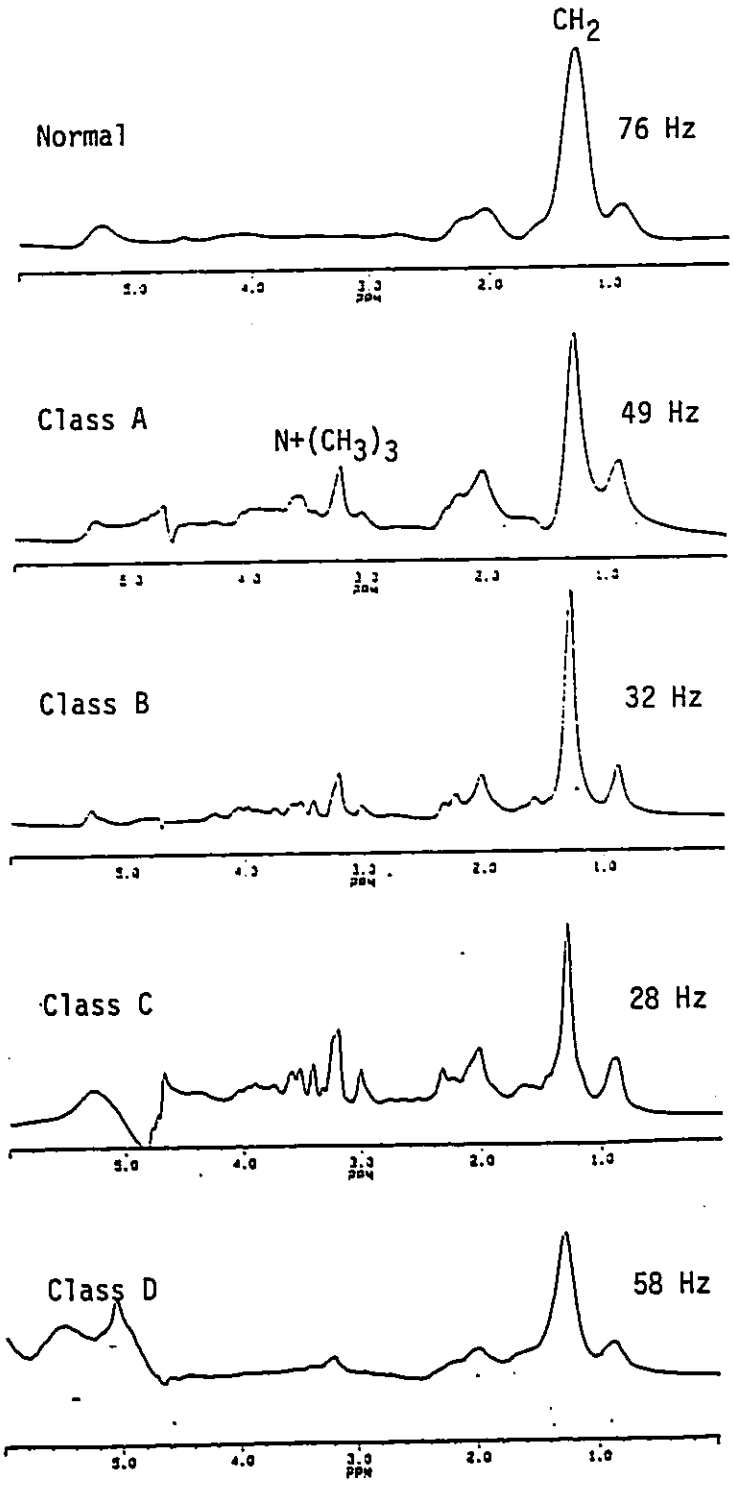

address this point, but their data indicate that the presence of free cholesterol is not the rate-limiting step in cholestrol ester formation, but the availability of fatty acid chains provided by the lipoprotein particle. The cholesterol-to-phospholipid ratio in lymphocyte cell membranes (whose cholesterol equilibrates with that in lipoproteins) decreases with lymphoma and leukemia (Shinitzky and Inbar 1974), resulting in line narrowing. Thus it appears that the lipid composition of tissue cell membranes reflects the composition of lipoproteins in the surrounding medium, the blood. We are observing lipoprotein-like domains of the cell membrane in our spectra (Williams et al. 1985). Whether produced by the tumour itself, or the result of the interaction of integral membrane domains with an incoming malignancy-associated-lipoprotein, the NMR spectrum of solid tissue should be comparable to that of lipoproteins in blood. The generally broader linewidth associated with solid tissue could result from restricted mobility and possibly greater variety of structure for the dynamic cell membrane.

Normal colonic mucosa gives a high resolution spectrum, characteristic of rapidly dividing tissue. There is a noticeable change in the linewidth at half-height of the lipid peak ($\Delta\nu_{\frac{1}{2}}CH_2$) with cancer progression (see Fig.4-10). A representative sample from each stage of the disease process was chosen at random. $\Delta\nu_{\frac{1}{2}}CH_2$ decreases by

Table 4-2. Linewidth at half-height of methylene peak for colon samples.

Sample Description	CH_2 (Hz)	Fossel No. $\frac{CH_2 + CH_3}{2}$
"Normal" colon	76	70
Benign tumour (cyst)	91	63
Benign polyp	52	54
Malignant Polyp (Class A)	49	49
Benign tumour	49	55
Class A	58	53
Class B	32	34
Class C	28	39
Class C (very metastatic)	97	68
Class D	58	60

Measurements are for one sample in each category.

approximately 20 Hz from the "normal" sample to the polyps and Class A. Classes B and C, the more dynamic, aggressive phase of the cancer, show a decrease in $\Delta\nu_{\frac{1}{2}}CH_2$ by another 20 Hz. For a very metastatic C and a Dukes D, the linewidth increases towards that of the "normal". The Dukes D spectrum resembles that of a "normal" sample, a rather featureless trace but for the CH_2 region.

As the lipid peak decreases in width, there is an increase in the number of peaks between 3.0 and 4.0 ppm attributable to carbohydrate. The $N^+(CH_3)_3$ peak narrows and increases in height. As the cancer reaches its terminal stages, the peaks in this region disappear under the broad envelope at the baseline. Whatever mobility they had previously is lost, or the molecules responsible for these peaks have completely disappeared!

Table 4-2 lists the CH_2 peak width at half-height and the Fossel number for one representative sample from each category.

The same trend is apparent numerically as in the spectra of Fig.4-10. To test the validity of this observed trend, the spectra of 10 "normal" and 57 tumour samples were examined. The complete data base consists of 15 "normal" samples and 128 tumour samples. Spectra for all samples were not printed out at the time of initial processing, since our initial interest was only in the T_2 values. At this later time it is time-consuming and often difficult to locate a

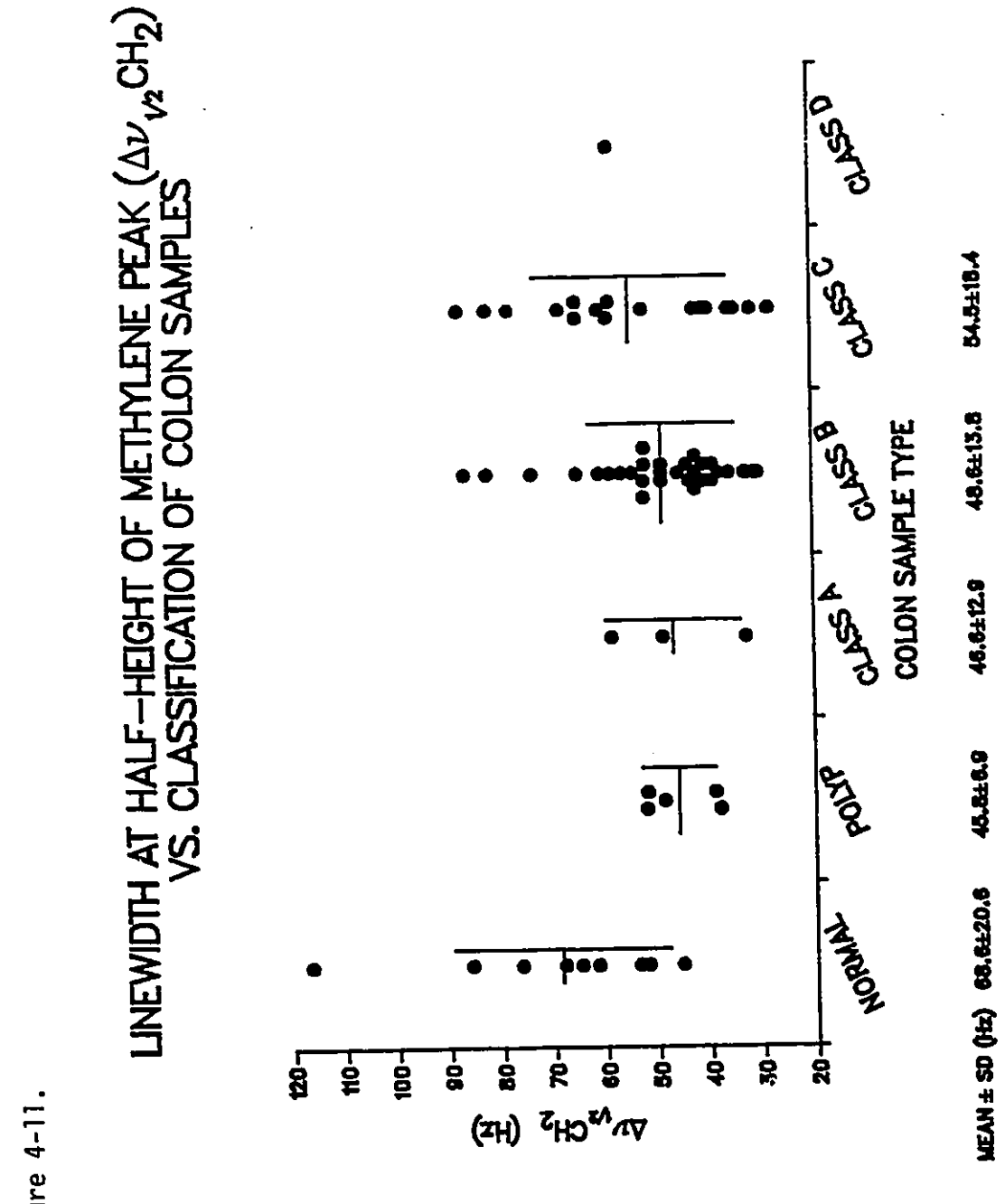
LINEWIDTH AT HALF-HEIGHT OF METHYLENE PEAK ($\Delta\nu_{1/2}CH_2$) VS. CLASSIFICATION OF COLON SAMPLES
$\Delta\nu_{1/2}CH_2$ (Hz)
120
110
100
90
80
70
60
50
40
30
20
NORMAL
POLYP
CLASS A
CLASS B
CLASS C
CLASS D
COLON SAMPLE TYPE
MEAN ± SD (Hz) 68.6±20.6 45.8±8.9 46.6±12.9 48.6±13.8 54.9±18.4

Figure 4-11.

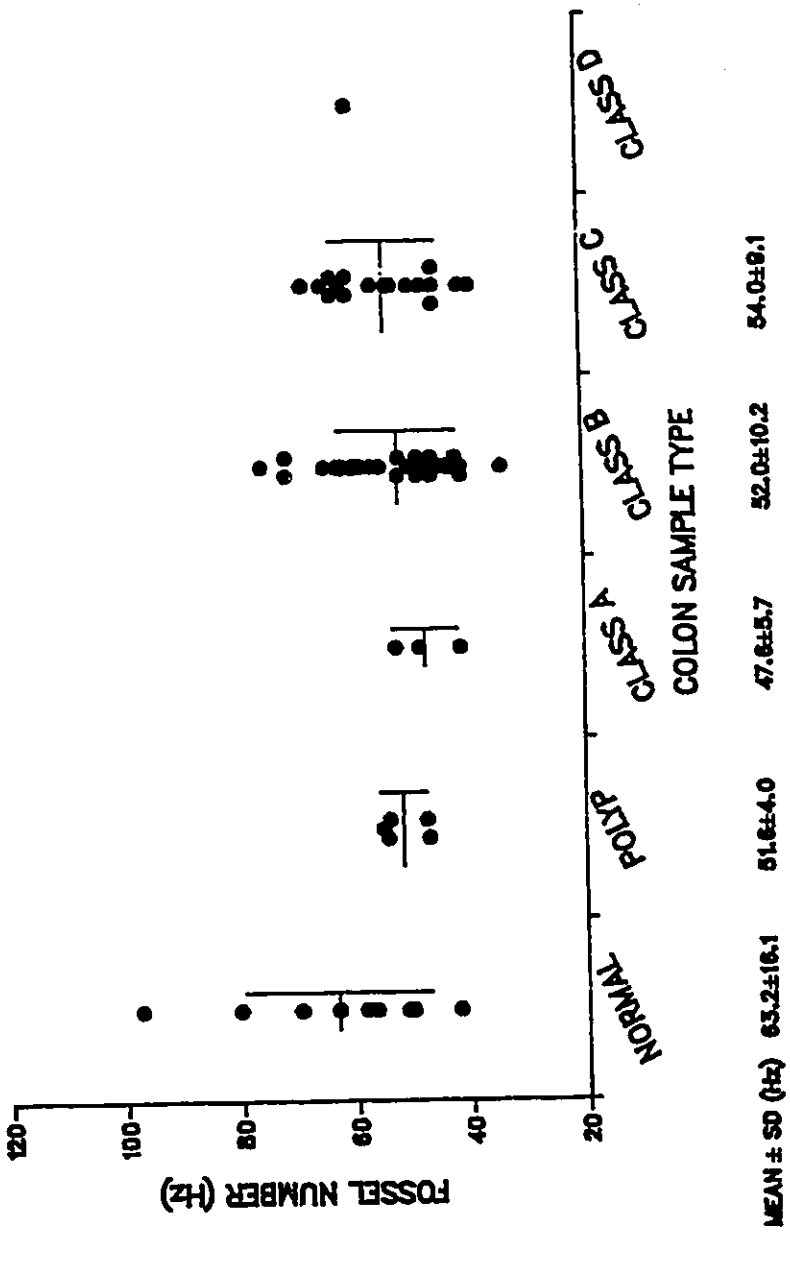
FOSSEL NUMBER VS. CLASSIFICATION OF COLON SAMPLES
FOSSEL NUMBER (Hz)
120
100
80
60
40
20
NORMAL
POLYP
CLASS A
CLASS B
CLASS C
CLASS D
COLON SAMPLE TYPE
MEAN ± SD (Hz) 63.2±16.1 51.6±4.0 47.6±5.7 52.0±10.2 54.0±9.1

Figure 4-12.

certain sample on our numerous tapes. Thus the following results are based on approximately half our data base.

The spread of $\Delta\nu_{\frac{1}{2}}CH_2$ and the Fossel numbers according to classification of colon samples by staging appear in Figs. 4-11 and 4-12, respectively.

In all but the original publication by Fossel, there is considerable overlap between normal and malignant samples for the Fossel numbers of plasma. The situation is similar for our solid tissue samples, as Fig.4-12 shows. Corresponding to the elevation in T_2 values at the initial stages of the disease process, however, polyp and Class A samples have Fossel numbers clustering around the lower range of the "normal" sample values. Yet the excellent separation apparent for T_2 values is clearly lacking. There is less overlap for the linewidth at half-height of the CH_2 peak with two polyps, one Class A, and about 50% of all Class B and Class C samples having smaller $\Delta\nu_{\frac{1}{2}}CH_2$ values than the "normal" colonic tissue samples. The Fossel numbers cover a narrower range of values - including the CH_3 linewidth from the end of the acyl chains averages the numbers closer together. Upon taking sample means, there is a decrease of 10 Hz for the Fossel numbers and 20 Hz for $\Delta\nu_{\frac{1}{2}}CH_2$ from "normal" to malignant tissue. Considering the amount of overlap, however, neither measurement can be used with confidence to discriminate between normal and malignant tissue.

Figure 4-13.

LINEWIDTH AT HALF-HEIGHT OF METHYLENE PEAK ($\Delta\nu_{1/2}CH_2$) VS. NUMBER OF LYMPH NODES AFFECTED

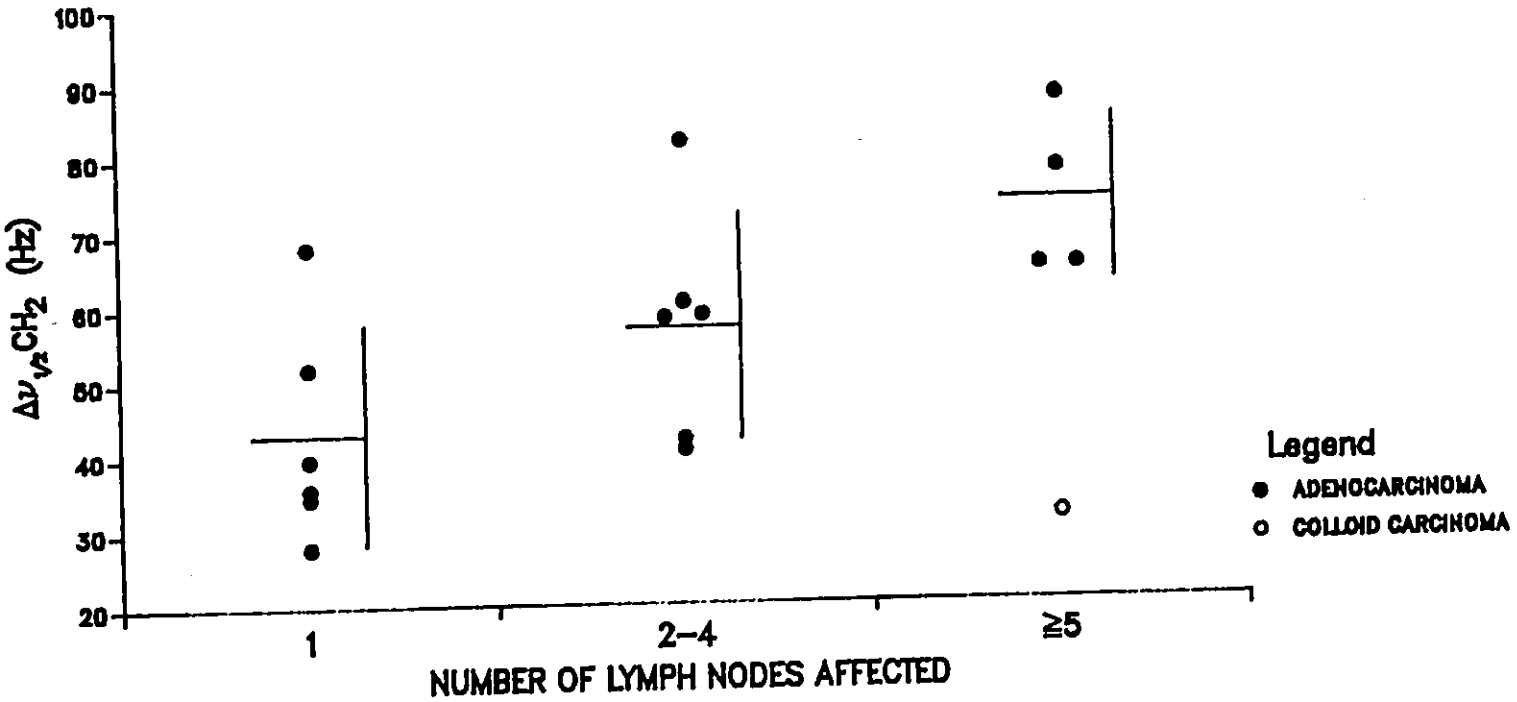

MEAN ± SD (Hz)	43.0±14.7	57.1±15.1	73.7±11.0 (• ONLY) 65.3±21.2 (• + ○)

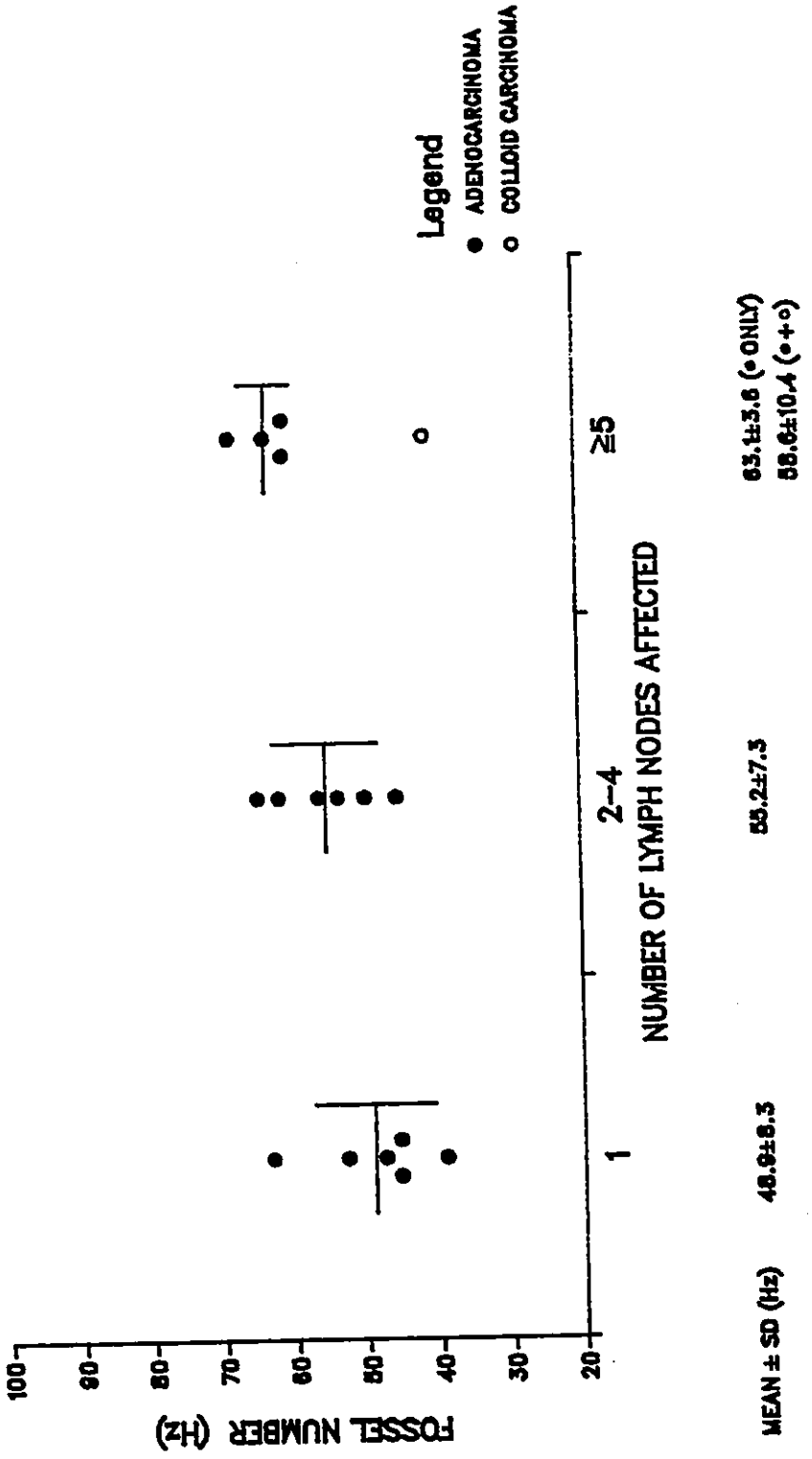
FOSSEL NUMBER VS. NUMBER OF LYMPH NODES AFFECTED
Legend
● ADENOCARCINOMA
○ COLLOID CARCINOMA
FOSSEL NUMBER (Hz)
100
90
80
70
60
50
40
30
20
1
2–4
≥5
NUMBER OF LYMPH NODES AFFECTED
MEAN ± SD (Hz)
48.6±8.3
55.2±7.3
63.1±3.6 (● ONLY)
58.6±10.4 (●+○)

Figure 4-14.

As with the T_2 values, $\Delta\nu_{\frac{1}{2}}CH_2$ and the Fossel numbers were examined with respect to the number of lymph nodes involved with metastasis. The results appear in Figs. 4-13 and 4-14. In general, both $\Delta\nu_{\frac{1}{2}}CH_2$ and the Fossel number increase with the amount of lymph nodes affected. The colloid carcinoma in the ≥5 lymph nodes affected category has a noticeably lesser $\Delta\nu_{\frac{1}{2}}CH_2$ and Fossel number than the adenocarcinomas. While all colon cancers secrete a certain amount of mucin, colloid carcinomas do it in such abundance as to give them a jellylike consistency. These mucinous adenocarcinomas differ from and have a worse prognosis than ordinary adenocarcinomas. The mean has been drawn excluding this sample.

The poorly differentiated tumours had low T_2 values. When $\Delta\nu_{\frac{1}{2}}CH_2$ and Fossel number were examined with respect to differentiation, the poorly differentiated samples lay in the upper third of all values obtained, although there was overlap between all the categories.

Why was the initially observed trend for the small group of random samples not followed upon examination of a larger data base? (The importance of a sufficiently large data base from which to gather conclusions is clearly emphasized).

Basically, two major factors can be considered : the composition and the mobility of molecules giving rise to the methylene peak. The CH_2 peak is composed mainly of resonances from the fatty acyl chains of triglycerides. It

has been shown by Dilman et al. (1981) that a rise in VLDL, the chief triglyceride carrier, is responsible for the increase in triglyceride levels in the blood of cancer patients. This phenomenon, by decreasing $\Delta\nu_{\frac{1}{2}}CH_2$, is held responsible for the smaller Fossel numbers obtained from the plasma of cancer patients (Holmes et al. 1988). Many of our samples have high $\Delta\nu_{\frac{1}{2}}CH_2$ values in the B and C stages, the peaks have not narrowed. According to the data published by Dilman et al., there is actually a significant decrease in total cholesterol and VLDL in the blood with the stage of cancer of the rectum, as well as a decreasing trend in the amount of triglyceride. Assuming the equilibration of lipoprotein components between tissue cell membranes and blood, this could well account for the widening of the CH_2 peak, and increase in Fossel number with the later stages of the disease process for our tumour spectra.

In one particular sample pair (#244) on which lipid analysis was performed, the amount of triglyceride for the normal sample was 1.2 times that for the tumour. The sample was from a male patient, and according to Dilman et al.'s data, a significant increase from normal levels in triglycerides and VLDL with cancer occurs only in females. Nonetheless, the $\Delta\nu_{\frac{1}{2}}CH_2$ for the tumour sample was 20 Hz less than for the normal sample. Since there was no significant difference in triglyceride levels, the difference must lie in the composition of the fatty acyl chains concerned.

What of molecular mobility? For small molecules with isotropic motion, an increase in mobility would produce line narrowing and longer T_2 values ($\Delta\nu = 1/\pi T_2$ in the theory of motional narrowing). In the case of the $N^+(CH_3)_3$ peak for transformed lymphocytes (Mountford et al. 1982), an increase in mobility apparently resulted in line narrowing. For the case of ≥5 lymph nodes involved, line broadening occurs together with a decrease in T_2 values. At the initial stages of cancer progression, there is a general decrease in linewidth, concomitant with an elevation in T_2 values. From the reciprocal relationship apparent for T_2 and $\Delta\nu_{\frac{1}{2}}CH_2$, it would appear that the phenomenon of motional narrowing holds for the CH_2 peak. The long T_2 value obtained for the peak, however, does not arise from the fatty acyl chains which are the major contributors to the peak width, but from a resonance of lesser proportion, but much greater mobility. It is possible, of course, that the carbohydrate sequences containing the fucose deemed responsible for the long T_2 are attached to the acyl chains in question. Block et al. (1974) found that concanavalin A, which bound to cell-surface carbohydrate chains, greatly broadened the CH_2 peak. There appears to be some sort of connection between T_2 and linewidth, but if it were purely motional narrowing, the linear upward trend of $\Delta\nu_{\frac{1}{2}}CH_2$ with number of lymph nodes involved would be parallelled by a linear downward trend of T_2 values, which was not the case, as Fig.4-10 clearly

demonstrates. Also the clear demarcation between T_2 values for "normal" samples (<450 ms) and polyps and Class A (>450 ms) does not appear for either $\Delta\nu_{\frac{1}{2}}CH_2$ or Fossel number. Thus linewidth appears to be more a reflection of tissue composition than of molecular mobility. As such, quantitative lipid analysis is necessitated before interpretation of linewidth results can be made. T_2 as an indicator of molecular mobility must be considered separately. Parl et al. (1987) pose a relevant question with regard to the measurement of Fossel numbers : "Is the difference in linewidth truly due to T_2 , or does it reflect the structural heterogeneity of lipids in normal and malignant tissues?" The breakdown of the initially observed trend in linewidths points to the latter proposition. The source of scatter in our data is most likely due to the structural heterogeneity of lipids from one sample to another.

Conclusions

A T_2 value greater than 450 ms is definitive for malignancy. For T_2 values less than this, a $\Delta\nu_{\frac{1}{2}}CH_2$ less than 45 Hz (using a 360 MHz spectrometer) is indicative of malignancy.

T_2 is an excellent criterion for early diagnosis of colon cancer, with no overlap apparent between "normal" tissue and samples at the initial stages of the disease

process (polyps and Class A). At later stages, the overlap of T_2 values with those from "normal" samples, although not relevant for early diagnosis, can be resolved by means of other NMR parameters, such as the presence of a narrow $N^+(CH_3)_3$ peak, but most notably by 2-D NMR (see Chapter 5).

$\Delta\nu_{\frac{1}{2}}CH_2$ and the Fossel number are inferior by far to T_2 values for diagnosis of malignancy and staging thereof, due to sample lipid heterogeneity in both "normal" and tumour samples.

There is a significant decline in T_2 values, and general increase in linewidths with very late stages of the disease process, as evidenced by the data for ≥ 5 lymph nodes affected. In the terminal stages of colorectal cancer, the NMR parameters revert to those indicative of "normal" tissue samples.

The successful diagnosis and staging of colorectal cancer by T_2 values, with assist from other NMR parameters, show tremendous potential for future non-invasive testing of patients with Magnetic Resonance Imaging in combination with Magnetic Resonance Spectroscopy.

References

Astler,V.B. and Coller,F.A. (1954) The prognostic extension of carcinoma of the colon and rectum. Ann.Surg. 139: 846.

Brown,M.S., Faust,J.R. and Goldstein,J.L. 1975. Role of the Low Density Lipoprotein Receptor in Regulating the Content of Free and Esterified Cholesterol in Human Fibroblasts. J. Clin. Investig. Vol.55 April:783-93.

Dilman,V.M., Berstein,L.M., Ostroumova,M.N., Tsyrlina,Y.V. and Golubev,A.G. 1981. Peculiarities of Hyperlipidaemia in Tumour Patients. Br. J. Cancer 43:637-43.

Dukes, C.E. (1932) The classification of cancer of the rectum. J. Pathol. Bacteriol. 35 : 323-332.

Dukes, C.E. and Bussey, H.J.R. (1958) The spread of rectal cancer and its effect on prognosis. Br. J. Cancer 12 : 309.

Fossel, E.T., Carr, J.M., and McDonagh,J. (1986) Detection of malignant tumours : Water-suppressed proton Nuclear Magnetic Resonance spectroscopy of plasma. New England J. of Med. Vol.135 No. 22 : 1369-1376.

Holmes,K.T., Mackinnon, W.B., May, G.L., Wright, L.C., Dyne, M., Sullivan, D., Tattersall, M.H.N. and Mountford, C.E. (1988) Hyperlipidemia as a biochemical basis of Magnetic Resonance plasma test for cancer. NMR in Biomed. Vol.1 No.1:44-9.

Hutter, R.V.P., and Sobin, L.H. (1986) A universal staging system for cancer of the colon and rectum. Let there be light. Arch.Pathol.Lab.Med. Vol. 110, May 1986. Editorial.

Jass, J.R., Atkin, W.S., Cuzick, J., Bussey, H.J.R., Morson, B.C., Northover, J.M.A., and Todd, I.P. (1983) The grading of rectal cancer : historical perspectives and a multivariate analysis of 447 cases. Histopathology 10, 437-459.

Jass, J.R., and Morson, B.C. (1986) A universal staging system for cancer of the colon and rectum revisited. Arch.Pathol.Lab.Med. Vol 110, Dec. 1986. Editorial.

Jass, J.R., and Morson, B.C. (1987) Reporting colorectal cancer. J.Clin.Pathol. 40: 1016-23.

Jass, J.R., Love, S.B., and Northover, J.M.A. (1987) A new prognostic classification of rectal cancer. The Lancet, June 6, 1987.

Kaufman,S., Steim,J.M. and Gibbs,J.H. 1970. Nuclear Relaxation in Phospholipids and Biological Membranes. Nature Vol.225 Feb.21:743-4.

Kyriakos, M. (1985) The President's Cancer, the Dukes Classification, and Confusion. Arch.Pathol.Lab.Med. Vol 109, Dec. 1985.

Mountford, C.E., Grossman, G., Reid, G. and Fox, R.M. (1982) Characterization of transformed cells and tumors by proton

Magnetic Resonance spectroscopy. Cancer Res. 42 : 2270-2276.

Mountford,C.E., Wright,L.C., May,G.L., Holmes,K.T., and Dyne,M. (1987) Inhibition of Metastatic Potential by Fucosidase: an NMR Study Identifies Fucoganglioside as a Cell Surface Metastasis Marker. J. Cell. Biol. Suppl. 0(11 part D):144.

Parl,F.F. and Harris,T.M. 1987. Lett. to Ed. New Eng. J. Med. Vol.316 No.22:1411-2.

Riddell, R.H., Goldman, H., Ransohoff, D.R., Appelman, H.D., Fenoglio, C.M., Haggitt, R.C., Ahren, C., Correa, P., Hamilton, S.R. Morson, B.C., Sommers, S.C., and Yardley, J.H. (1983) Dysplasia in inflammatory bowel disease : standardized classification with provisional clinical applications. Human Pathol. Vol.14 No.11 : 931-968.

Rosi, A., Guidoni, L., Luciani, A.M., Mariutti, G., and Viti, V. (1988) RNA-lipid complexes released from the plasma membrane of human colon carcinoma cells. Cancer Lett. 39(2) Mar.:153-60.

Schmidt, W.A. Principles and Techniques of Surgical Pathology. Addison-Wesley Publishing Co. 1983.

Small,D.M. and Hamilton,J.A. 1987. Lett. to Ed. New Eng. J. Med. Vol.316 No.22:1412-3.

Wieczorek, A.J., Rhyner, C., and Block, L.H. (1985) Isolation and characterization of an RNA-proteolipid complex associated with the malignant state in humans. Proc.Natl.Acad.Sci.USA 82 : 3455-9.

Williams,P.G., Helmer,M.A., Wright,L.C., Dyne,M., Fox,R.M., Holmes,K.T., May,G.L. and Mountford,C.E. 1985. Lipid domain in cancer cell plasma membrane shown by H NMR to be similar to a lipoprotein. FEBS Lett. Vol.192 No.1 Nov.:159-64.

Wolmark, N., Fisher, E.R., Wieand, H.S., and Fisher, B. (1984) The relationship of depth of penetration and tumor size to the number of positive nodes in Dukes C colorectal cancer. Cancer 53 : 2707-2712.

Wright, L., May, G.L., Dyne, M., and Mountford, C.E. (1986) A proteolipid in cancer cells is the origin of their high resolution NMR spectrum. FEBS Lett. 203, 164-168.

Zinkin, L.D. (1983) A critical review of the classifications and staging of colorectal cancer. Dis. Colon Rectum 26 : 37-43.

CHAPTER 5

2-D NMR OF COLON TUMOUR AND "NORMAL" SAMPLES : IN SEARCH OF THE MOLECULAR SPECIES RESPONSIBLE FOR THE LONG T_2 VALUES

Introduction

The prominent CH_2 peak apparent on the 1-D spectrum at 1.3 ppm of both normal and malignant colonic tissue contains a multitude of overlapping resonances. The fatty acyl chains ($(CH_2)n$) of triacylglycerols in lipoprotein molecules associated with the cell membrane (Mountford et al. 1984) comprise the bulk of the peak, but several smaller molecular species, such as lactate, threonine and fucose have resonances with the same chemical shift. In plasma samples, it has been possible to move the resonances of lactate and threonine downfield by acidifying the sample to pH 2.5, and to attenuate the broader lipid components by a sufficiently long relaxation delay, leaving a doublet at 1.29 ppm which is stronger in patients with malignant tumours (Nicholson and Nicholson 1987). Mountford et al. (1987a) have suggested that high levels of fucosylated proteolipids in the plasma of patients with malignant tumours are the source of this resonance. The resolution of this resonance is not as simple for solid tumours. Unlike the situation for plasma samples, it is not possible to deconvolute individual peaks under the CH_2 peak mathematically in the solid tumour spectrum. 2-D NMR, however, provides a powerful tool by which some of the resonances under the lipid peak can be

separated.

2-D NMR is possible because the signals from individual spins vary with time after excitation. They are sinusoidally modulated, either in amplitude or in phase, as a result of spin-spin interactions. We have used the homonuclear chemical shift correlated (COSY) experiment for our 2-D NMR spectra. The four main time-sections of a general 2-D NMR experiment will be explained with respect to the COSY sequence - t_0-90°-t_1-90°-t_2 -acquisition.

The preparation period (t_0-90°) establishes the condition of the spin system at the beginning of t_1. Multiple, separate experiments are required for 2-D NMR and the nuclear spins must be brought to the same well-defined state at the start of the experiment for all the separate values of t_1. The time period t_0 usually involves a delay to give equilibrium magnetization for all nuclei, and is followed by a 90° pulse to generate transverse magnetization.

During the evolution period t_1 the magnetization induced by the last part of the preparation period is allowed to evolve over a fixed time in a well-defined magnetic and radiofrequency (rf) environment. This period t_1 is varied systematically and regularly from 0 to some upper limit, and spectra are obtained for each new value. In this way phase and intensity variations with time can be monitored.

The second 90° pulse gives rise to the mixing period,

Figure 5-1. The 2-D NMR experiment.

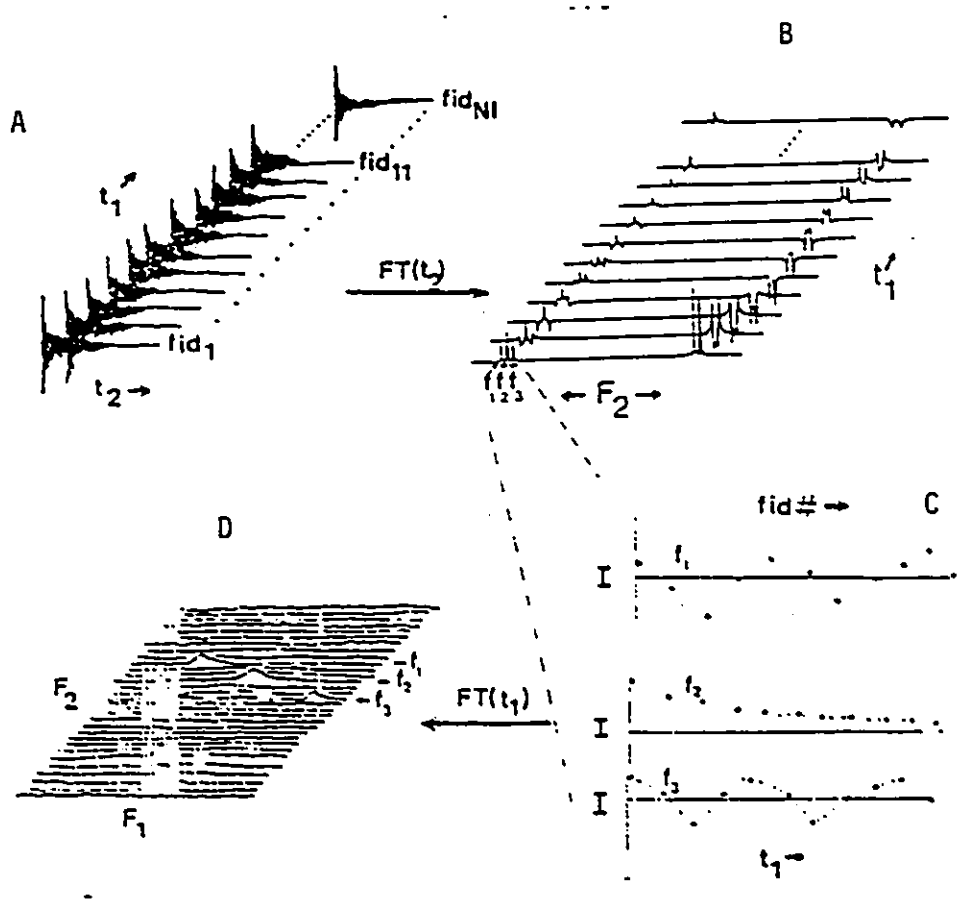

A - NI FID's are acquired, with t_2 constant and t_1 regularly increasing

B - each FID is Fourier transformed, giving NI chemical shift spectra

C - after rotation of the F_2-vs-t_1 data matrix by 90°, the second Fourier transform is performed

D - resulting 2-D spectrum, with frequency axes in both dimensions

from Gray, G.A. (1987) In: Two-Dimensional NMR Spectroscopy. Applications for Chemists and Biochemists. (VCH Publishers Inc. New York)

where nuclear magnetization is redistributed among the spins. Spin communication is allowed for a fixed period of time. The 90° pulse acting on coupled homonuclear spins transfers magnetization from one proton to another that is coupled to it, thus mixing the spin states within a spin system.

The detection time is given by t_2, a constant time period. The signal from the sample is detected and recorded in the form of an FID.

The processing of a 2-D spectrum involves two sets of Fourier transformations (see Fig.5-1). The first transformation is a function of t_2, the constant time-slice for detection, and results in normal chemical shift spectra (the F2 domain), one for each value of the evolution time t_1. The second transformation is a function of t_1, the varied evolution time, where the resulting modulation in the signal is picked up. This is the F1 domain. The frequency characteristic plotted in the F1 domain, whether chemical shift or J-coupling, depends on the environment of the spins during the evolution time, which is determined by the pulse sequence. The environment felt by the nuclei during either the detection or evolution time can be controlled and modified by various means such as pulses, decoupling, and pulsed field gradients. Modulations arising from interactions not of interest can be suppressed. The 2-D experiment can be tailored to provide the information

Figure 5-2. 2-D COSY spectrum of a colon tumour sample.

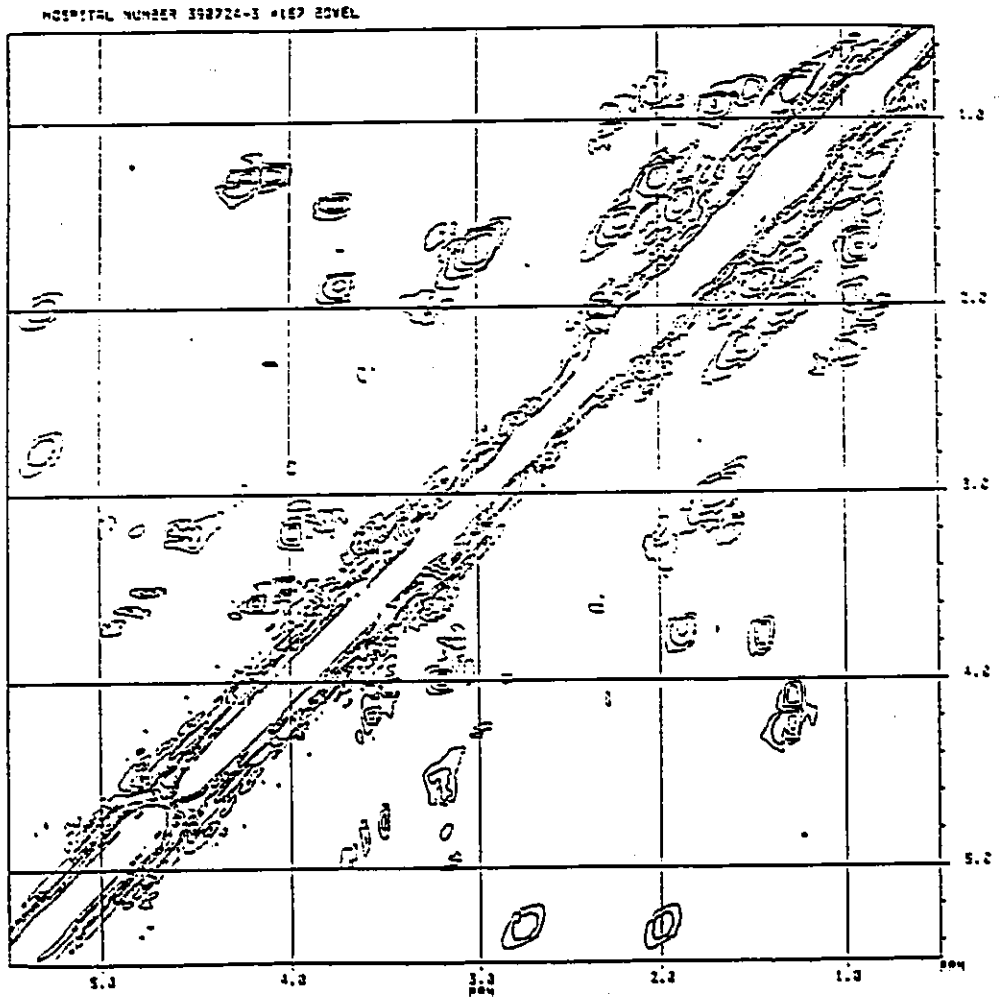

required by the user. These methods have been feasible since the early 1980's with the advent of new, larger and faster computers capable of implementing the Fast Fourier Transform algorithm on large data bases.

The COSY experiment plots chemical shift in both dimensions (see Fig.5-2) and can identify all the scalar coupling interactions (i.e. through-bond coupling to a limit of 2-3 bonds) of the proton species in our samples. The couplings are evidenced from the presence of off-diagonal cross peaks linking protons of one chemical shift with those of another chemical shift. This can aid in identifying the molecular species hiding under the broader CH_2 peak.

Dr. Mountford's group (Holmes et al. 1986) observed a prominent cross peak, which they have designated as Cross Peak Y, in the COSY spectrum of the metastatic 13762 tumour cell line, which was absent in the spectrum of the non-metastatic J-clone line. Cross Peak Y indicated ccupling between protons at 4.2 ppm, attributable to a proton neighbouring to a C-O moiety, with protons at 1.3 ppm, attributable to protons from a methyl (CH_3) group. Lactate, threonine and fucose all contain this coupling (see Fig. 5-3).

In this chapter will be presented the results of our 2-D NMR COSY experiments on some of the colon tumour and "normal" samples.

Figure 5-3. Possible sources of Cross Peak Y.

lactate

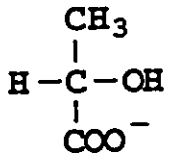

threonine

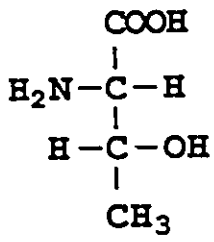

fucose

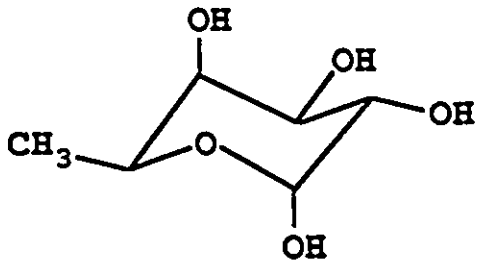

Materials and Methods

Colon Tumour and "Normal" Samples

The same samples were used as for the T_2 experiments of Chapters 3 and 4. The "normal" samples, as before, were pieces of colon obtained from the resection margin, 10 to 20 cm away from the location of the tumour, and declared "clean" (i.e. having the appearance of normal colonic tissue) by histological analysis.

NMR

The COSY experiment (t_0-90°-t_1-90°-t_2 acquisition) was run on the Bruker AM-360 MHz machine. For a listing of the automated sequence and typical parameters, see Appendix A.

On some of the samples a T_2COSY (90°-(τ-180°-τ)$_n$-t_1-90°-t_2 -acquisition) was run. The CPMG T_2 experiment sequence replaced the usual t_0-90° preparatory period of the COSY. Three separate COSY experiments comprised a T_2COSY run, one with n = 0, one with n = 160 ms, and one with n = 320 ms. Thus with the total initial delays of 320 and 640 ms before the start of the t_1-90°-t_2 part of the COSY sequence, resonances with relaxation times less than these values relax to 1/e (approx. 1/3) of their previous intensity. Certain resonances will consequently have much diminished intensities, and possibly disappear

Figure 5-4. COSY spectra of colon tumour and "normal" samples.

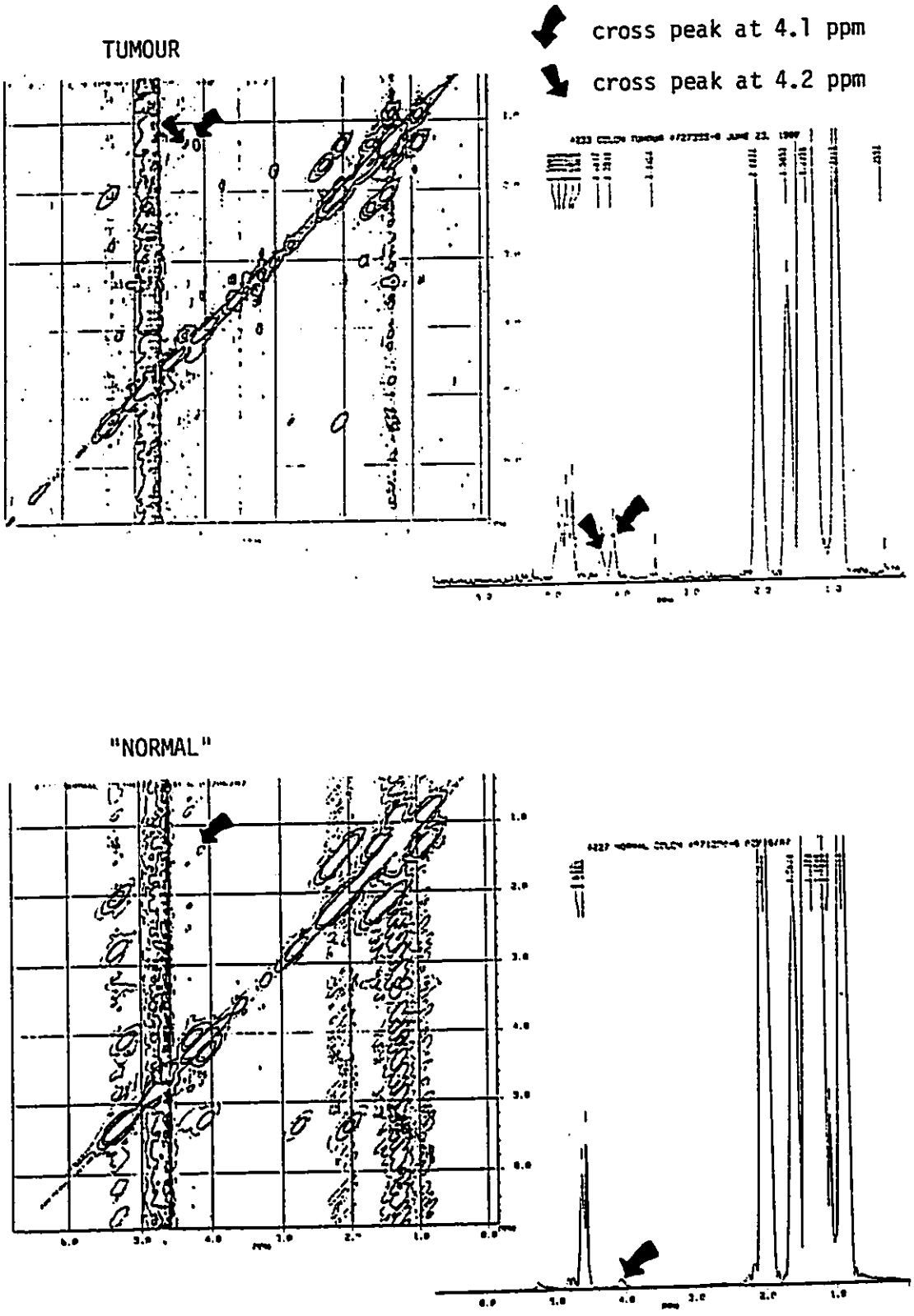

from the COSY spectrum, indicating which cross peaks result from molecules with relaxation times shorter than 320 or 640 ms.

In order to compare intensities of Cross Peak Y, linking resonances at 4.2 and 1.3 ppm, 1-D cross-sections at the level of the 1.3 ppm peak were plotted from the COSY contour plots.

Results

COSY

A typical COSY for a colon tumour and a "normal" colon sample appears in Fig. 5-4. Note the two cross peaks (arrows) at 4.2 and 4.1 ppm (horizontal scale) and 1.3 ppm (vertical scale) for the tumour sample. The "normal" sample yields one cross peak at 4.1 and 1.3 ppm. The 1-D cross-sections underneath the COSY plots illustrate the difference in magnitude of the cross peaks at 4.1 ppm for the tumour and "normal" samples.

The appearance of cross peaks indicating scalar coupling between protons at 4.1 and 1.3 ppm and at 4.2 and 1.3 ppm in all the colon tumour and "normal" samples examined by 2-D NMR are summarized in Table 5-1.

Table 5-1. 2-D NMR (COSY) Cross Peaks of Colon Samples

Sample #	Tissue Type	Cross Peak		Comments
		4.1 ppm	4.2 ppm	
167	tumour	X	X	
199	"	X	X	
201	"	X	X	
205	"	X	-	benign sample
207	"	X	X	
227	"	-	X	large H_2O peak
230	"	X	x	4.25 peak in 1-D
233	"	X	X	
235	"		X	
237	"	X	X	
243	"	X	X	
227	"normal"	X	-	
230	"	X	-	
233	"	X	-	
237	"	X	-	

In the COSY of tumour sample #227, the cross peaks are completely hidden under a wide water peak. A relatively wide 4.2 ppm peak was apparent on the 1-D cross-section along the column at 1.3 ppm on the horizontal axis. It is likely that the 4.1 ppm peak is included in this wide peak because in the T_2COSY experiment the peak narrows with a longer initial delay time, disclosing a sharp peak on the right (upfield) side, centred above 4.1 ppm. For tumour sample #230, the 2-D COSY experiment shows a prominent cross peak at 4.1 ppm, and a peak shifted 0.05 ppm downfield from 4.2 ppm just above the noise level. Upon inspection of the 1-D cross-section, the peak at 4.25 ppm is apparent with S/N equal to 2. This particular sample is a very metastatic Dukes' C tumour (all

Figure 5-5. T_2COSY of a colon tumour sample.

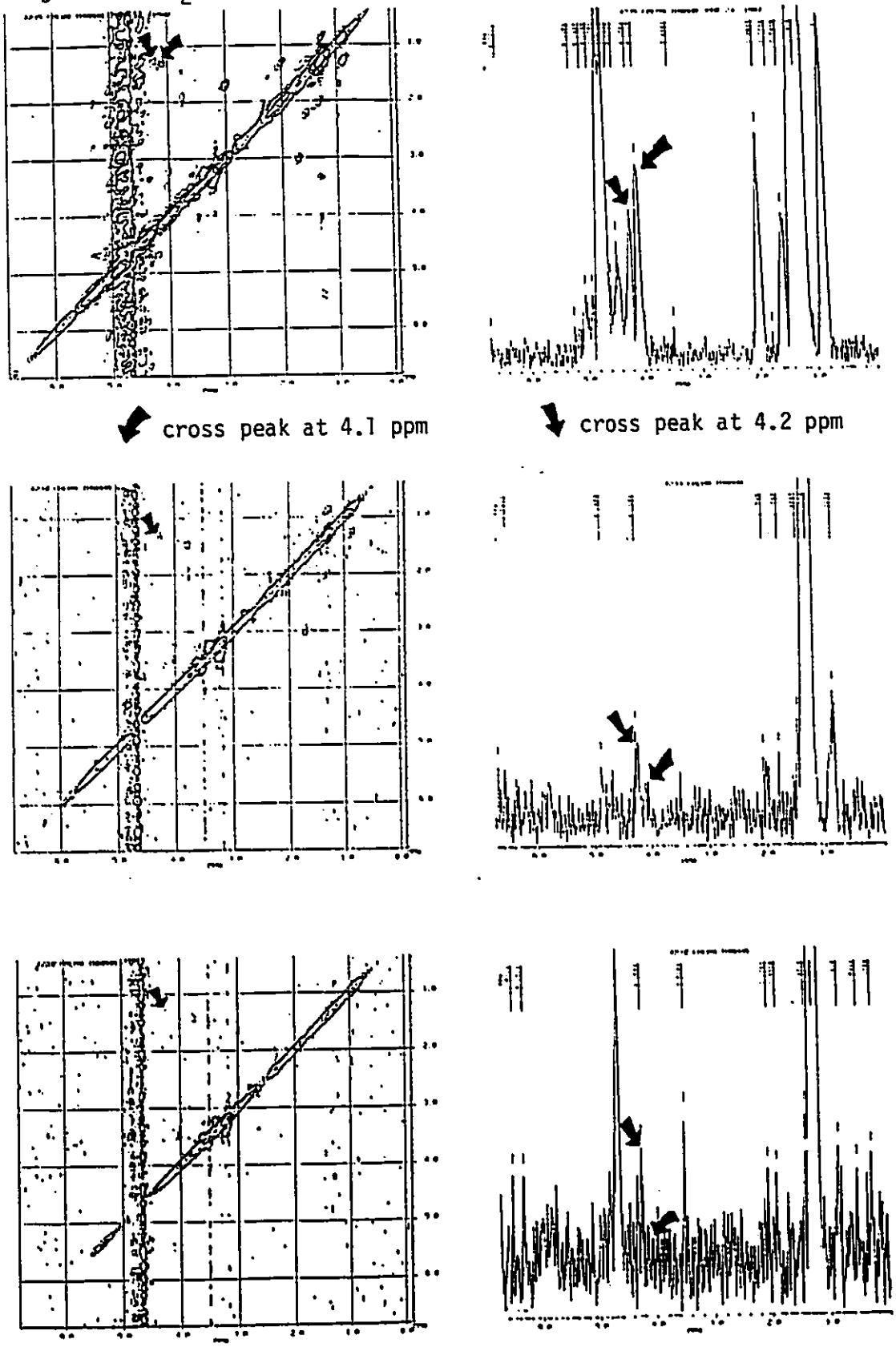

Figure 5-6. T_2COSY of a colon "normal" sample.

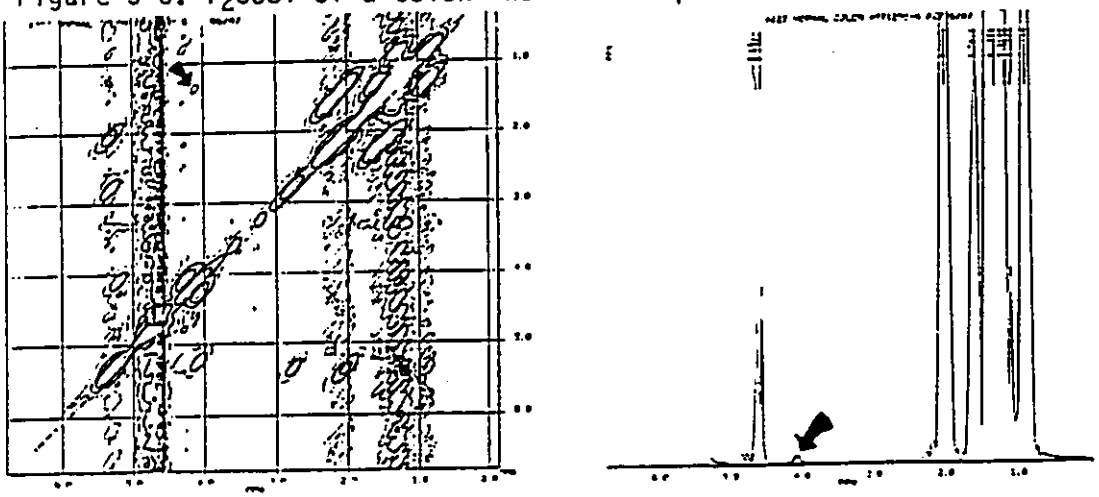

Note absence of cross peak at 4.2 ppm. ← cross peak at 4.1 ppm

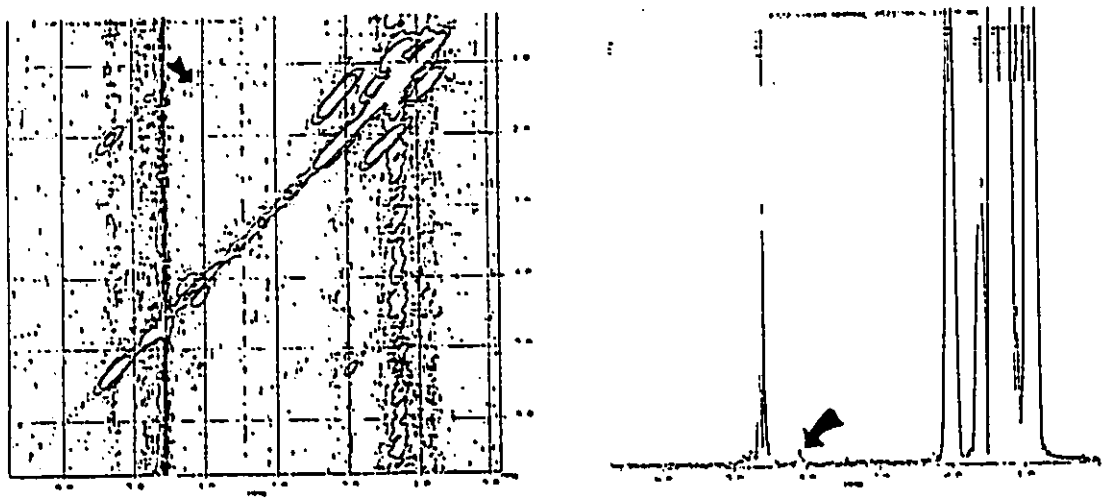

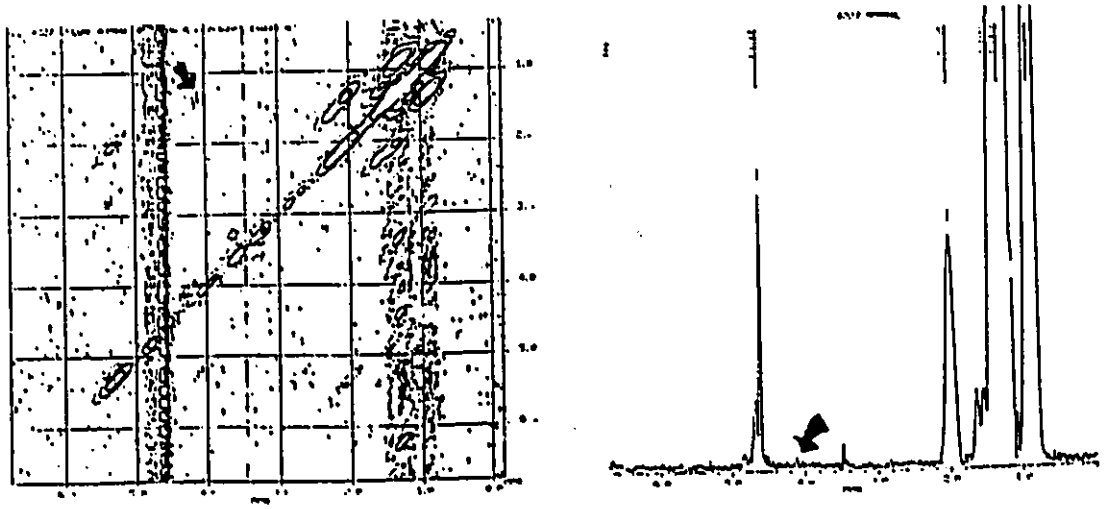

9 lymph nodes inspected had metastasis). The tumour was poorly differentiated, indicating a very poor prognosis. Its T_2 was low - 363 ms. The Fossel number of the tumour sample was in fact higher than that of the "normal". It appears that the 2-D spectrum verifies the observation made from T_2 values and methylene peak widths at half-height, that as colon cancer worsens to a late stage, the NMR characteristics indicative of malignancy revert to those of normal tissue. The "normal" #230 sample also possessed a cross peak at 4.25 ppm with S/N equal to 2 in the 1-D cross-section. At such a late stage of the cancer's progression, the "normal" classification of this sample is indeed questionable.

In summary, all the malignant tumour samples (n=10) can be seen to possess two cross peaks, one at 4.2 ppm and one at 4.1 ppm. In 9 of these the cross peaks were readily apparent on the 2-D COSY spectrum, while in the remaining one (#230), its observation necessitated a 1-D cross-section. One tumour sample lacking the cross peak at 4.2 ppm was later found to be a benign tumour sample by histological analysis. All four "normal" samples yielded only one cross peak at 4.1 ppm on the 2-D COSY spectrum.

T_2COSY

The T_2COSY run of a tumour sample is illustrated in Fig. 5-5, and that of a "normal" sample is shown in Fig. 5-6. The

T_2COSY results appear in Table 5-2.

Table 5-2. T_2COSY Results for Colon Tumour and "Normal" Samples *

Sample #	COSY Delay (ms)	Cross Peak			
		Tumour		"Normal"	
		4.1 ppm	4.2 ppm	4.1 ppm	4.2 ppm
227	0	?	XXXXX	XXXXXx	+
	320	+[a]	XXXX	XXX	-
	640	-	-	-	-
233	0	XXXXX	XXX	XX	-
	320	XX	XX	-	-
	640	-	+	ND	ND
235	0	XXXXXXx	XXXXX	ND	ND
	320	-	XX	ND	ND
	640	-	XX	ND	ND
237	0	XXXX	XXXXx	**	-
	320	XX	XXX	ND	ND
	640	-	XXx	ND	ND

* The number of X's signifies S/N ratio, e.g. XXx = 2.5
\- in noise level
\+ just above noise level
? cannot determine
ND no data available
** very strong signal (triplet for #237 normal)
[a] apparent as sharp peak tip on right side of peak

When comparing the heights of the cross peaks in the 1-D cross-sections, one must take into account the level of noise in the spectrum. The cross peak intensity is expressed as the ratio of signal-to-noise (S/N) for the peak, in order to compare intensities from one spectrum to another.

Possibly a better means of measurement would have been comparing the heights of the cross peaks at 4.1 and 4.2 ppm to either the CH_2 or CH_3 peaks. In either case the measurements are more qualitative than quantitative, in order to obtain a rough estimate of the relaxation times involved.

For both the tumour and "normal" samples, the cross peak at 4.1 ppm is much diminished in height with an initial delay time of 320 ms. For two samples (tumour #235 and "normal" #233) the peak disappears entirely into the noise. With the 640 ms delay, the peak disappears for all samples.

The cross peak at 4.2 ppm in the tumour samples also decreases in intensity (as measured by S/N peak height) with an initial COSY delay time, but not to the same extent as the 4.1 ppm peak. In two of the samples (tumours #235 and #237), after the initial decrease at 320 ms, the peak appears to stabilize. A small decrease is noted in the peak at 640 ms for sample #237. For sample #227 the cross peak disappears into the noise at 640 ms. It must be noted, however, that this peak was examined differently from the others due to the strong water signal. The peak persists for sample #233, but barely above the noise level. To summarize, the peak at 4.2 ppm, in three out of four cases, does not relax away with delay times exceeding 640 ms, as does the peak at 4.1 ppm.

Discussion

Both colon tumour tissue and "normal" colonic mucosa give rise to the cross peak connecting resonances at 4.1 ppm and 1.3 ppm in the 2-D COSY experiment. This cross peak has a T_2 relaxation time greater than 320 ms but less than 640 ms, i.e. longer than that for lipid (200 ms) but shorter than that for lactate (1000 ms). The molecule giving rise to the cross peak is common to both malignant and normal colonic tissue. Its relaxation time rules out the possibility that it is lactate, the end-product of anaerobic glycolysis.

The cross peak connecting resonances at 4.2 ppm and 1.3 ppm appears to be unique for tumours, and can thus be used as a criterion for malignancy in colonic tissue. A 2-D COSY would differentiate between Dukes' B and C cancers with T_2 values less than 450 ms and normal colonic tissue (Chapter 4).

From the T_2COSY runs it can be seen that a sizeable proportion of the 4.2 ppm cross peak decays with the initial relaxation delays while the rest does not, this latter part probably attributable to lactate. In the samples examined, the tumour samples had approximately twice the lactate content of the "normal" samples. The "normal" samples contain about 200 ug lactate per gram of wet weight tissue. Why do they not have a cross peak at 4.2 ppm ? Either the amount of lactate is insufficient or lactate assumes a

certain configuration or position that does not manifest itself as the cross peak unique to tumour tissue, i.e. it has a short T_2. Sample #227, yielding a very small cross peak at 4.2 ppm on the 1-D cross-section contained 10 times the lactate content of the other "normal" samples, yet this peak decayed away quickly when the initial delay was 320 ms, indicating that it was not due to lactate of unrestricted mobility. In the tumour samples, the part of the cross peak that is not due to lactate, the faster relaxing component, could possibly be due to the same entity as for the 4.1 ppm peak, but again in a different configuration or environment unique to tumour tissue, yielding a slightly different chemical shift.

As mentioned in the introduction, there are three compounds that could give rise to the cross peak at 4.2 ppm which is specific for tumour tissue in our colon samples. What are their connections with cancer ?

Lactate is not specific for cancer, but it is generally assumed that tumour cells produce more lactate than do normal cells, possibly from lack of adequate oxygenation of the rapidly-growing tumour tissue, and an increase in the enzyme lactate dehydrogenase in tumour tissue. This will be examined in greater detail in Chapter 6.

L-threonine is a dietary essential amino acid which cannot be made by mammalian cells. Wellner et al. (1979) used L-threonine deaminase (which catalyzes the conversion

of L-threonine to α-ketobutyrate and ammonia) to test the effect of L-threonine depletion on four cell lines in culture - two murine leukemias, mouse L cells and normal human fibroblasts. The leukemia cells died, whereas the normal cells stopped growing but did not lose viability, and resumed growth upon replenishment of L-threonine in the medium. The malignant cells, with their lack of growth regulation, continued to proliferate and remained metabolically active, resulting in their death from lack of essential L-threonine. Since L-threonine appears necessary for the growth and division of tumour cells, these authors recommend further investigation of the use of L-threonine deaminase as an anticancer agent. If tumour cells in vivo have the same requirements as tumour cells in vitro, L-threonine should be present in our biopsy samples.

Threonine most notably is one of the anchoring amino acids for the addition of carbohydrate chains to nascent polypeptides in the rough endoplasmic reticulum of cells. More specifically, the amino acid sequence Asp-X-Ser/Thre is the signal for the glycosylation of proteins resulting in the large class of asparagine- or N-linked oligosaccharides. With its position at the base of a branched carbohydrate chain, it is highly unlikely that threonine in this position would possess the mobility to yield a long relaxation time.

Fucose, a methylpentose, and the only sugar in the body assuming the L-configuration, is the third possibility for the source of the cross peaks. L-fucose is a terminal sugar on cell surface oligosaccharides attached to either lipid or protein molecules. GDP-L-fucose, the activated form of fucose, is synthesized by cells either by a de novo pathway from D-mannose precursors, or by a salvage pathway from L-fucose. The enzyme fucosyltransferase transfers the fucose from GDP-L-fucose onto an N-acetylglucosamine (GlcNAc) residue during carbohydrate processing in the cell's Golgi apparatus. The final glycoprotein exits from the Golgi via vesicular transport to the plasma membrane.

Fucose can be found in immunoglobulins, blood group antigens, human milk - serving as growth factor for intestinal flora in infants - in certain placental proteins such as human chorionic gonadotropin, and even on the coating of the sea urchin egg, where it is a vital element for fertilization. Fucose acts as a signal for growth or proliferation, and also as an antigenic determinant, a signal for the immune system. Possibly its L-configuration singles it out for its signal giving properties.

What is its connection with cancer ? Glycoproteins containing fucose have been characterized in the serum of human cancer patients (Kannagi et al. 1986). In rapidly proliferating tissue, glycolipids rather than glycoproteins are the major sources of fucose. Yamamoto et al. (1985)

report fucose-containing glycolipids in developing embryonic brain of rodents which are expressed mainly on proliferating cells. They suggest that these glycolipids may modulate the cell-cell interactions in the normal developmental processes in particular regions of the brain. Normal human intestinal epithelium, a tissue with a great turnover of cells, contains fucolipids (McKibbin et al. 1982). Liepkalns et al. (1985) found that by adding butyric acid, a cell differentiation inducer (thereby arresting cell division), to human colonic tumour cell lines, the cells' capacity for fucosylation of cell surface antigens is diminished. They propose that fucolipid antigens are associated more with dividing, undifferentiated tumour cell populations, and that fucolipids play a role in tumour cell division.

Neutral glycolipids containing fucose have been isolated and characterized from human colonic cancer samples (Nudelman et al. 1986). Monoclonal antibodies directed towards these fucolipids have been produced to identify colon cancer, notably KH1 antibody for a branched chain containing 3 fucose residues, a glycolipid present in all colonic cancers tested (Kaizu et al. 1986). This glycolipid was absent from normal colonic extract and normal blood cell membranes. In these glycolipids fucose is joined to GlcNAc, a characteristic of blood group glycoproteins and glycolipids with Lewis blood group activity. They are ceramides of simple oligosaccharides containing 5 to 7

sugars. A high proportion of hydroxylated, unsaturated fatty acids are present in these ceramides with phytosphingosine and sphingosine as the predominant long chain bases. The carbohydrate chains are classed according to the position of the linkage of galactose (Gal) to GlcNAc. Type 1 has the β1→3 linkage and type 2 has the β1→4 linkage. Normal human intestine contains the type 1 chain, e.g. the Lewis a isomer fucolipid :

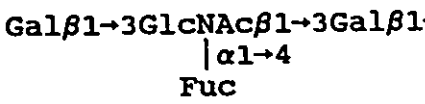

Fucose is attached to GlcNAc in an α1→4 linkage. Magnani et al. (1982) isolated a ganglioside (sialylated lacto-N-fucopentaose II) from gastrointestinal cancer with this structure, except that sialic acid (N-acetylneuraminic acid) is attached in an α2→3 linkage to the terminal Gal.

Fucolipids isolated from human colonic adenocarcinoma contain the type 2 chain, e.g. the trifucosyl Le^Y antigen (lactotrifucononaosylceramide, $III^3FucV^3FucVI^2FucnLc6$) for the KH1 antibody :

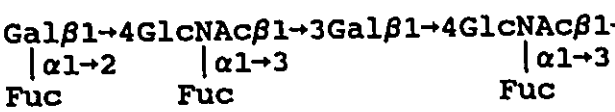

Fucose is attached to GlcNAc in an α1→3 linkage. Wherever fucose is attached to Gal, it is via an α1→2 linkage.

The chemical shift of the H-5 of the terminal fucose (Fuc α1→2) in these chains is between 4.01 and 4.3 ppm. The H-5 of Fuc α1→3 has a chemical shift of about 4.6 ppm which

would be hidden under the water peak at 4.7 ppm in our spectra. These NMR studies were done on isolated glycolipids in non-aqueous solvents. The fucolipids in their natural biological setting would be in a completely different environment, with various neighbouring molecules either shielding or deshielding their proton nuclei, resulting in different chemical shift values. Also, the isolation procedure itself could alter the molecular configuration. The beauty of NMR is that one can study molecules in their natural environment. The challenge of NMR in this case is to discover exactly what one is studying! The ongoing dilemma in biological systems is that if one isolates or removes a part of it for more detailed analysis, the physiological relevance is potentially lost. Nonetheless, the published chemical shift values of the isolated glycolipids are in the vicinity of the 4.2 ppm peak observed for our cross peak.

Several fucolipid antigens associated with cancer have been characterized and compared to blood group antigens. The exact residue sequence and points of attachment of fucose vary, but the Fuc α1→2 link to Gal and Fuc α1→3 link to GlcNAc are always present. In their 3-dimensional structure of the trifucosyl Le^Y antigen specific for the KH1 antibody, Kaizu et al. propose that a large hydrophobic area with adjacent polar sites from the sugar molecules form the binding site for the antibody. The addition of fucose may well be the component necessary to achieve the proper 3-D

configuration. Fucose has a definite role in immune system interactions.

In a study with α-L-fucosidase, a glycosidase which splits terminal α-L-fucose from oligosaccharides, Cameron (1985) found that macrophages incubated with the enzyme were no longer able to respond to lipopolysaccharide (LPS), a macrophage activating factor. Fucose must comprise an essential part of the macrophage receptor for LPS. After incubation of tumour cells with α-L-fucosidase, they became resistant to activated, cytotoxic macrophages. The effect was blocked upon addition of α-L-fucose to the incubation mixture. Fucose appears necessary for macrophage-tumour cell interactions.

Amongst all the work in progress to find an antigenic determinant unique to tumour cells, Fidler and Poste (1982) take a different approach. They reason that with all the diversity of cell surface carbohydrates, something more basic must be the key by which macrophages home in on target tumour cells, specifically the lipid composition of the cell membrane. Macrophages recognize old blood cells ready for termination by the appearance of phosphatidylserine on the cell surface (Schroit et al. 1985), which is absent from the surface of ably functioning younger cells. Macrophages are the scavengers of the immune system that recognize "self" from "non-self", and once activated, destroy the latter. Activated macrophages recognize and destroy neoplastic

cells without regard to their phenotypic diversity. Lymphocytes in animals with large tumour burdens, however, often lack the ability to release macrophage-activating lymphokines. Fidler and Poste circumvent the problem with macrophage-activating factors encased in liposomes. The macrophages engulf the liposomes, become activated, and destroy tumour cells. The authors class this as "passive" targetting, and although admitting that this method is insufficient for large tumour burdens, they claim that it would be an excellent way of ridding the body of small metastatic deposits and residual tumour burden that remains after elimination of the bulk of the tumour by other means. Liposome-encapsulated activating factors bypass the need for receptors on the macrophage surface, but the carbohydrate chains containing fucose could still be vital for tumour cell recognition, according to Cameron's findings.

Fucose appears to play a role in ridding the body of metastatic deposits, yet it also appears to play a role in formation of metastases. Low-metastatic variants of a highly metastatic murine tumour cell line were found to be deficient in the L-fucose salvage pathway (Dennis and Kerbel 1981) since they could not synthesize GDP-L-fucose from fucose 1-phosphate and GTP. The authors speculate that salvaged fucose may be important for fucosylation at the cell surface by specific fucosyltransferases. A block in this process could result in a decrease in specific

cell-surface fucosylated molecules necessary for metastatic behaviour. The lack of ^{3}H-fucose incorporation did not affect the tumorigenicity of these tumour lines, only their metastatic capacity. Schwartz et al. (1984) confirmed these findings. For each tumour system studied, weakly metastasizing tumour lines were deficient in ^{3}H-fucose incorporation and in its conversion to GDP-L-fucose. The level of fucose incorporation differs between tumour systems. The highly metastatic parent cell line of Dennis and Kerbel's study incorporated less fucose than another highly metastatic cell line. As well, each tumour line exhibited a unique glycoprotein pattern. Mountford et al. (1987b) found that the metastatic 13762 tumour cell line incorporated more ^{14}C-fucose than the non-metastatic J-clone line. It was the metastatic cell line that yielded Cross Peak Y at 4.2 ppm. When the cells were treated with fucosidase, Cross Peak Y disappeared, as did the long T_2 value for the cells, and the fucosidase treated cells failed to produce metastases when injected into rats. All the evidence strongly points to fucose as the metastatic marker.

The seemingly inevitable stage-by-stage progression of colon tumours to metastases in the surrounding lymph nodes seems to indicate that all colon tumours have the potential for metastasis. The long T_2 values at the initial stages of colon cancer also indicate metastatic potential. The cross

peak at 4.2 ppm is unique for the tumour samples, therefore the source of the long T_2 value, and is in accord with Dr. Mountford's findings. Whereas Cross Peak Y from a washed cell suspension appears to arise solely from fucose (washing would eliminate extracellular lactate), it is not surprising that our Cross Peak Y from a heterogeneous tumour biopsy sample contains more than one component - probably lactate, and the metastatic marker fucose. Since normal colon also contains fucolipids, it seems probable that the cross peak at 4.1 ppm is also fucose, but in a different structure.

Afterthought - Speculation by the author

All the parameters we have examined, i.e. T_2, $\Delta\nu_{\frac{1}{2}}CH_2$, $N^+(CH_3)_3$, cross peaks, tumour marker (fucose), we have considered as separate variables. However, they are all part of the cell's total plasma membrane profile. We have seen that sometimes T_2 alone is insufficient for diagnosis, but a combination of parameters (T_2, $\Delta\nu_{\frac{1}{2}}CH_2$, presence of a certain cross peak, e.g.) correctly describes the state of the tissue. Therefore the answer appears to lie in the total membrane picture. Fidler and Poste recognized the importance of the plasma membrane composition when they proposed that it is the major factor in macrophage recognition of tumour cells. Once activated, macrophages home in on tumour cells. Activated macrophages give rise to a high resolution spectrum (Holmes et al. 1988). By the activation process,

Figure 5-7. NMR membrane profiles of various cell types.

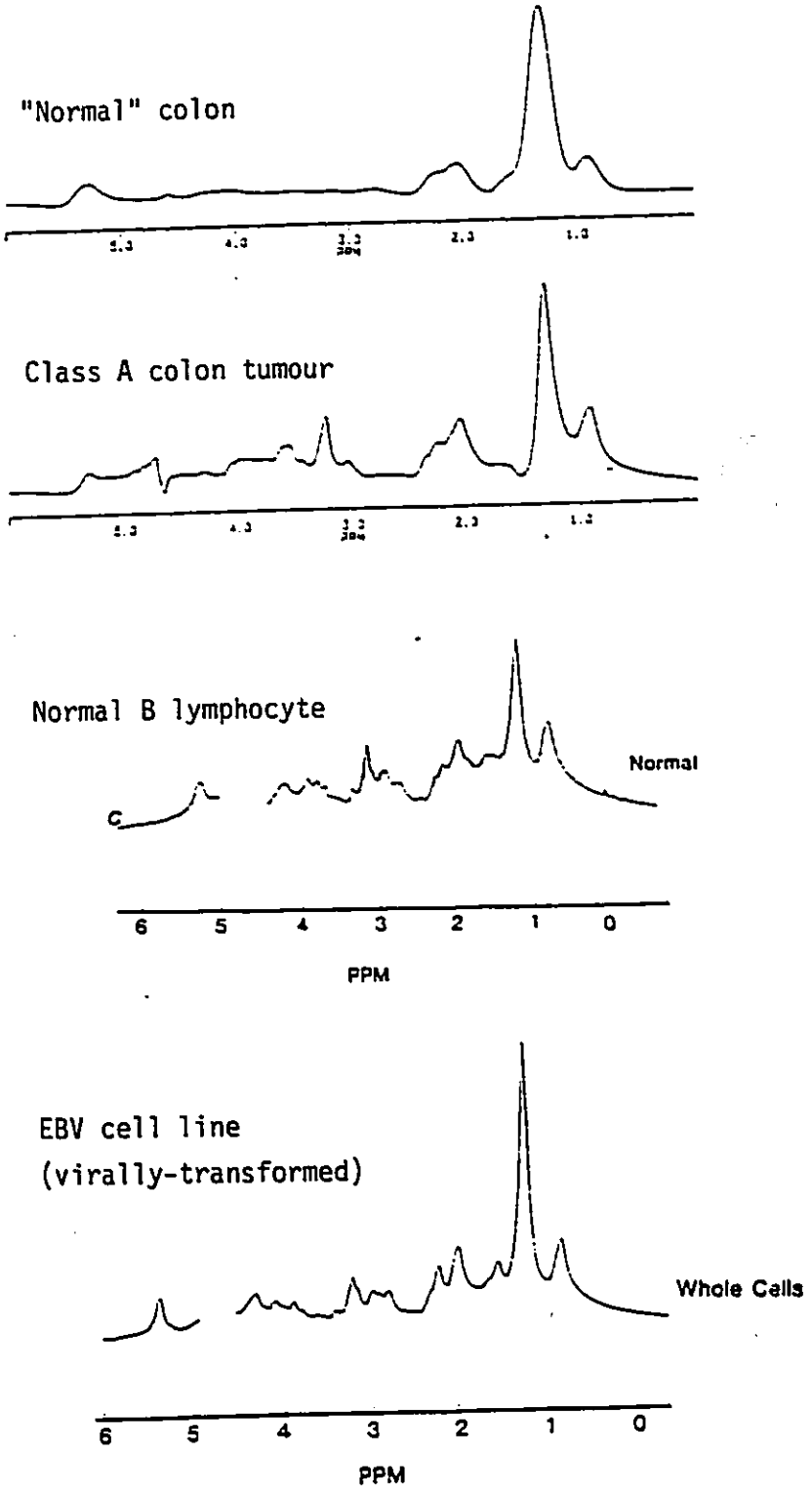

Spectra of normal B lymphocyte and EBV cell line are from Mountford, C.E. et al. (1982) Cancer Res. Vol.42: 2270-6.

macrophages somehow acquire a membrane profile similar to that of a typical tumour cell. This seems to be a necessary requirement (possibly in conjunction with certain cell antigens) for their uncanny ability to track down and kill tumour cells. In cells, as partly synthesized proteins for export are transported via vesicles through the various layers of the Golgi apparatus, their membrane composition matches that of the Golgi layer with which they are to fuse, and finally that of the plasma membrane. It appears that membranes need to match in chemical composition for efficient fusion to occur.

Nonetheless, tumour cells evade the immune system. Why aren't the macrophages activated ? Perhaps tumour cells escape immune surveillance because they are masquerading as part of the immune system. If one compares the spectra, representing the plasma membrane profile, of normal resting B lymphocytes, virally-transformed cells, and an early stage (Class A) colon tumour sample (Fig. 5-7), one cannot help noticing the similarities between them. All are high resolution spectra, with the prominent CH_2 peak, and a noticeable $N^+(CH_3)_3$ peak. Block noted in 1977 the similarity of lymphocyte and tumour cell spectra in their high resolution lipid resonances, in comparison with the typical broad protein resonances in the spectrum of erythrocytes. Most cell NMR profiles are indeed broad, indicative of relatively rigid bilayer lipids and proteins.

The body's immune system has often been compared to an army, fighting off invaders. What better way to infiltrate an army than to don its uniform? One can speculate that by natural selection, a virus capable of transforming the cell in this particular manner has initiated the very successful and dreaded disease cancer. It is an interesting and frightening proposition. How does one selectively break the pattern of the tumour cell membrane without affecting similar immuno-cells ? Perhaps fucose will play a role in this. It has been noted that with increase in differentiation of leukemic cells transplanted into rats, the tumour is rejected by the rat's immune system (Jimenez and Yunis 1987). The incorporation of cell surface fucose decreases with differentiation (Liepkalns et al. 1985). This implies that the increase of fucose on undifferentiated cells plays a role in their proliferation (differentiation and cell division are reciprocally related) and somehow modulates the immune system. The changes in the plasma membrane profile together with the incorporation of cell surface fucose could be the makings of the successful tumour cell.

Conclusions

A 2-D COSY experiment can be used to differentiate between malignant and "normal" colonic tissue by the presence of a cross peak (Cross Peak Y) connecting

resonances at 4.2 and 1.3 ppm.

From the approximate relaxation times apparent in a T_2COSY experiment, it is hypothesized that lactate and the metastatic marker fucose are the molecular species responsible for the cross peak.

To prove the above hypothesis, a tumour homogenate could be prepared, and lactate oxidase (to convert lactate to acetate) and α-L-fucosidase could be used in turn to test their effect on the cross peaks in sequential COSY experiments. α-L-fucosidase cleaves terminal fucose from the carbohydrate chain, so that free L-fucose would remain in the sample. Its chemical shift would probably differ from that for the attached fucose. L-fucose could then be added to the sample, to discern the location of the free fucose peak. Alternatively, the sample could be washed to eliminate the free fucose and any accumulated lactate produced by the cells in the interim. A single cell suspension of the tumour sample would be a cleaner experiment, but technically more difficult to prepare.

COSY experiments have been done using lactate oxidase on placental homogenate, and these will be described in the following chapter.

The proposed experiment for the cross peak at 4.2 ppm for the tumour samples was not carried out due to physical constraints because of the author's advancing pregnancy. Experimental work was stopped in August 1987, in order to

analyze the large data base already accumulated, and to summarize our findings in the current thesis.

References

Bax,A. (1984) A Simple Description of Two-Dimensional NMR Spectroscopy. Bulletin of Mag.Res. Vol.7 No.4:167-83.

Benn,R. and Gunther,H. (1983) Modern Pulse Methods in High-Resolution NMR Spectroscopy. Angew.Chem.Int.Ed.Engl. 22:350-80.

Blaszczyk-Thurin,M., Thurin,J., Hindsgaul,O., Karlsson,K.-A., Steplewski,Z, and Koprowski,H. (1987) Y and Blood Group B Type 2 Glycolipid Antigens Accumulate in a Human Gastric Carcinoma Cell Line as Detected by Monoclonal Antibody. J.Biol.Chem. Vol.262 No.1 January 5:372-9.

Cameron,D. (1985) Specificity of Macrophage-Mediated Cytotoxicity: Role of Target and Effector Cell Fucose. Immun.Letters,11:39-44.

Gray, G.A. (1987) Introduction to Two-Dimensional NMR Methods. In: Two-Dimensional NMR Spectroscopy. Applications for Chemists and Biochemists. Eds. Croasmun,W.R. and Carlson,R.M.K. (VCH Publishers Inc. New York).

Dennis,J.W., and Kerbel,R.S. (1981) Characterization of Deficiency in Fucose Metabolism in Lectin-resistant Variants of a Murine Tumor Showing Altered Tumorigenic and Metastatic Capacities in Vivo. Cancer Res. 41, January:98-104.

Farrar,T.C. (1987) Two-Dimensional NMR Spectroscopy. Analytical Chem. Vol.59 No.11, June 11:749A-61A.

Fidler,I.J. (1985) Macrophages and Metastasis - A Biological Approach to Cancer Therapy: Presidential Address. Cancer Res. 45, October:4714-26.

Fidler,I.J., and Poste,G. (1982) Macrophage-mediated Destruction of Malignant Tumor Cells and New Strategies for the Therapy of Metastatic Disease. Springer Semin. Immunopathol. 5:161-74.

Holmes,K.T., Williams,P.G., May,G.L., Gregory,P., Wright,L.C., Dyne,M. and Mountford,C.E. (1986) Cell surface involvement in cancer metastasis: an NMR study. FEBS Lett. Vol.202, No.1 June: 122-6.

Holmes,K.T., Mackinnon,W.B., King,N.J.C., May,G.L., Dyne,M. van Hafften-Day,C., and Mountford,C.E. (1988) Generation and modulation of lipoprotein-like domains in cell membranes. Abstract for the Seventh Annual Meeting of the Society of Magnetic Resonance in Medicine, San Francisco, U.S.A.

Jimenez,J.J. and Yunis,A.A. (1987) Tumor Cell Rejection Through Terminal Cell Differentiation. Science Vol.238 Nov.27 :1278-80.

Kaizu,T., Levery,S.B., Nudelman,E., Stenkamp,R.E., and Hakomori,S. (1986) Novel Fucolipids of Human Adenocarcinoma: Monoclonal Antibody Specific for Trifucosyl Le ($III^3FucV^3FucVI^2FucnLc6$) and a Possible Three-dimensional Epitope Structure. J. Biol. Chem. Vol.261 No.24, August 25:11254-8.

Kannagi,R., Fukushi,Y., Tachikawa,T., Noda,A., Shin,S., Shigeta,K., Hiraiwa,N., Fukuda,Y., Inamoto,T., Hakomori,S., and Imura,H. (1986) Quantitative and Qualitative Characterization of Human Cancer-associated Serum Glycoprotein Antigens Expressing Fucosyl or Sialyl-Fucosyl Type 2 Chain Polylactosamine. Cancer Res. 46:2619-26.

Koerner,T.A.W., Prestegard,J.H., and Yu,R.K. (1987) Oligosaccharide Structure by Two-Dimensional Proton Nuclear Magnetic Resonance Spectroscopy. Methods in Enzymology Vol. 138:38-59.

Kornfeld,R., and Kornfeld,S. (1985) Assembly of Asparagine-Linked Oligosaccharides. Ann.Rev.Biochem. 54:631-64.

Liepkalns,V.A., Herrero-Zabaleta,E., Fondaneche,M.C., and Burtin,P. (1985) Alterations in Expression and Synthesis of Glycolipid Antigens in Human Colonic Tumor Cell Lines. Cancer Res. 45, May:2255-63.

Magnani,J.L., Nilsson,B., Brockhaus,M., Zopf,D., Steplewski,Z.,Koprowski,H., and Ginsburg,V. (1982) A Monoclonal Antibody-defined Antigen Associated with Gastrointestinal Cancer Is a Ganglioside Containing Sialylated Lacto-N-fucopentaose II. J. Biol. Chem. Vol.257 No.23 December 10:14365-9.

McKibbin,J.M., Spencer,W.A., Smith,E.L., Mansson,J.-E., Karlsson,K.-A., Samuelsson,B.E., Li,Y.-T., and Li,S.-C. (1982) Lewis Blood Group Fucolipids and Their Isomers from Human and Canine Intestine. J. Biol. Chem. Vol.257 No.2 January 25:755-60.

Mountford,C.E., May,G.L., Mackinnon,W.B., Dyne,M., Holmes,K.T., Vanhaaften-Day,C., and Tattersall,M.H.N. (1987a) Proteolipid Identified by Magnetic Resonance Spectroscopy in Plasma of a Patient with Borderline Ovarian Tumor. Lancet 1:829-34.

Mountford,C.E., Wright,L.C., May,G.L., Holmes,K.T., and Dyne,M. (1987b) Inhibition of Metastatic Potential by Fucosidase: an NMR Study Identifies Fucoganglioside as a Cell Surface Metastasis Marker. J. Cell. Biol. Suppl. 0(11 part D):144.

Nicholson,J.K., and Nicholson,F. (1987) Proton Spectroscopy of Plasma and Testing for Malignancy. Lancet Aug.1.

Nudelman,E., Levery,S.B., Kaizu,T., and Hakomori,S. (1986) Novel Fucolipids of Human Adenocarcinoma: Characterization of the Major Le Antigen of Human Adenocarcinoma as Trifucosylnonaosyl Le Glycolipid ($III^3FucV^3FucVI^2FucnLc6$). J. Biol. Chem. Vol.261 No.24 August 25:11247-53.

Schroit,A.J., Madsen,J.W., and Tanaka,Y. (1985) In vivo recognition and clearance of red blood cells containing phosphatidylserine in their plasma membranes. J. Biol. Chem. 260:5131-8.

Schwartz,R., Schirrmacher,V., and Muhlradt,P.F. (1984) Glycoconjugates of Murine Tumor Lines with Different Metastatic Capacities. I.Differences in Fucose Utilization and in Glycoprotein Patterns. Int. J. Cancer 33:503-9.

Turner,D.L. (1985) Basic Two-Dimensional NMR. Prog. in NMR Spectroscopy Vol.17:281-358.

Wellner,D., and Greenfield,R.S. (1979) L-Threonine Deaminase as a Possible Antitumor Agent. Cancer Treat. Rep. 63:1089-94.

Williams,P.G., May,G.L., Holmes,K.T., Wright,P.E., Ekiel,I., Smith,I.C.P., and Mountford,C.E. (1986) Two Dimensional Proton NMR Studies of Intact Cancer Cells. Magnetic Resonance in Cancer; International Conference, Banff, Alberta, Canada, Apr.30-May 4,1985. Allen,P.S.,D.P.J. Boisvert and B.C. Lentle (Ed.) Pergamon Press Inc.:127-128.

Yamamoto,M., Boyer,A.M., and Schwarting,G.A. (1985) Fucose-containing glycolipids are stage- and region-specific antigens in developing embryonic brain of rodents. Proc.Natl.Acad.Sci.USA Vol.82 May:3045-9.

CHAPTER 6

LACTATE EXPERIMENTS

Part I. Lactate Analysis of Colon Tumour and "Normal" Samples

Introduction

An elevation in lactate production is generally associated with tumour tissue. The amount produced varies from one type of tumour to another, and even in clones from the same tumour line (Kaplan et al. 1985). To determine whether the colon tumour samples contained greater amounts of lactate than the normal colonic samples, and to test for a correlation between these amounts and the T_2 relaxation value for the sample, it was decided to assay for lactate in the biopsy samples. A greater proportion of lactate with its extremely long T_2 (greater than 1 second) would be expected to yield a higher resultant T_2 value for the tissue concerned. Also, since the T_2COSY's of the previous chapter indicated that lactate was present in the cross peak at 4.2 ppm, it was important to determine to what extent the amount of lactate influenced either the presence or the magnitude of this cross peak.

Part I of this chapter will describe the lactate analysis of the biopsy samples and the results of the comparison between lactate content and T_2 values.

Part II will describe further experiments with lactate on human placenta - a more in-depth analysis of lactate, T_2 and the 2-D cross peak.

Materials and Methods

Preparation of Biopsy Samples for the Lactate Assay

Colon tumour and "normal" biopsy samples obtained for NMR analysis from January 20, 1987 onwards were used for lactate determination.

For pre-NMR lactate analysis, the total chopped-up sample (for both NMR and lactate analysis) was placed into a pre-weighed 2-dram glass vial with a teflon-lined screw-on lid and the wet weight of tissue determined. For post-NMR samples, 2 or 3 small pieces of tissue from the NMR tube were weighed similarly.

After the addition of 1 ml 1N KOH to break down the tissue cell structure, the glass vials were stored at 4°C. Within a week accumulated vials were heated in a water bath with their lids loosened and boiled for 15 minutes to dissolve the tissue completely. The vials were allowed to cool, and 1 ml of 8% perchloric acid (PCA) was added to each. This neutralized the KOH to bring the solution to the optimum pH (9.0) for the enzymes of the lactate assay kit. Also, the immediate formation of the precipitate $KCLO_3$ removed salt from the solution which could have interfered with the assay. The vials were shaken, then allowed to sit for 15 minutes to allow the precipitate to settle. The liquid was pipetted into 1.5 ml Eppendorf micro test tubes and spun in a Brinkmann Eppendorf centrifuge 5414 for 5

Table 6-1. Resuspension of lyophilized samples for lactate analysis.

Vial #	Sample Weight (g)	Amount of H_2O to add (ml) (0.2ml/0.1g wet wt.tissue)	Dilution Factor (F)
48	0.40	0.80	1
49	0.46	0.92	1
50	0.49	0.98	1
51	0.18	0.36 x 2 = 0.72	2
52	0.13	0.26 x 2 = 0.52	2
53	0.15	0.30 x 2 = 0.60	2

Table 6-2. Calculation of the amount of lactate in tissue samples.

Vial #	A	Concentration (g/l) (c = 0.33A x F)	μg lactate/g tissue ($2c \times 10^3$)	lactate in NMR tube (g)
48	0.908	0.303	606	467
49	0.586	0.195	390	285
50	0.703	0.234	468	370
51	0.426	0.284	568	
52	0.865	0.576	1152	
53	0.578	0.386	772	

minutes. The supernatants were pipetted into clean, labelled glass vials with screw-on lids and lyophilized. The lyophilized samples were kept at 4°C until further processing.

The lyophilized samples were resuspended with double-distilled water, 0.2 ml water per 0.1 g wet weight tissue (Table 6-1). After vortexing briefly, the solutions were pipetted into 1.5 ml Eppendorf tubes and spun for 5 minutes in the Eppendorf centrifuge. The supernatants were pipetted into clean labelled glass vials, ready for the lactate assay.

The Lactate Assay

The Boehringer-Mannheim L-Lactic Acid Assay kit, UV Method (Catalogue No. 139084) was used. A Bausch & Lomb Spectronic 2000 spectrophotometer was used to measure the absorbance at 340 nm. From the concentration value (g lactic acid per l of test solution) obtained, ug lactic acid per g of wet weight tissue was calculated. The amount of lactic acid in the NMR tube could be calculated from the known weight of sample in the tube. Table 6-2 gives an example of these calculations.

T_2 and Normalized α Calculations for the Samples

As discussed previously in Chapter 4, the longest T_2 value for each sample is the resultant of the relaxation

times of several components under the CH_2 peak which can occur in varying proportions from sample to sample. Lactate has the longest relaxation time of these components, being a small mobile particle. It was of relevance, therefore, to determine whether the amount of lactate in a sample influenced the magnitude of the long T_2 value as well as the proportion (α-value, or pre-exponential) of this long T_2 value among all the T_2 values for the sample. The T_2 values were calculated from the best non-linear least squares fit to the experimental data, as explained in Chapter 3. The α-values corresponding to the T_2 values were normalized as follows :

$$\text{normalized } \alpha_i = \text{actual } \alpha_i / \Sigma\alpha_i$$

where i=1,2,or 3, depending on the number of exponentials in the T_2 fit

Plots were made of the longest T_2 value and its normalized α-value vs. the amount of lactate in the sample. Comparisons were also made of the lactate content in colon tumour vs. "normal" samples.

Lactate Assay Reliability

A standard test was performed on known concentrations of a Lithium Lactate solution to test the reliability of the L-Lactic Acid Assay kit and the spectrophotometer readings. Results were well within experimental error. Six tissue samples were assayed at one time, along with a test sample of a 0.5mM Lithium Lactate solution to ensure that readings

were accurate. For some assays, a lactate standard (0.4 mg L[+]Lactic Acid per ml solution - catalogue no. 826-10) from SIGMA DIAGNOSTICS was used. A small amount (0.1 ml) of the standard solution was diluted with an equal amount of double-distilled water.

To test for stability of the lactate present with the sample preparation procedure, 0.5 ml aliquots of a 0.5mM Lithium Lactate solution were processed several different ways. The complete procedure as described above was followed for 1 aliquot, as well as for a control using double-distilled water instead of the lactate solution. To another aliquot 1 ml 1N KOH was added but the solution was not heated prior to addition of 1 ml 8% PCA. Two ml of water was added to yet another 0.5 ml of solution in place of the KOH and PCA, with no heating. One aliquot was simply lyophilized and resuspended, while another was not processed in any way prior to the lactate assay. All assays were within 0.006 g/l of the 0.048 calculated value for the concentration used. It was concluded that the preparation process did not affect the stability of the lactate in the samples.

After addition of 1 ml 1N KOH, the samples were usually kept in the refrigerator for a week before further processing. To ensure that this delay time did not affect the lactate determination, one sample was split three ways - one was processed immediately, one was left in the

Figure 6-1.

AMOUNT OF LACTIC ACID IN COLON TUMOUR SAMPLES VS. T_2 VALUES

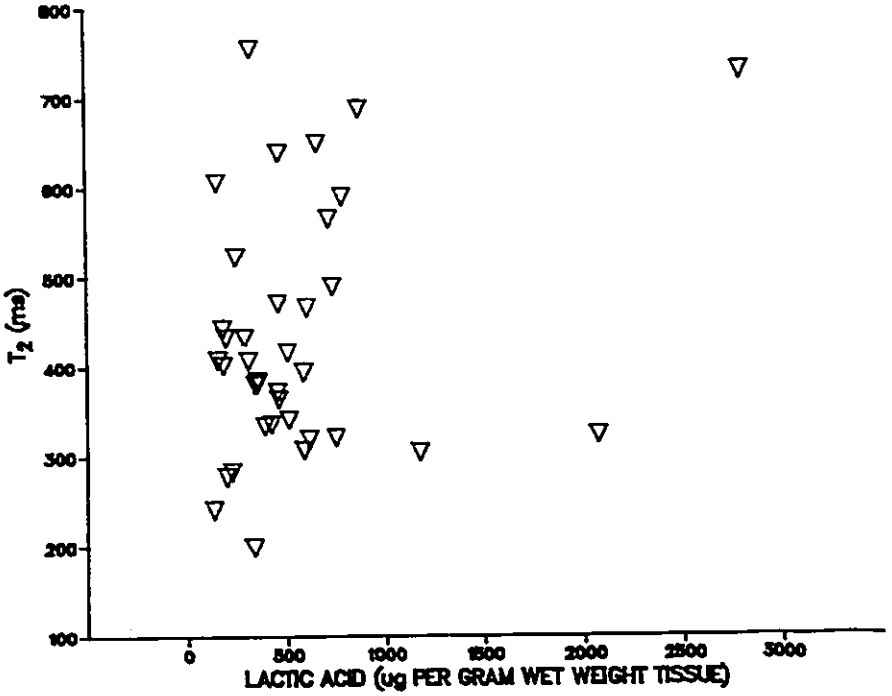

AMOUNT OF LACTIC ACID IN COLON TUMOUR SAMPLES VS. T_2 PRE-EXPONENTIALS (α)

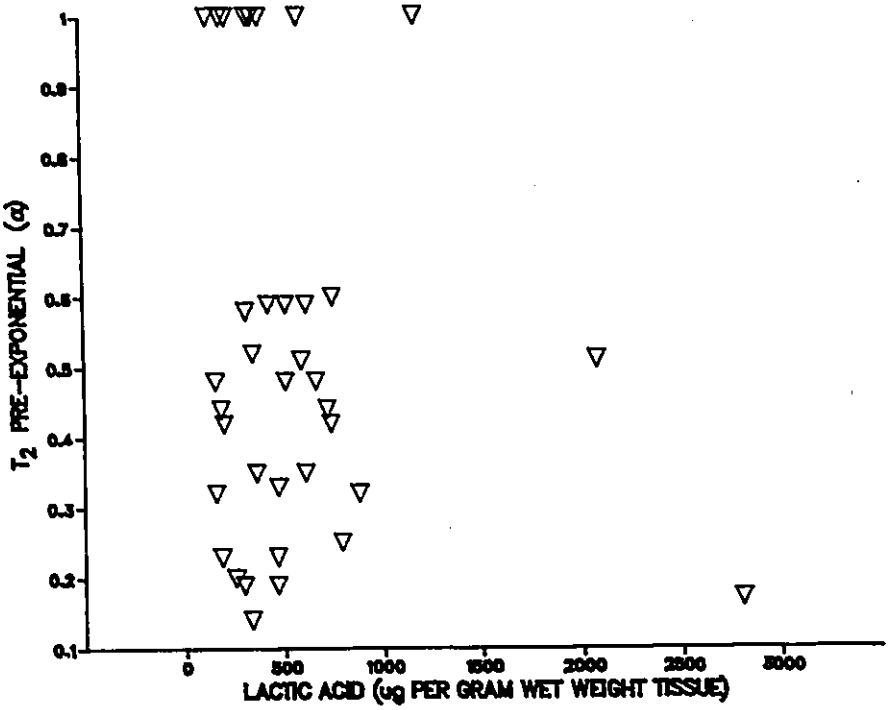

refrigerator for 2 weeks, and the third for 2.5 weeks. From extrapolation of the values obtained, it was determined that in one week the measured lactate in the sample dropped by 32 ug per g wet weight tissue, a drop of less than 1% from the value obtained by immediate processing.

One sample was split into two equal portions, to test consistency of measurement. The concentration of lactate in the two samples (c) varied by 0.01 g/l to give a 20 ug difference in the amount of lactate per gram of wet weight tissue, a 0.4% variability for the amount of lactate in the samples.

All the test results for lactate assay reliability were considered to be within experimental error, and the lactate assay used was thus deemed reliable.

Results

Amount of Lactic Acid in Colon Tumour Samples vs. T_2 and α-Values (Fig. 6-1).

"Normal" colon samples were included in these scatterplots.

The T_2 values range from 198 ms to 754 ms for amounts of lactic acid in the samples varying from 133 to 2806 ug per g wet weight tissue. For the same lactic acid content there exist a whole range of T_2 values, and the same T_2 value can result from a great variation in lactic acid content. A very long T_2 value (727 ms) is given by a tumour sample having 2806 ug lactic acid/g wet weight tissue, yet the longest T_2

Figure 6-2.

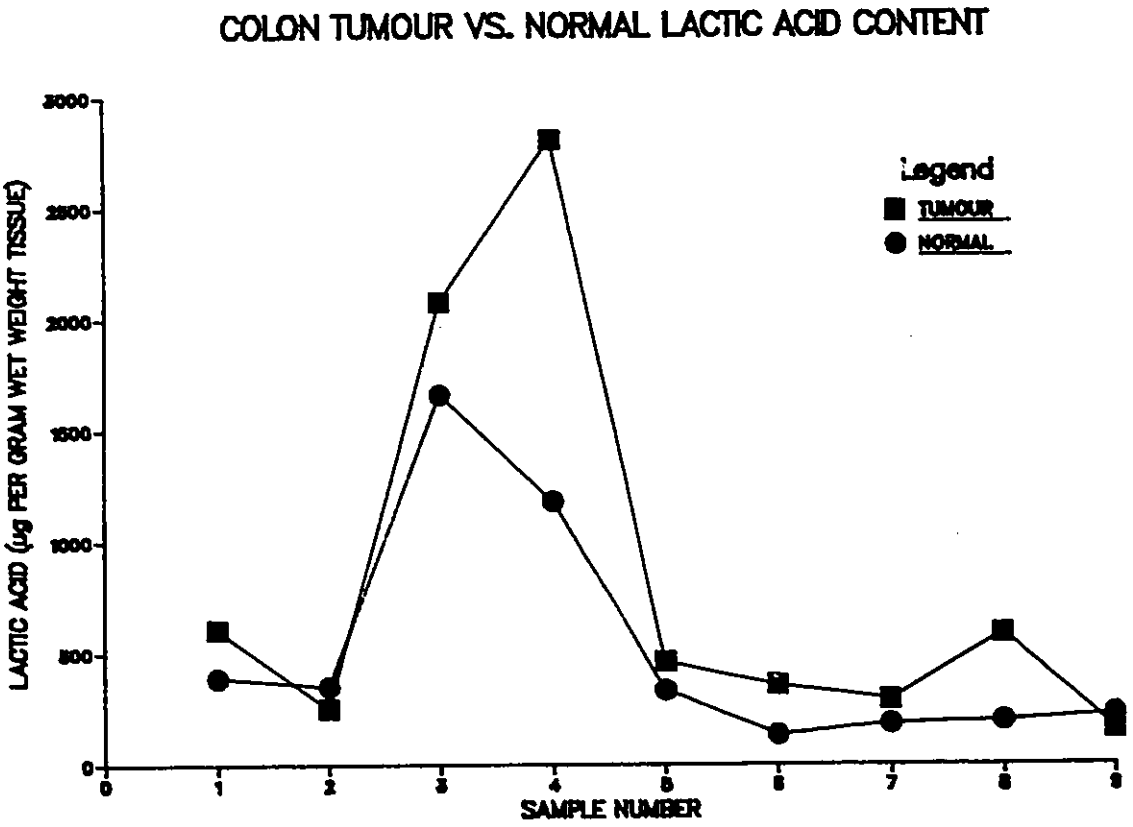
COLON TUMOUR VS. NORMAL LACTIC ACID CONTENT
LACTIC ACID (µg PER GRAM WET WEIGHT TISSUE)
3000
2500
2000
1500
1000
500
0
0
1
2
3
4
5
6
7
8
9
SAMPLE NUMBER
Legend
TUMOUR
NORMAL

Table 6-3. Comparison of lactate content in colon tumour and "normal" samples.

Sample #	pre-NMR ug lactate/g tissue Tumour	"Normal"	Ratio Tumour/"Normal"	Longest T_2 T.	"N."	post-NMR ug lactate/g tissue Tumour	"Normal"	post/pre-NMR Ratio Tumour/"Normal"	
209	606	390	1.55	465	333	1152	568	1.90	1.46
224	252	352	0.72	522	380	984	424	3.90	1.20
226	2076	1660	1.25	322	-*				
227	2806	1180	2.38	727	303				
230	460	332	1.39	363	198	924	410	2.01	1.23
233	356	133	2.68	383	240				
235	291	184	1.58	432	401				
243	586	197	2.97	306	277				
244	158	227	0.70	407	283				

* could not be fit by computerized nonlinear least squares fitting procedure due to systematic error in data

value (754 ms) is given by a sample containing only 330 ug. The pre-exponentials of the longest T2 component in these samples are almost identical - 0.17 for 727 ms and 0.14 for 754 ms - the shorter T_2 components for these samples, due to lipids, comprising 0.83 and 0.86 respectively of the total T_2 relaxation times.

Similar results are apparent for the scatterplot of pre-exponential values vs. the amount of lactic acid in the samples. The same ratio of the longest T_2 value to all the T_2 values for the sample, as yielded by the multi-exponential fit, can result from differing amounts of lactate. The same lactic acid content can yield a whole range of α-values for the longest T_2 component.

Lactate Content in Colon Tumour vs. "Normal" Samples

Fig. 6-2 and Table 6-3 present the results of the comparison between colon tumour and "normal" samples with respect to lactic acid content.

Tumour samples generally do contain more lactate than their "normal" counterparts, by ratios ranging from 1.25 to 2.97. In two samples, the "normal" tissue contains more lactate, giving ratios of 0.72 and 0.70, yet the tumour samples still yield longer T_2 values than the "normals" : 522 ms vs. 380 ms and 407 ms vs. 283 ms respectively.

Post-NMR lactate content data were acquired for only three tumour/"normal" sample pairs. It is noteworthy that

the tumour samples are capable of producing greater quantities of lactate than their "normal" counterparts in the same period of time. Even the tumour sample with less lactate content pre-NMR produced greater than 3 times the amount of lactate than the "normal" tissue when compared to their pre-NMR values.

Discussion

It is not surprising that tumours are capable of greater lactate production than normal tissue. As tumours grow, often the accompanying vasculature is insufficient to deliver an adequate supply of oxygen to the tissue, and anaerobic pathways prevail, resulting in an abundance of lactate. With lesser blood supply, metabolic waste products are not carried away, adding to the accumulation of lactate. Another reason for lactate proliferation in tumours could well be an increase in the amount of lactate dehydrogenase (LDH), the enzyme responsible for converting the pyruvate of glycolysis to lactate. Several researchers claim to have found an increase in LDH in tumour tissue. Bourrat and Müller-Klieser (1986) have found that tumour spheroids grown in culture medium containing large quantities of lactate were smaller in size with significant decrease in the size of the necrotic portion (the central dead region of the tumour, resulting from lack of proper nourishment) than spheroids grown in control medium or culture medium with

lesser amounts of lactate. Perhaps the increase in lactate maintains the level of viable tissue in a tumour.

If lactate were the major component influencing the value of the long T_2 , one would expect some correlation of T_2 value with the amount of lactate in the sample. Since no correlation is apparent, it would indicate that something else is the determining factor, or possibly a delicate interplay of several factors.

We have been assuming that the amounts of lipid and lactate in a sample would have a marked influence on the T_2 values obtained for our samples. Lipid and lactate analysis were performed for colon tumour #244 and colon "normal" #244. Considering only the amounts of lipid and lactate in a sample, it would be interesting to determine the theoretical resultant T_2 value. Using the model of discrete T_2 values as obtained by the multi-exponential least squares fitting procedure, a 2-exponential equation would describe the relaxation decay curve :

$$I = I_{1ip}\, e^{-(t/T_{2lip})} + I_{1ac}\, e^{-(t/T_{2lac})}$$

where

I_{1ip}	is the initial intensity of the lipid peak, proportional to the amount of lipid in the sample times its proton ratio
I_{1ac}	is the same for the lactate peak
T_{2lip}	is the lipid relaxation time, taken to be 200 ms
T_{2lac}	is the lactate relaxation time, taken to be 1000 ms

For the lipid peak intensity, the amount of triglyceride in the sample was used, since the high resolution lipid peak

results from the mobile triglycerides in domains associated with the plasma membrane. The phospholipids in the bilayer would not give the high resolution peak observed in the ^1H NMR spectrum. From the amounts of triglycerides and lactate in the samples as discerned by biochemical analysis, and an approximate lipid/lactate proton ratio of 28:1 (using an 18-C fatty acid as an average chain length), the equations are :

$$\text{Tumour} : \quad I = 83.72e^{-(t/200)} + e^{-(t/1000)}$$
$$\text{"Normal"} : \quad I = 72.24e^{-(t/200)} + e^{-(t/1000)}$$

The fitting program gave a 2-exponential as the best fit to the simulated data, as expected :

$$\text{Tumour} : \quad I = 81.9e^{-(t/198)} + 2.9e^{-(t/494)}$$
$$\text{"Normal"} : \quad I = 71.5e^{-(t/200)} + 1.7e^{-(t/671)}$$

The results are very close to the original equation, but with large errors in the long T_2 value (494 ± 360 ms and 671 ± 561 ms). The program found the two components but had difficulty resolving the longer one because of its small proportion and possibly because the delay times do not exceed 960 ms. Nonetheless, the expected ratio of components are recovered. The normalized α's indicate the much larger proportion of the lipid component :

Tumour : 0.97(198 ms) + 0.03(494 ms)
"Normal" : 0.98(200 ms) + 0.02(671 ms)

The actual experimental NMR data, on the other hand, gave quite different results. Tumour #244 was fit by a 2-exponential equation, giving upon normalization of α :

0.52(122 ms) + 0.48(407ms)

The shorter lipid component carries equal weighting with the longer T_2 component. Clearly something other than the lactate present in the sample is involved (as the T_2COSY experiments suggested) to make such a large difference in the weighting. The actual long T_2 value is shorter also, possibly due to the strong lipid component's influence.

"Normal" sample #244 was fit by a monoexponential decay of T_2 value 283 ms. A longer T_2 component was not resolved at all, but possibly averaged in, resulting in an essentially lipid-range T_2 value. The results are close to the simulated data, i.e a strong (α=0.98) lipid-range T_2.

The actual triglyceride/lactate ratios for the samples did not differ by much, yet the experimental NMR data yielded strikingly different results for the tumour and the "normal" sample. The evidence is strong for the existence of a strong longer-T_2-yielding entity other than lactate that is unique to tumours.

To identify and quantitate all the components of a sample by biochemical analysis and NMR would be an extensive and difficult task, especially since micromolar quantities are necessary for NMR visibility. The actual absolute composition of a sample is not as important as the resultant product of the relative proportions as evidenced in the T_2 value, if this gives a sufficient discrimination between malignant and normal samples. The initial purpose of this project was for diagnosis, to discover if a biochemical

difference does exist between tumour and normal samples, and if its magnitude can give an indication of metastatic potential for the tumour. This biochemical difference would be linked to an NMR parameter, or combination of parameters, as illustrated for colon samples in Chapter 4.

Eventually, the identity of the source of the difference will matter, for purposes such as antibody targetting. Further biochemical analysis and NMR experiments - notably 2-D - are then warranted to find the compound(s ?) responsible, or at least eliminate the ones that are not, in order to narrow down the search. The experiments on human placenta samples in Part II of this chapter were undertaken for this latter purpose, to determine whether changing the amount of lactate in a sample influences the long T_2 value and the cross peak in the 2-D COSY spectrum.

Conclusions

The amount of lactate in a tumour or "normal" sample has no direct bearing on either the magnitude or the proportion of the longest T_2 value for that sample. It is becoming more and more apparent that this T_2 value is the result of a complex interplay of relaxation times from all the resonances under the spectral peak at 1.3 ppm, possibly with one particular resonance peculiar to tumours having the greatest influence.

LACTATE EXPERIMENTS

Part II. Lactate Experiments on Human Placenta Samples

Introduction

One of the two sources of false positives in Fossel's diagnostic blood test for cancer (Fossel et al. 1985) was pregnant women (for the curious, men with non-cancerous prostate problems was the other). Apparently the blood of pregnant women and cancer patients have something in common. The developing fetus and its nourishing placenta immediately come to mind as probable sources of this mimicry of cancer.

There appear to be basic similarities between placental and cancerous growth. Both are rapidly developing and proliferating tissues with one fundamental difference - the placental growth is regulated by the body whereas tumour growth is aberrant, having escaped the body's normal control mechanisms. The placenta can be thought of as invading the uterine endometrium much as a cancerous growth invades its host tissue, colon cancer invading the bowel wall, for example. The cancer continues growing, eventually spreading to other body sites if left unchecked, whereas the placenta separates from its host tissue of nine months, after delivery of the baby. The exact mechanism by which this occurs is not known but some placental proteins have been singled out as playing a part in this separation. The placenta is an extremely rich tissue, with an abundant blood supply, and producing many different proteins such as

hormones, enzymes, immunoregulatory proteins, transport and receptor proteins, to name a few. Some of these proteins contain substantial amounts of carbohydrates.

One important similarity with tumour tissues is the placenta's immunoregulatory properties. Here is a tissue that is part of the mother, yet part also of the developing fetus, which is half foreign to the mother, namely the paternal half. The mother is still resistant to infections, but her immune system has been tampered with, deviated from its normal workings in order to allow this partly foreign fetus and placenta to grow and develop.

This immunoregulatory capacity of the placenta has been demonstrated in grafting experiments on mice (Voisin et al. 1984). Mice immunized with A/J spleen cells in the presence or absence of liver extract rejected an A/J sarcoma tumour graft, while mice immunized together with a placental extract did not reject the tumour graft. The placental extract suppressed the immunization factor. Voisin et al. point out that the outcome of an immune reaction launched against a foreign invader or graft depends on the balance between a rejection reaction and a facilitation reaction. They propose that during gestation the balance would be in favour of the facilitation reaction which protects the antigen-bearing target and that the placenta plays a role in this immunodeviation. Several placental proteins have been isolated as being part of this immunodeviatory system, but

its actual workings are still a mystery.

It is apparent that a tumour growth fools the immune system in some way also, in order to gain a foothold in the tissue where it is growing. We are under the assumption that it is something on the cell surface (specifically the sugar fucose at an oligosaccharide terminus), an immunomodulatory antigen, that is the source of our long T_2 values and Cross Peak Y. The antigenic determinants on the placental trophoblast at the maternal/fetal interface are also cell surface constituents. Thus it appears to be of great interest and relevance to this project to study placental tissue.

We had also planned to study embryonic tissue, particularly gut (because of our concentration on colonic tissue) and brain, because increases in fucose levels have been documented in embryonic brain from various mammalian sources (Yamamoto et al. 1985). There was only time, however, to do the studies on placenta, so the investigation of embryonic tissue is left for others to pursue.

The basic plan for work with placentas was first of all to compare its T_2 values with those of tumour tissue, and to note the presence or absence of Cross Peak Y in a 2-D NMR experiment. The lactate content of the placental tissue was to be compared with its T_2 values, as for the colonic tumour samples. If the occurrence of Cross Peak Y was noted, enzymatic experiments were planned to remove lactate from

the sample in order to determine whether lactate was the source of this Cross Peak in placenta. With the experimental protocol worked out on placental samples, the same type of experiment could later be done on tumours. The findings for one type of tissue do not necessarily hold for another type of tissue, yet the same method could be employed for both.

Materials and Methods

Placenta Samples

Pieces of fresh, human, full-term placentas were obtained from the Civic Hospital Pathology Laboratory. The samples were placed in test tubes containing either PBS, Growth Medium (RPMI with Fetal Calf Serum, HEPES buffer, and $NaHCO_3$), or Imidazole buffer (0.05 M). All buffers were of pH 7.4. The samples were kept in ice water.

The placental samples were dark burgundy in colour, rich in blood, with a bluish white membrane on the outer side. The texture was similar to liver, but upon cutting, the tough fibrous nature of the tissue was apparent. The same general procedure as for the tumours was followed in preparing the samples for NMR, and in preparing small sample pieces for lactate analysis.

NMR Experiments, T_2 Determination

As for the tumour samples, a CPMG automated sequence with the number of experiments (NE) equal to 30 was run. The

number of scans (NS) per experiment was usually 24, but NS = 16 or 8 was sometimes used. The non-linear least squares fitting program was used to obtain the T_2 values. A COSY experiment was run to obtain 2-D NMR spectra. Three 1-D cross-sections were plotted per COSY, to obtain maximum intensity measurements for the methylene (CH_2), methyl (CH_3) and 4.2 ppm peaks.

Lactate Oxidase Experiments

Lactate oxidase (L-Lactate:oxygen 2-oxidoreductase, decarboxylating, EC 1.13.12.4) was obtained from Boehringer Mannheim (catalogue no. 396 745). A bacterial flavoenzyme (using flavin mononucleotide (FMN) as cofactor) prepared from Mycobacterium smegmatis, lactate oxidase catalyzes the oxidation of L-lactic acid to acetic acid and carbon dioxide :

$$\text{L-lactate} + O_2 \longrightarrow \text{acetate} + CO_2 + H_2O$$

In the absence of oxygen a reaction still takes place, but yields pyruvate as the product. Pyruvate is not a substrate for the enzyme. The enzyme forms an intermediate with pyruvate which decarboxylates in the presence of oxygen but dissociates from the enzyme in its absence. The proposed mechanism of action for the enzyme (Lockridge et al. 1972)

is as follows :

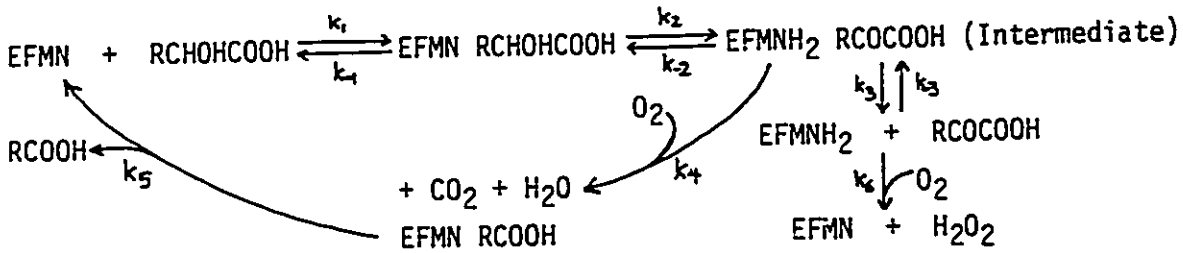

The rate limiting step is k_5, the dissociation of the reaction products. The optimum pH for enzyme activity was found to be 5.75 (Sullivan 1968) at 37°C reaction temperature. The pH of most of our samples, as measured by immersing the pH meter electrode into the contents of the NMR tube, was 6.8, at which pH there is still 80% of maximum enzyme activity. Sullivan performed all his experiments on lactate oxidase using a phosphate-based buffer. Lockeridge et al. later found that phosphate is a competitive inhibitor of the enzyme, resulting in the biphasic formation of a long wavelength absorbing intermediate. This resulted from the lactate being able to reduce only enzyme uncomplexed with phosphate (the rapid phase), while the slow phase resulted from the rate of dissociation of phosphate from the inactive enzyme-phosphate complex. Lockridge et al. therefore used 0.01 M imidazole-HCl buffer, pH 7.0 for all their experiments.

At first our placental samples were obtained in PBS/D_2O,

as had been the tumour samples. After noting that the lactate oxidase did not cut down tremendously on the amount of lactate in our samples, and after reading the paper by Lockridge et al., it was decided to put our samples into Growth Medium (in order to improve on sample viability for preparation of placental cell suspensions). When cell suspensions proved to be a lengthy procedure requiring the use of collagenase and many centrifugations, and of dubious merit for enzymatic elimination of intracellular as well as extracellular lactate, homogenate of placental tissue was tried. The results proved rewarding for the NMR experiments, and consequently homogenates were prepared.

To determine exactly to what extent the phosphate buffer inhibited the enzyme, solutions of 0.5mM Lithium Lactate in phosphate or imidazole buffer were reacted with lactate oxidase solutions prepared in D_2O. The lactate oxidase oxidized 60% of the lactate in phosphate buffer, 96% of the lactate dissolved in D_2O, 97% of the lactate in imidazole buffer incubated at room temperature, and 99% of the lactate in imidazole buffer incubated at 37°C. Thus the enzyme was noticeably inhibited by phosphate. From placenta #19, therefore, all the placenta samples were obtained in imidazole buffer. Samples were incubated with lactate oxidase at 37°C for 15-20 minutes, swirling in an open scintillation vial to ensure an adequate oxygen supply for the reaction.

Figure 6-3. Spectra of placenta, lactate oxidase and imidazole buffer.

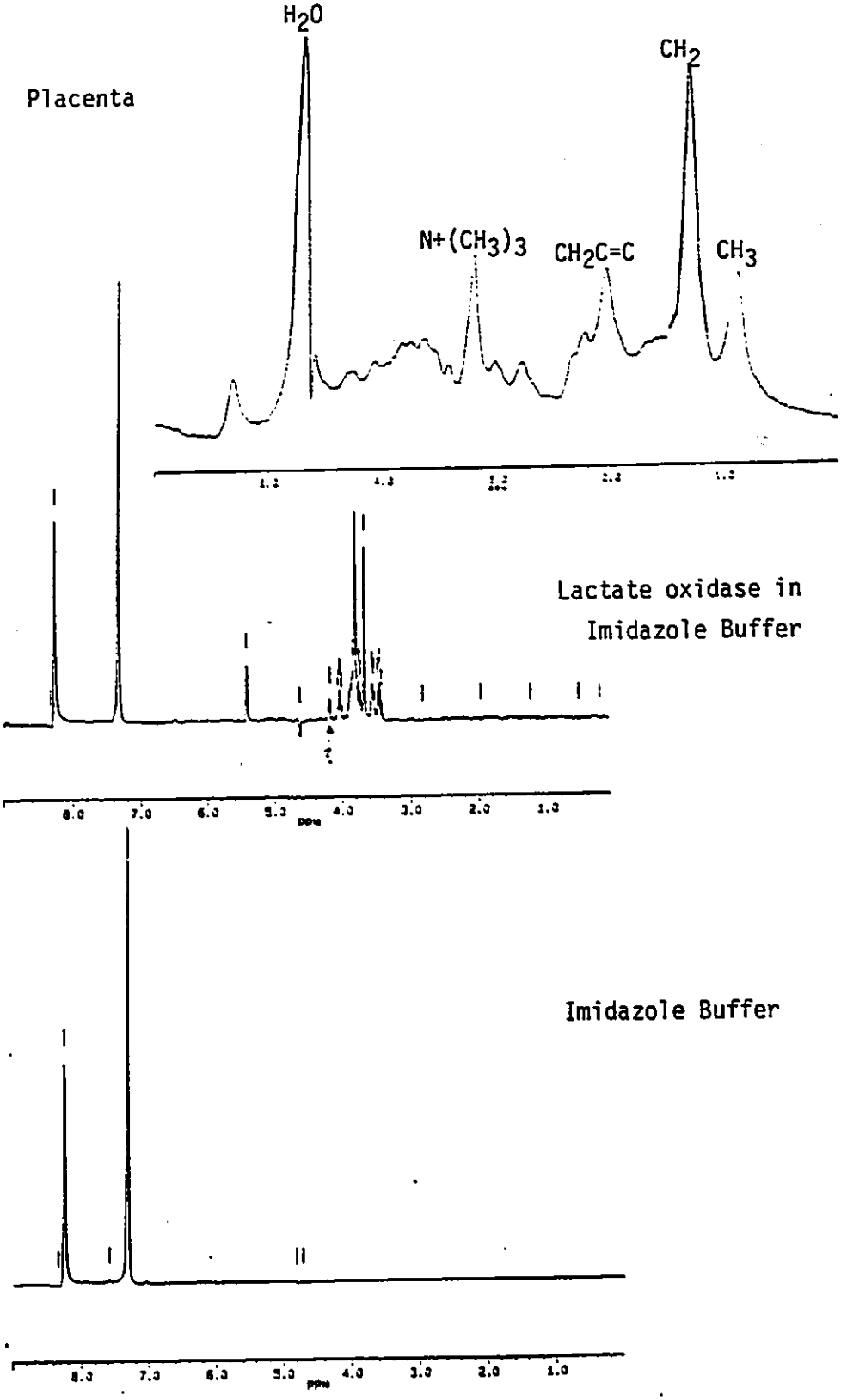

Enzymatically reducing the amount of lactate in our samples by its conversion to other compounds, whether acetate in the presence of oxygen or pyruvate in its absence, is useful for monitoring the effect of changing the lactate concentration in an NMR experiment. By changing the compound's chemical composition, its chemical shift is moved elsewhere in the NMR spectrum. The resonance due to lactate under the CH_2 peak at 1.3 ppm would thus decrease in height, and a peak corresponding to acetate (2.1 ppm) or pyruvate (2.55 ppm) would grow in its place. In the one-dimensional cross-section from the 2-D NMR COSY, the peak at 4.2ppm is coupled to the resonance at 1.3 ppm under the CH_2 peak. If the source of this peak is lactate, it will fluctuate in height as the amount of lactate in the sample fluctuates during the lactate experiment. The imidazole buffer is good buffer from an NMR point-of-view, since its resonances occur at 7-8 ppm, in no way interfering with the peaks of interest at 1.3 and 4.2 ppm. Lactate oxidase likewise has no interfering peak at 1.3 ppm (see Fig. 6-3). Since there is no peak at 1.3 ppm, the small peak at 4.2 ppm in the 1-D spectrum of lactate oxidase bears no relationship to the peak at 4.2 ppm resulting from scalar coupling with the resonance at 1.3 ppm in the cross-section of the 2-D spectrum of the placental sample.

Preparation of Lactate Oxidase Solution

Figure 6-4. Typical 2-D COSY and 1-D CPMG spectra of placenta. Note single cross peak at 4.1 vs. 1.3 ppm.

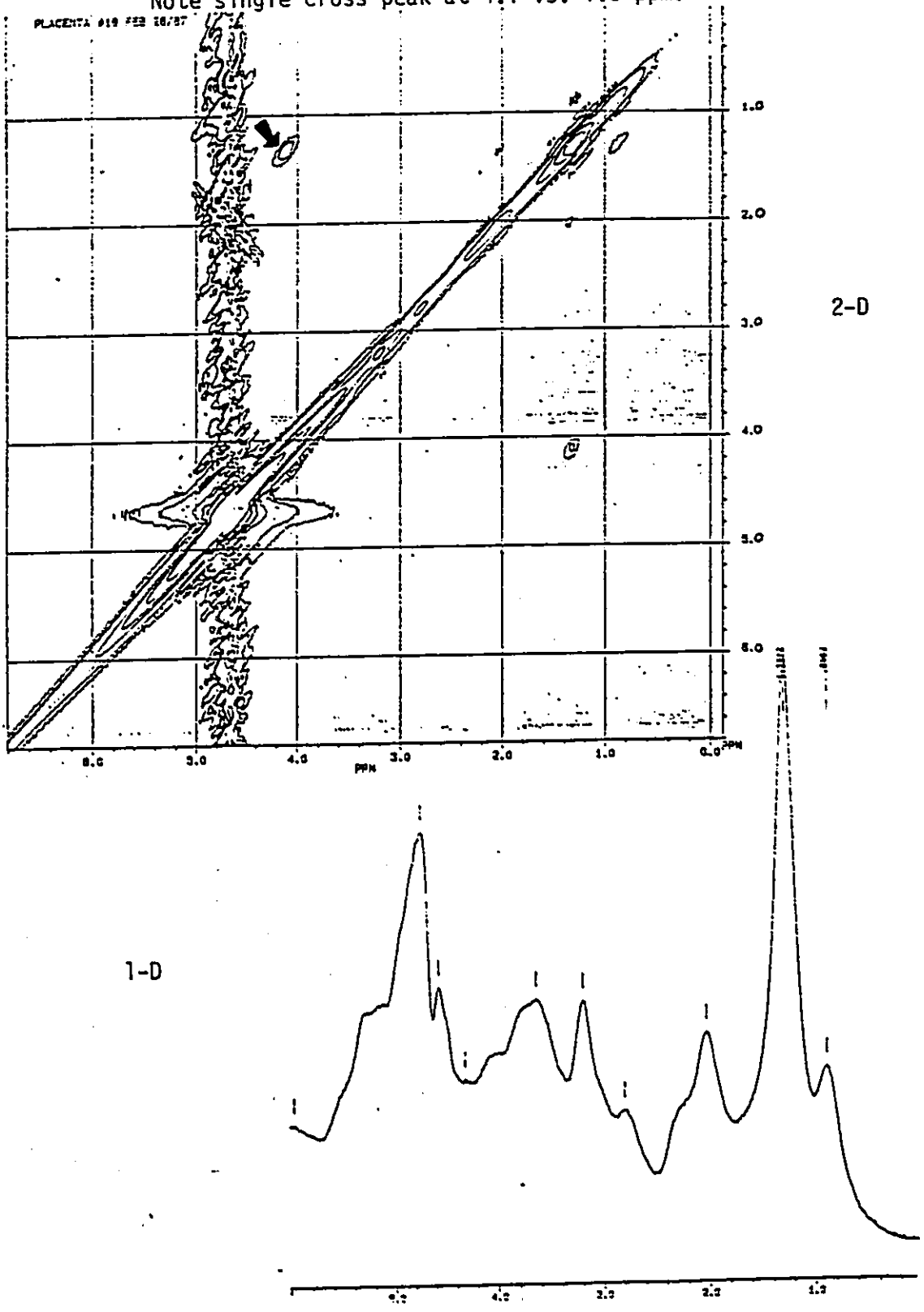

Stock Solution

0.0024g lactate oxidase crystals made up to 2ml in 0.01 M Imidazole Buffer in D_2O

0.1 ml of solution will deliver 112 ug of lactate oxidase

The specific activity of the enzyme is 15U, which means that 1350 ug lactate are transformed per minute per mg lyophilized lactate oxidase crystals. For transforming 300 ug lactate, the average amount in our samples, 0.2 ml of the Stock Solution would be sufficient. Two times this amount was used, however, to ensure a decrease in the net amount of lactate. As lactate was removed by the enzyme, the tissue would produce more.

Preparation of Placental Homogenates

To a weighed piece of placental tissue was added a known volume of imidazole buffer, and the mixture homogenized. A known volume (usually 0.7 ml) was then pipetted into a 5 mm NMR tube. For lactate analysis pre- and post-NMR, 0.1 ml of the homogenate was used. In this way the actual amount of placental tissue as well as the amount of lactate in the NMR tube could be calculated.

Results and Discussion

NMR Experiments

A typical 1-D spectrum and 2-D COSY spectrum of a placenta sample are shown in Fig. 6-4. Note the presence of

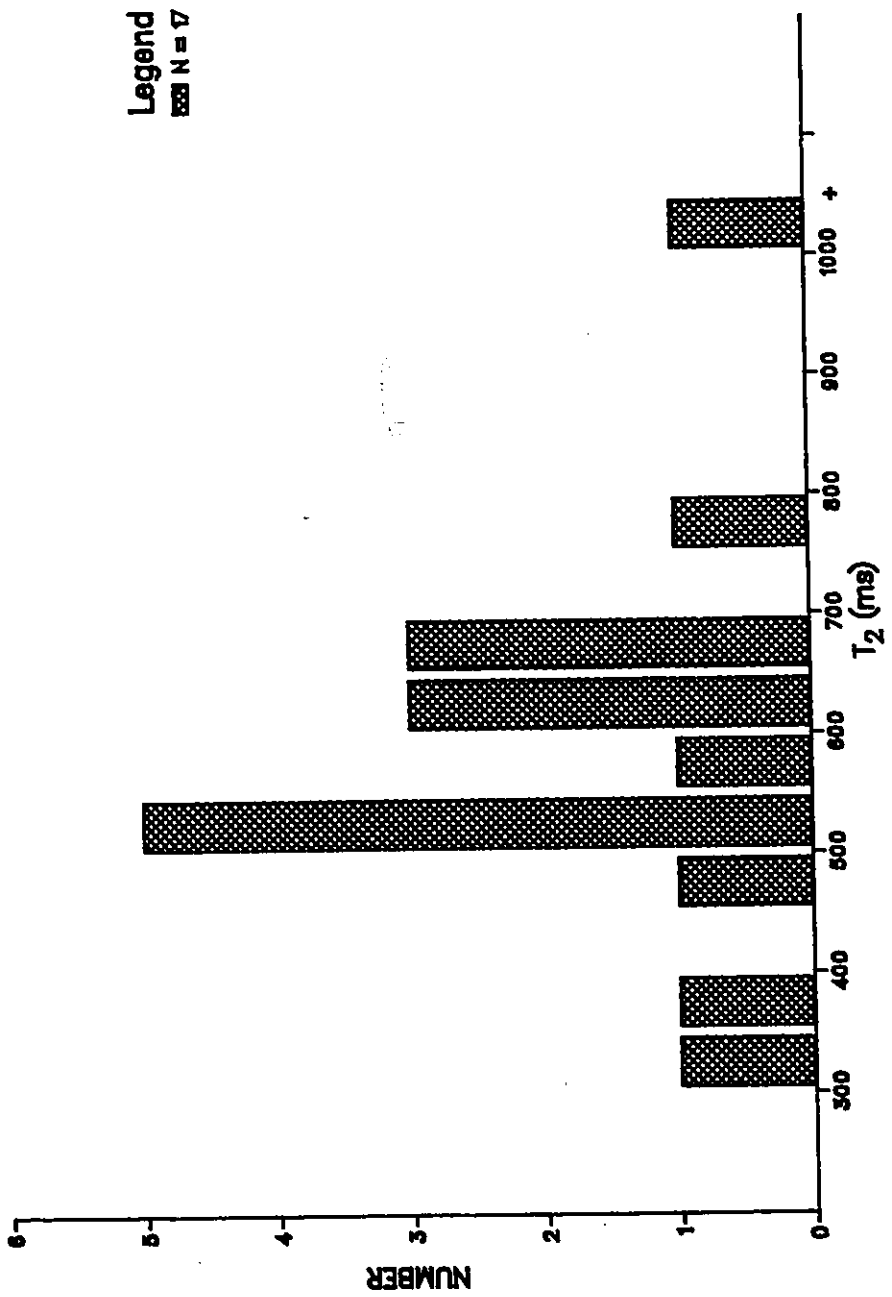
HISTOGRAM OF T_2 VALUES FOR PLACENTA
Legend
N = 17
NUMBER
0
1
2
3
4
5
6
300
400
500
600
700
800
900
1000 +
T_2 (ms)

Figure 6-5.

Figure 6-6.

AMOUNT OF LACTIC ACID IN PLACENTA SAMPLES VS. T_2 VALUES

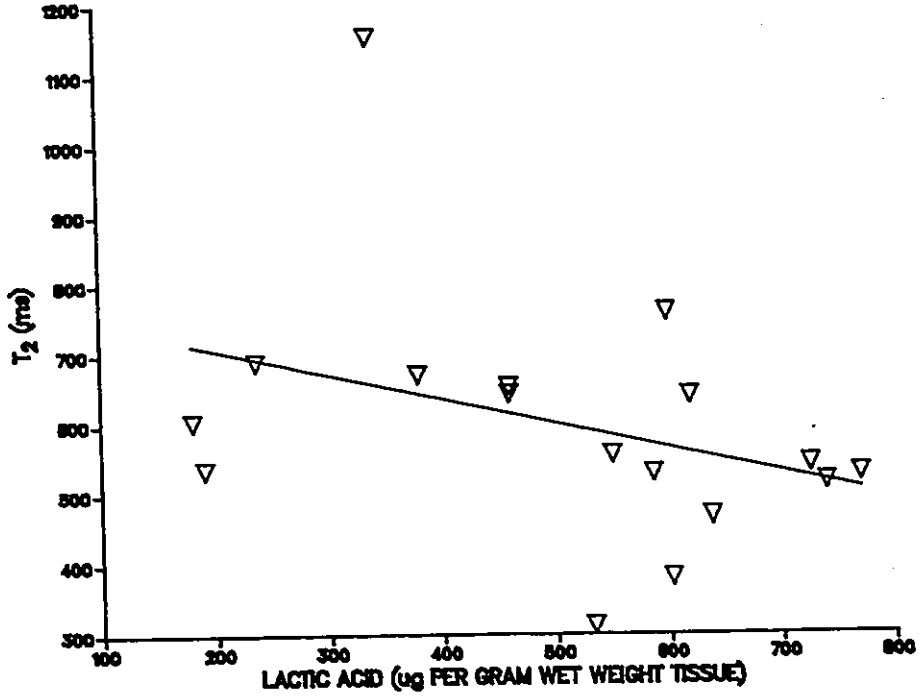

AMOUNT OF LACTIC ACID IN PLACENTA SAMPLES VS. T_2 PRE-EXPONENTIALS (α)

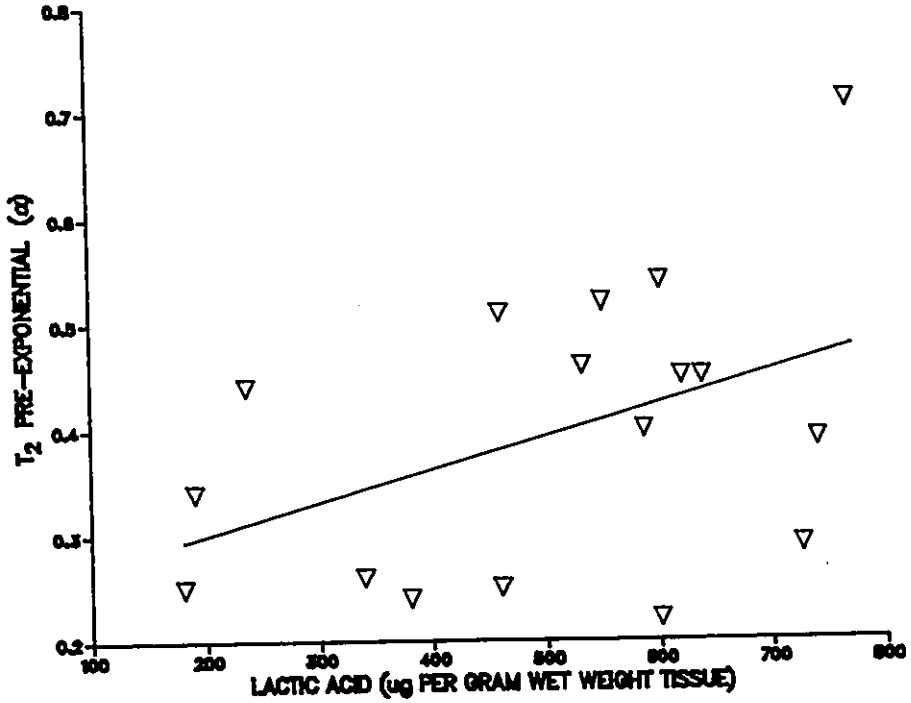

a cross peak at the intersection of 1.3 and 4.1 ppm, indicating coupling between protons at these resonances. As for the "normal" colon samples, only this cross peak is evident for placentas, whereas the colon tumour samples have the additional cross peak indicative of metastatic potential at 4.2 ppm.

Range of T_2 Values for Placenta (Fig. 6-5)

T_2 values for the 1.3 ppm resonances of 17 placenta samples were obtained. The decays were multi-exponential. The longest T_2's of 76% of the samples fall in the range 450 to 700 ms; 90% are above 450 ms, comparable to the long T_2 values of the tumour samples.

Amount of Lactic Acid in Placenta Samples vs. T_2 and Pre-exponential Values (Fig. 6-6)

Results differ from those for the tumour samples, where no correlation at all could be found between lactate content and T_2, or α-value. For the placentas, lactic acid content ranges from 180 to 770 ug/g wet weight tissue with all the T_2 values but one ranging from 300 to 760 ms. The greatest variation in T_2's occurs in the proximity of 600 ug/g wet wt. tissue. At 450 and 750 ug lactic acid content there are several samples with virtually the same T_2 value, hinting at some correlation between the two parameters. A regression line fit to the data points has a slight negative slope, indicating a trend opposite to what one would expect, i.e.

Figure 6-7. 1-D spectra of Placenta # 21 : chopped sample, homogenate and homogenate after addition of lactate oxidase.

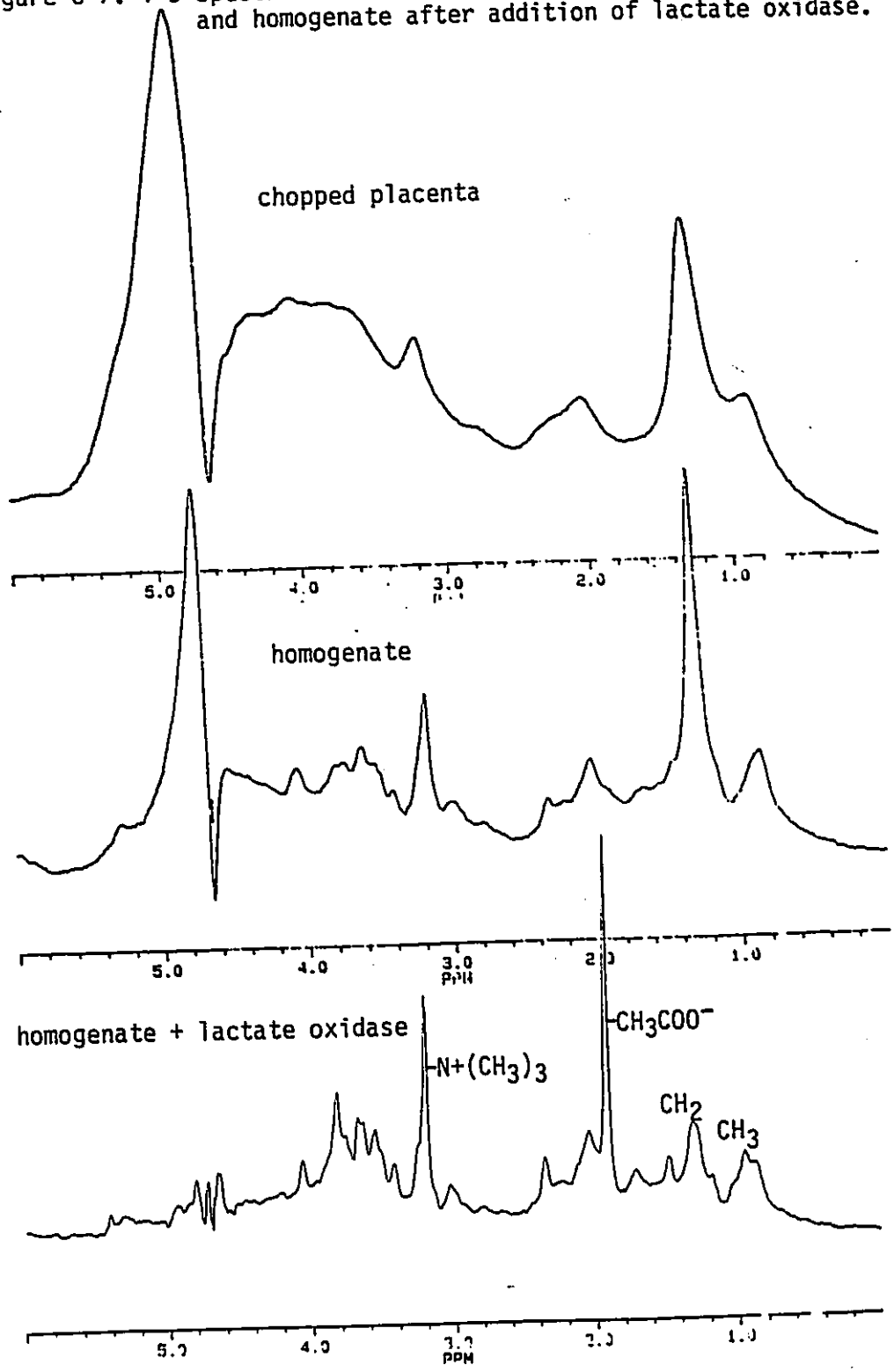

T_2 decreases with increase in lactate content rather than increases. The regression line through the α-values is surprising again; as the long T_2 value decreases with increasing lactate content, the relative population of this T_2 component increases at about the same rate.

If one asssumes that lactate with its extremely long T_2 is the major determinant of the longest T_2 for the sample, the plot of lactate content vs. pre-exponentials agrees with this assumption. Yet the actual T_2 value appears to decrease with increasing lactate content. One can only infer that another factor is involved, lending even greater weight than the lactate content, in order to reverse the incline of the regression line. It must be noted, however, that the above-mentioned trends are very general, with a large scatter of data points about the regression line. However, we have demonstrated clearly that in placenta the long T_2 value measured is not strongly influenced by the presence of lactic acid.

Lactate Oxidase Experiments with Placental Homogenates

T_2 Experiments

Representative spectra of a chopped placenta sample, a placental homogenate, and the latter after addition of lactate oxidase are shown in Fig. 6-7. The results of T_2 calculations for the methylene peak of these spectra appear in Table 6-4.

Table 6-4. T_2 Results for Placenta Homogenate Samples.

Sample #	Description	α	T_2	ug lactate in NMR tube	lactate ratio
19	chopped	0.40	530	434	
	homogenate	0.53	568	203	1.00
	h.+lac.oxid.	0.50	755	27	0.13
20	homogenate	0.29	542	610	1.00
	h.+lac.oxid.1	0.27	591	360	0.60
	h.+lac.oxid.2	0.33	474	63	0.10
21	chopped	0.54	380	452	
	homogenate	0.75	494	756	1.00
	h.+lac.oxid.1	0.36	557	122	0.16
	h.+lac.oxid.2	0.40	398	72	0.10

Several patterns emerge from Table 6-4. The placental homogenates yield longer T_2 values with larger α-values than do the chopped placenta samples. This is probably due to the homogenization process as molecules from previously rigid positions experience greater freedom of motion either as a result of mechanical action or the action of enzymes released from intracellular vesicles. In the case of placenta #19, the increases in T_2 and α are certainly not caused by an increase in lactate, since the amount of lactate is halved in the homogenized sample. For placenta #21, on the other hand, it is a possibility, since the amount of lactate in the homogenate is twice that in the chopped sample.

Upon addition of the enzyme, the T_2 is seen to increase initially, with a negligible decrease in α in two of the samples, and a large decrease in α for placenta #21. In all

cases the amount of lactate is decreased substantially by the enzyme. In samples #20 and #21, a subsequent T_2 experiment, run immediately after 0.1 ml of the sample was removed for lactate analysis, yielded a lower T_2 value by approximately 100 ms with no significant change in α-values. The amount of lactate was still decreasing, but not to the same extent as in the previous experiment. An explanation for the shorter T_2 values could be that as the lactate decreases, other molecules with shorter relaxation times, such as lipid, would rise in proportion, wielding greater influence on the resultant T_2 value. But why the initial increase in T_2 with decreasing lactate ? Could this imply the presence of another long-relaxation-time molecule ? One can reason that the 50 ms increase in samples #20 and #21 is insignificant, within the error of the T_2-fitting procedure, but the 200 ms increase for placenta #19 is not as easy to explain. Nonetheless, the T_2's are all long. It is the proportion of these long T_2 values that has greater relevance. Does it correlate with the amount of lactate ? Only for placenta #21 is there evidence of some correlation. Possibly the amount of lactate with respect to all the other molecular species present is insufficient to show a correlation for the other samples, i.e. it is not lactate that influences the α-value.

COSY Experiments

Figure 6-8. 2-D COSY's and 1-D cross-sections of a lactate oxidase experiment with placenta.

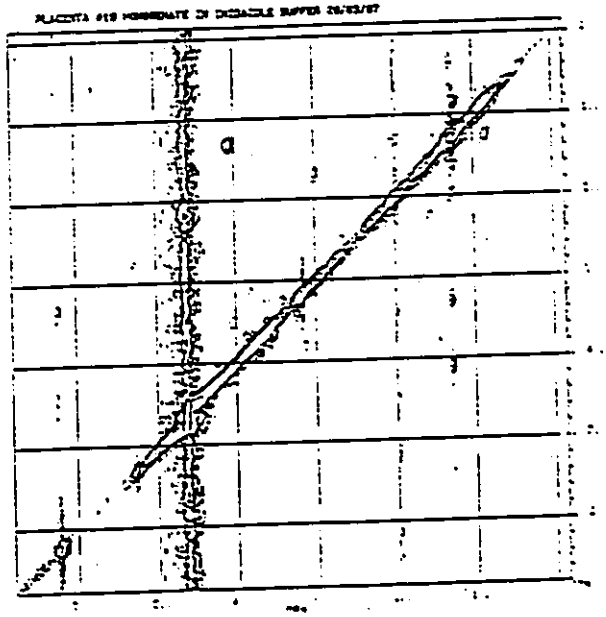

COSY's

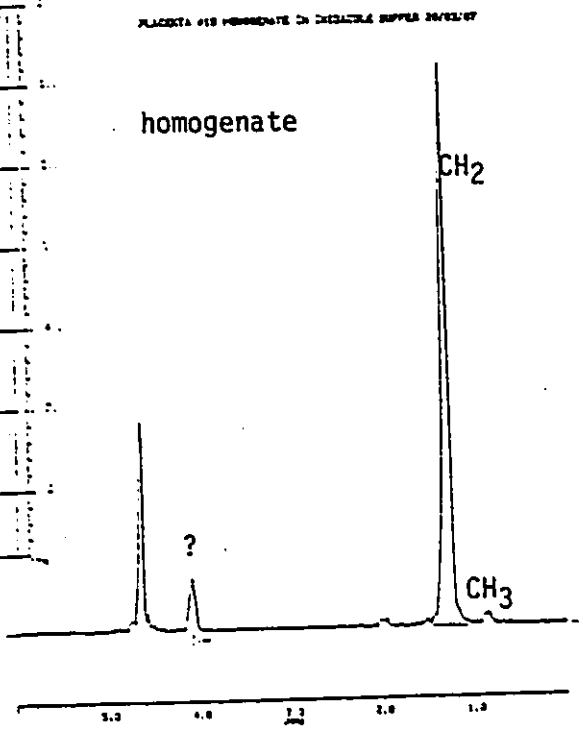

1-D cross-sections showing magnitude of cross peak before and after addition of lactate oxidase

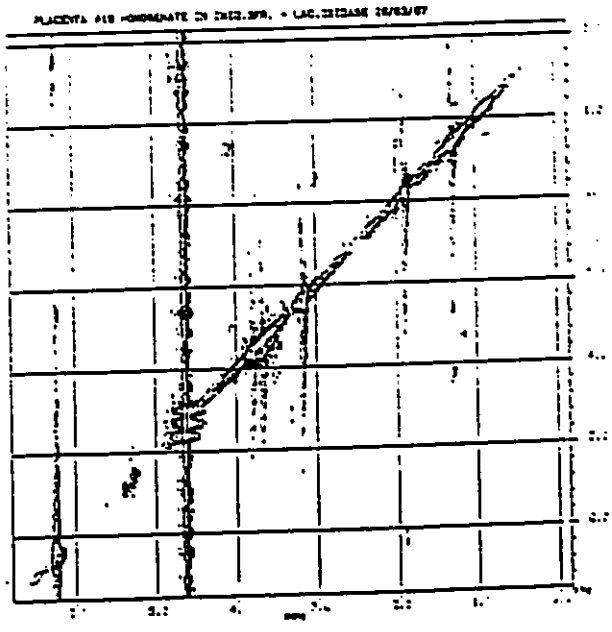

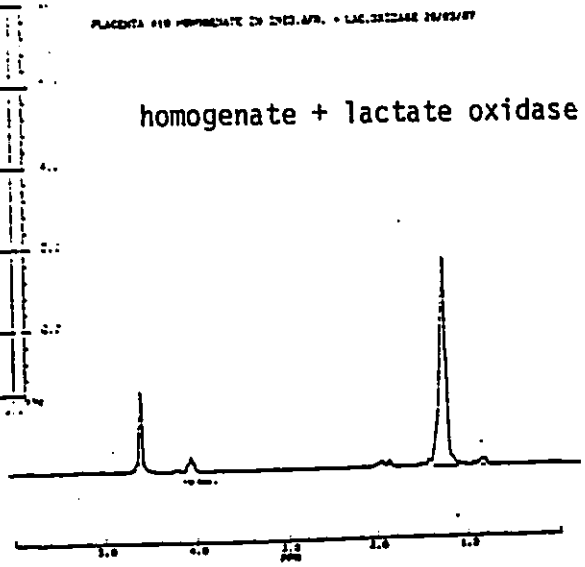

The COSY run for placenta #19 is shown in Fig. 6-8. The results for both placenta #19 and #21 are given in Table 6-5.

Table 6-5. Placenta COSY Results : Measurements.

Sample	Description	CH_2 Peak Height (cm)	4.1 Peak Height (cm)	CH_3 Peak Height (cm)	Lactate in NMR t. (ug)	Tissue in NMR t. (g)
#19	Homogenate	20.9	1.9	0.70	203	0.53
	+lac.oxid.	7.7	0.6	0.35	27	0.28
#21	Homogenate	467.0	44.0	8.30	756	0.63
	+lac.oxid.1	166.0	4.0	4.30	122	0.32
	+lac.oxid.2	90.0	2.8	3.75	72	0.28

Because of the great differences in peak heights for placenta #21, the 1-D cross-sections were plotted out at different scaling factors. The CH_2 and 4.1 ppm peak heights were multiplied to bring them to the same scaling level as the CH_3 peak. The homogenate was diluted with addition of the enzyme. The CH_3 (the methyl group at the end of the fatty acyl chains) peak height was taken as the reference for the amount of tissue in the NMR tube. A quick glance down the column marked "tissue in NMR tube" and comparison with the CH_3 peak heights will justify this choice. In order to calculate the decreases in the CH_2 and 4.1 ppm peak heights attributable to the decrease in lactate, it was necessary to know the decrease expected from decrease in tissue content alone. The "expected value" is that due to

dilution of the sample, as if lactate had no effect at all. The fraction of each peak affected by lactate is therefore equal to :

$$\left[\frac{\text{"expected value"} - \text{actual value}}{\text{"expected value"}}\right]$$

Table 6-6 summarizes these results.

Table 6-6. Placenta COSY Results : Changes in Peak Heights with Lactate.

Sample #	Description	4.1 ppm fraction	CH_2 peak fraction	reduction in lactate
19	homog.+enz.	0.37	0.26	0.87
21	homog.+enz.1	0.83	0.31	0.84
	homog.+enz.2	0.86	0.57	0.90

For both placentas, the fraction of the CH_2 peak affected by lactate is less than that of the 4.1 ppm peak. This is to be expected considering the multitude of resonances under the methylene peak. For placenta #19, the fraction of the 4.1 ppm peak affected does not match the reduction in lactate. For placenta #21 the peak fraction parallels the lactate reduction. These observations are in keeping with the T_2 experiment results : for placenta #19 lactate has negligible effect on the α-value whereas for placenta #21 lactate has a major effect. There was a great difference in experimental time span for the two placentas

Figure 6-9. T_2COSY of Placenta #13.

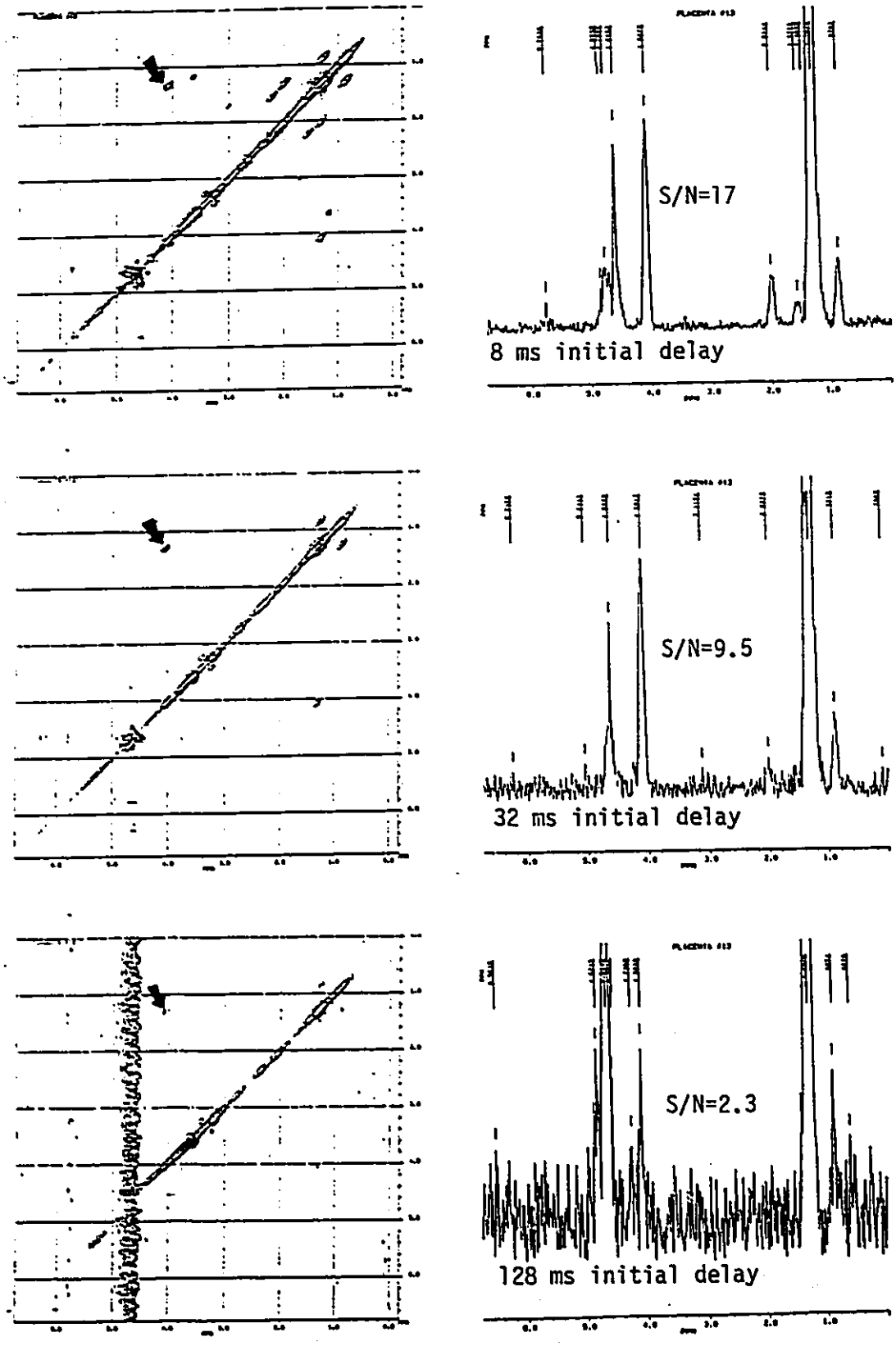

which probably resulted in the much greater initial lactate concentration for placenta #21. Alterations in the biological material with time could have had an effect also. The fact that for placentas #19 and #20 in the T_2 experiments lactate did not appear to alter the α-values, and the fact that 0.63 of the 4.1 ppm peak for placenta #19 was unaffected by a change in lactate indicate that further experiments, particularly 2-D COSY experiments, would be worthwhile. The non-lactate component of the 4.1 ppm cross peak could be fucose, as proposed for the same peak in the colon tumour and "normal" samples. In a T_2COSY experiment run on placenta #13 (Fig.6-9) the cross peak at 4.1 ppm can be seen to diminish rather quickly. With a relaxation delay between 300 and 800 ms (i.e. longer than that of lipid but shorter than that of lactate) the cross peak disappeared completely. More samples are necessary for a proper statistical data base. Controls are imperative, where buffer without enzyme is added to the homogenate to ensure that the decreases in peak heights are indeed due to lactate reduction and not to natural relaxation or homogenization-induced processes. The use of fucosidase after addition of lactate oxidase in the 2-D NMR experiment as well as biochemical analysis for fucose are warranted before definitive assignment for the source of the cross peak can be made.

The rationale for studying placenta, because of its

similarities to tumour tissue as outlined earlier, was finding a non-hazardous (as opposed to cancerous tissue) source of the long-T_2-and-Cross-Peak-Y-yielding antigen peculiar to tumours. The placental marker is in a slightly different configuration (4.1 ppm as opposed to 4.2 ppm) but it is not unlikely, from these preliminary findings, that the same molecule is responsible.

The role of cell surface carbohydrates for cell recognition and antigen specificity is well recognized. As mentioned earlier, tumours and placentas share immunoregulatory properties. Placental proteins believed to have immunoregulatory properties are situated at the maternal-fetal interface, the trophoblast (precursor of the placenta in the early embryonic stage, becoming the chorion later on - it is the chorionic villi that project into the uterine wall as the embryo implants itself), or are released into the maternal bloodstream. It is of interest that fucose appears as a carbohydrate-chain component in some of these proteins : e.g. in pregnancy-specific glycoprotein (Tatarinov 1978), in placental tissue factor (Scheefers et al. 1986), and in human chorionic gonadotropin (Kessler et al. 1979) where 25% of the carbohydrate chains contain the terminal sugar fucose (Mizuochi and Kobata 1980). The evidence linking fucose, the immune system, tumours, and placentas is more than circumstantial and worth further investigation.

Conclusions

The T_2 range and the presence of the cross peak at 4.1 ppm justify the use of placentas as a tissue comparable to tumour tissue. The 4.1 ppm peak in placenta is composed of lactate, as well as another component, as indicated in results from all samples but one. From a T_2COSY experiment, the entity could well be the same as in the colon samples. Further experiments are warranted. The protocol developed in these proceedings, with suitable controls, and the 2-D experiments proposed at the end of Chapter 5 with lactate oxidase and fucosidase could be used for future experiments on placentas and tumour samples to pinpoint the exact source of the cross peak not attributable to lactate.

Differences between placental and tumour tissue are to be expected. The tissues have great contrast of purpose : one for the continuation of the species, the other for its early demise. Yet the mode of their existence involves the key to regulation of the immune system. What one learns from placental tissue can thus be applied to our understanding of the unretarded growth of tumour tissue.

References

Bischof,P., Klopper,A.(Eds.) Proteins of the Placenta : Biochemistry, Biology and Clinical Application. 5th International Congress on Placental Proteins, Annecy, France. June 13-15, 1984.(Kargel, Basel 1985)

specifically :
Bohn,H. Biochemistry of Placental Proteins. pp.1-25.

Rosen,S.W. Ectopic Production of Placental Proteins and Their Subunits. pp.84-101.

Voisin,G.A., Duc,H.T., and Bobe,P. Immunomodulatory Proteins of the Placenta. pp.54-67.

Bourrat,B. and Müller-Klieser,W. (1985) Influence of Lactate Acculation on Growth, Viability and Oxygenation of Multicellular Tumor Spheroids. Pfluegers Archiv. 405(Suppl.2):R23.

Kaplan,N.O., McClure,D.B., and Esty,K. (1985) Lactic Acid Formation in Human Tumor Cells. Biochem. Med. 33(2):273-4.

Kessler,M.J., Reddy,M.S., Shah,R.H., and Bahl,O.P. (1979) Structures of N-Glycosidic Carbohydrate Units of Human Chorionic Gonadotropin. J. Biol. Chem. Vol.254 No.16 Aug.25:7901-8.

Lockridge,O., Massey,V. and Sullivan,P.A. (1972) Mechanism of Action of the Flavoenzyme Lactate Oxidase. J. Biol. Chem. Vol. 247 No.24 Dec.25:8097-106.

Mizuochi,T. and Kobata,A. (1980) Different Asparagine-linked Sugar Chains on the Two Polypeptide Chains of Human Chorionic Gonadotropin. Biochem. Biophys. Res. Commun. Vol.97 No.2 Nov.28:772-8.

Scheefers,H., Kobus,A., Geyer,R. and Mueller-Berghaus,G. (1986) Composition and Lectin Binding Properties of the Carbohydrate Moiety of Human Placental Tissue Factor. Haemostasis 16(Suppl.5):73-4.

Sullivan,P.A. (1968) Crystallization and Properties of L-Lactate Oxidase from Mycybacterium smegmatis. Biochem. J. 110:363-71.

Tatarinov,Y.S. (1978) Trophoblast-specific beta -glycoprotein as a marker for pregnancy and malignancies. Gynec. and Obstet. Investig. 9:65-97.

Yamamoto,M., Boger,A.M. and Schwarting,G.A. (1985) Fucose-containing glycolipids are stage- and region-specific antigens in developing embryonic brain of rodents. Proc.Natl.Acad.Sci.USA Vol.82 May :3045-9.

CONCLUSION

From the initial working hypothesis that a long T_2 value is indicative of metastatic potential in human tumours has emerged the new finding that the observed long T_2, in combination with other NMR parameters, is useful for the diagnosis of malignancy, in so far as colorectal cancer is concerned. The question of metastasis requires longer than the time span of this thesis for its verification, and clinical follow-up must be continued.

Before any disease can be successfully treated, the disease process, or pathology must be understood. The pattern of the disease must be elucidated, before means can be taken to disrupt it. Through the use of NMR, we have observed changes in the plasma membrane profile of the cell with the progression of cancer. Initially there is a marked elevation in T_2 value, a narrowing of the methylene (CH_2) peak, and the emergence of the choline ($N^+(CH_3)_3$) peak. The magnitude of these phenomena suggest profound changes both in composition and mobility in the cell membrane with the onset of cancer. In the intermediate stages, there is great variation in these values, parallelling the heterogeneity of the samples involved. In the terminal stages all the parameters revert to those indicative of normal tissue, although by other observations the patient is obviously very ill.

The cross peak at 1.3 vs. 4.2 ppm in the 2-D NMR COSY spectrum is unique to colon tumours, therefore is the source of their long T_2 value, and is definitive for malignancy. From the presence of this cross peak and the long T_2 values at the premalignant and initial stages of colon cancer, NMR parameters indicative of metastatic potential in the rat system (Mountford et al. 1987), it appears that most colon tumours possess the potential for metastasis. Although lactate comprises part of the cross peak, the bulk of this peak arises from another entity, which we propose to be fucose, a terminal sugar on cell-surface oligosaccharide chains, cell-surface antigens with possible immunoregulatory properties. The approximate relaxation times obtained from T_2COSY experiments and the chemical shift coordinates of the cross peak support this claim. The connection of fucose with cancer and metastasis has been well documented.

Lactate analysis of tumour and "normal" samples and experiments with human placentas prove that lactate content is not the determining factor either for the long T_2 or the cross peak. Further work with placenta and tumour samples are warranted, however, to prove that fucose is responsible for the parameters observed. Similar studies of fetal tissue would complete the investigation. Oncomodulin, an oncodevelopmental protein found in placentas and tumours in humans (Brewer and MacManus 1987), is lacking in rat fetal tissue (Brewer and MacManus 1987). It would be of interest

to discern if the long T_2 and cross peak common to placenta and tumour tissue appears also in fetal tissue. The similarity of the plasma membrane profiles of normal B lymphocytes and tumour cells was noted. This would also be worth investigation by NMR.

Our results from study of the colon data base, notably the elevation in T_2 values at the initial stages of colon cancer, demonstrate excellent potential for non-invasive early diagnosis and staging of colorectal cancer.

Henkelman et al. (1985) have addressed the role of Magnetic Resonance Imaging (MRI), still an evolving technology, in tumour staging. Better images are constantly emerging, but the practical uses of MRI depend on the user's ability to interpret the results. Because of the high cost of implementation, MRI must be shown to be more accurate or provide more information than other imaging modalities. These authors consider MRI for cancer management only if it will have beneficial effects for the medical outcome of the patient. They concur that non-invasive diagnosis by MRI would eliminate the trauma of other means of investigation such as biopsy by surgery. In my opinion, early diagnosis would have the additional advantage of earlier and possibly less aggressive treatment of the patient. A major problem with cancer is its usually late discovery. MRI has proven useful for cancer management in certain cases, e.g. in the brain and extremities. Henkelman et al. point out, however,

that most cases involve the rest of the body, in which MRI had shown little or no advance over other modalities at the time. With technological advances providing better contrast, resolution, and elimination of motion artifacts, the outlook for MRI in cancer management is constantly improving. Tissue contrast has been attained by differences in signal intensity as a result of the pulse sequence used. If the lipid peak T_2 could be implemented for contrast between normal and malignant tissue, the situation would be vastly improved.

In the introduction to this thesis, it was noted that tumour-distinguishing characteristics could not be recognized with ^{31}P spectroscopy until later in the cancer process. Using ^{1}H NMR, relaxation times for the water peak have been extensively reviewed by Bottomley (1987) and shown to be unreliable for cancer diagnosis. Bottomley et al. (1985) have suggested using localized ^{1}H NMR spectroscopy in combination with imaging to monitor the lactate CH_3 peak at 1.3 ppm as an indicator of hypoxia and ischemia. Because of the sensitivity of the hydrogen nucleus as compared to phosphorus, this would be superior to examining changes in the P_i peak with ^{31}P NMR for metabolic studies and clinical applications. The lipid (CH_2) peak is a problem, because of the overlap of its resonances with that of lactate. Our results indicate that rather than being an obstruction, it is the lipid peak that would provide relevant information,

as far as monitoring colon cancer progression is concerned. ^1H NMR localized spectroscopy focussing on the CH_2 peak in a section of colon could be used with confidence to diagnose malignancy as well as the stage of the disease process. Localization of the relevant section of colon is a major problem, especially at the premalignant and initial stages when tumour growths are small. As Henkelman et al. point out, however, MRI is evolving, and the technology for fast and accurate resolution of small tissue sections will one day be realized.

Our findings have shown NMR to be a sensitive tool for monitoring the plasma membrane changes in cancer progression, notably for colon. The information acquired could be useful for early diagnosis and staging of colorectal cancer in the future. Subsequent work, perhaps in another field, could further elucidate the nature of the malignancy/metastasis marker (fucose) singled out through NMR, possibly for the purpose of antibody targetting. It is hoped that this thesis work has added new and useful insight into the difficult problem of cancer.

References

Bottomley,P.A., Edelstein,W.A., Foster,T.H. and Adams,W.A. (1985) In vivo solvent-suppressed localized hydrogen nuclear magnetic resonance spectroscopy: A window to metabolism? Proc.Natl.Acad.Sci.USA Vol.82 April:2148-52.

Brewer,L.M. and MacManus,J.P. (1985) Localization and Synthesis of the Tumor Protein Oncomodulin in Extraembryonic Tissues of the Fetal Rat. Dev. Biology 112, 49-58.

Brewer,L.M. and MacManus,J.P. (1987) Detection of Oncomodulin, an Oncodevelopmental Protein in Human Placenta and Choriocarcinoma Cell Lines. Placenta 8, 351-63.

Henkelman,R.M., Poon,P.Y., Bronskill,M.J. and Dunlap,H.J. (1985) Evaluation of the role of MRI in tumour staging. Magnetic Resonance in Cancer. Eds. Allen,P.S., Boisvert,D.P.J. and Lentle,B.C. International Conference, Banff, Alberta, Canada, Apr.30-May 4, 1985. (Pergamon Press Inc.) pp 99-110.

Mountford,C.E., Wright,L.C., May,G.L., Holmes,K.T. and Dyne,M. (1987) Inhibition of Metastatic Potential by Fucosidase: an NMR Study Identifies Fucoganglioside as a Cell Surface Metastasis Marker. J. Cell. Biol. Suppl. 0(11 part D):144.

APPENDIX A

Program to suppress the water peak in spectra of biological samples.

```
;  PRESAT.AUR
;HOMO-NUCLEAR PRESATURATION (SOLVENT SUPPRESSION)

1 ZE                ;ZERO MEMORY
2 D1 HG S3          ;APPLY CW DEC. AT FREQ. C2, POWER S3, DURING D1
3 GO=2 DO           ;GATE DEC. OFF DURING AQ.
4 EXIT              ;EXIT WITH DEC. OFF

;RD=0
;D1 TYPICALLY 1-3 TIMES T1
;S3 TYP. 20-30L
```

Typical values :

D1 - 4 us to 5 us

S3 - 12L to 15L

Automated sequence (CPMG) for T_2 determinations

```
CPMGHG.AU
; THIS AUTOMATED SEQUENCE PERFORMS A
; CARR-PURCELL-MEIBOOM-GILL SPIN-ECHO FOR T2
; ELIMINATES J-MODULATION, 180 DEG PULSE ERRORS,
; AND DIFFUSION EFFECTS. SAMPLE SPINNING CAN MODULATE
; THE ECHO DECAY RATE.

;   D1 - 90 - (D2 - 180 - D2)*C - FID

RF #1.001
1 ZE
2 D1 HG S1          ;RELAX TO EQUILIBRIUM
3 P1:A              ;90 DEG PULSE, GP PHASE CONTROL
4 D2                ;DEPHASE
5 P2 PH2            ;180 DEG PULSE SHIFTED 90 DEG REL. TO P1
6 D2                ;REPHASE
7 LO TO 4 TIMES C       ;VARIABLE LOOP TO 4 FOR 'C' ECHOES
8 GO=2 DO           ;ACQUIRE FID, LOOP TO 2
  VD
9 WR #1             ;STORE FID
10 IF #1            ;INCREMENT FILE EXTENSION
11 VC               ;INCREMENT POINTER FOR VC LIST (NEXT VALUE OF 'C')
12 IN=1
TE
13 EXIT

PH2=A1 A3 A1 A3 A2 A0 A2 A0


;PROGRAM REQUESTS FILENAME FOR FIDS
;NE DEFINES THE NUMBER OF EXPERIMENTS, NO. OF ITEMS IN VC LIST.
;CURRENT VC LIST MUST CONTAIN A SERIES OF VALUES FOR THE LOOP
;   COUNTER 'C'. THESE MUST BE EVEN NUMBERS TO PROVIDE FOR
;   CANCELLATION OF 180 DEG PULSE ERRORS.
;D2 = A SHORT FIXED ECHO TIME TO ALLOW ELIMINATION OF DIFFUSION
;. AND J-MOD. EFFECTS. THE MIN. VALUE FOR D2 IS 0.6 MSEC TO ALLOW
;   FOR VARIABLE LOOP IN STEP 7. SHORTER VALUES OF D2 ARE
;   POSSIBLE WHEN A FIXED HARDWARE LOOP IS USED.
;   D2 SHOULD BE << 1/J  BUT > CA. 50*P2 TO
;   AVOID EXCESSIVE AVE. POWER OUTPUT FOR TRANSMITTER.

;D1 = 5*T1 FOR COMPLETE RELAXATION  (value from PRESAT.AUR used)
;P1 = 90 DEG  (usually from 6.9 to 7.3 us)
;P2 = 180 DEG (usually from 13.8 to 14.6 us, i.e. 2 x 90° pulse)
;RD=PW=0, GP, NS= MULTIPLE OF 8 (usually 24)
```

D2 was set to 1 ms, "C" in statement 7 is taken from VC list on following page

VC list for CPMG sequence - this gives the value for n in the sequence

$90^{\circ} - (\tau - 180^{\circ} - \tau)_n$

(τ = 1 ms)

1 = 4
2 = 304
3 = 112
4 = 240
5 = 480
6 = 400
7 = 384
8 = 48
9 = 432
10 = 80
11 = 464
12 = 200
13 = 352
14 = 144
15 = 277
16 = 8
17 = 176
18 = 448
19 = 320
20 = 32
21 = 336
22 = 288
23 = 216
24 = 416
25 = 96
26 = 368
27 = 64
28 = 128
29 = 256
30 = 160

The total time before acquisition is 2τx n, i.e. double the values in the VC list.

Program for acquisition of 2-D spectra (COSY)

```
; COSY.AUR
; HOMONUCLEAR SHIFT-CORRELATED 2-D NMR (JEENER)
; W.P.AUE. E.BARTHOLDI, R.R.ERNST, J.CHEM.PHYS. 64. 2229 (1976)
; K.NAGAYAMA ET AL, J.MAGN.RES. 40, 321 (1980)

;  D1 - 90 - D0 - 90 OR 45 - FID

; SYMMETRIC MATRIX WITH SHIFTS AND COUPLINGS IN F1, F2
; OFF-DIAGONAL PEAKS CORRELATE SPINS WHICH SHARE A
; SCALAR COUPLING J.

1 ZE
2 D1 HG              ;RELAXATION
3 P1 PH1            ;90 DEG EXCITATION PULSE
4 D0                ;EVOLUTION OF SHIFTS AND COUPLINGS
5 P2 PH2            ;MIXING PULSE, 90 OR 45 DEG
6 GO=2 D0             ;ACQUIRE FID
7 WR #1             ;STORE FID
8 IF #1             ;INCREMENT FILE NUMBER
9 IN=1              ;INCREMENT D0 AND LOOP FOR NEXT EXPER.
10 EXIT

PH1=A0 A0 A0 A0 A1 A1 A1 A1      ;PHASE PROGRAMS CANCEL AXIAL
    A2 A2 A2 A2 A3 A3 A3 A3      ;PEAKS (SCANS 1-2), SELECT N-TYPE
                                 ;PEAKS (SCANS 3-4), SUPPRESS F2
PH2=A0 A2 A1 A3 A1 A3 A2 A0      ;QUAD IMAGES (SCANS 5-8), AND CANCEL
    A1 A3 A2 A0 A2 A0 A3 A1      ;ARTEFACTS FROM P1 (SCANS 9-16).

;PROGRAM REQUESTS FILENAME WITH .SER EXTENSION
;NE DEFINES NUMBER OF FIDS = TD1
;USE QP, NS = 4,8, OR 16 (COMPLETE PHASE CYCLE)
;DS = 2 OR 4
;RD=PW=0
;D1 = 1-5*T1
;P1 = 90 DEG
;P2 = 90 DEG FOR MAX. SENSITIVITY
;   = 45 DEG FOR MINIMAL DIAGONAL (GOOD FOR TIGHT AB SYSTEMS)
;        AND 'TILTED' CORREL. PEAKS (SIGNS OF COUPLINGS).
;D0 = 3E-6 INITIAL DELAY
;IN = 0.5/SW1 = 2*DW
;NDO = 1
;I2D = 1, SW1=SW/2

;CHOOSE SW AND SI SO THAT HZ/PT = CA. 2-6 HZ
;TYPICALLY USE TD = SI, NO ZERO-FILLING IN F2
;              NE = SI/4, ZERO-FILL IN F1
;MATRIX CAN BE SYMMETRIZED ABOUT DIAGONAL
```

P1 and P2 are the 90° pulse values, NE was upwards of 96
SW (Sweep Width) was 2500 Hz, centred about O1 of 6100 Hz